EFFECTS OF REINFORCEMENT CORROSION ON THE STRUCTURAL PERFORMANCE OF REINFORCED CONCRETE BEAMS

Gavin De Vos Theron

A dissertation submitted to the Faculty of Engineering, University of Cape Town, in partial fulfilment of the requirements for the degree of Master of Science in Engineering.

Cape Town, 1994

Declaration

I declare that this dissertation is my own unaided work. It is being submitted in partial fulfilment for the degree of Master of Science in Engineering in the University of Cape Town. It has not been submitted before for any other degree or examination in any other University.

_____

_____day of_____199_

Abstract

This dissertation is an investigation into the effect of reinforcement corrosion on the structural performance of reinforced concrete beams. Two types of specimens are investigated, the first without any stirrups and the second with stirrups. The specimens were corroded galvanostatically as well as by subjecting them to alternate cycles of wetting and drying with a saline water. An attempt is made at classifying the extent of corrosion of the reinforcing steel and its effects on the concrete. The effect of the corrosion on the structural performance is measured by establishing its effect on the maximum load carrying capacity, the deflections, energy requirements and ductility ratio. The main conclusions made in respect of the effect of reinforcement corrosion are that it causes : a decrease in the load carrying capacity; an increase in the deflections at the equivalent load level; a decrease in the energy requirements to reach the maximum load; and a smoothing of the load-deflection relationship. A limited literature review is also presented to provide background information of corrosion in concrete and general structural behaviour. Guidelines for the development of an analytical model to predict the load carrying capacity of corrosion affected reinforced concrete beams are also given.

Acknowledgements

I would like to thank to the following people for their assistance and guidance in preparing this dissertation :

Professor M.G. Alexander	My supervisor, Department of Civil Engineering, University of Cape Town.
Professor R.D. Kratz	My co-supervisor, Department of Civil Engineering, University of Cape Town.
Professor A.R. Kemp	Department of Civil Engineering, University of the Witwatersrand.
Mr J. Mackechnie	Research officer, Department of Civil Engineering, University of Cape Town.
The workshop staff	Department of Civil Engineering, University of Cape Town.
Mr J. Lemmetjies	Departmental assistant, Department of Civil Engineering, University of Cape Town.
Mr J. Williams	Departmental assistant, Department of Civil Engineering, University of Cape Town.

This research was conducted with support from the 'Special Programme on Concrete Durability', funded by the South African Cement Industry and the Foundation for Research Development. I would also like to acknowledge the support of an FRD bursary.

Contents

Structural properties, behaviour of reinforced concrete beams under load, and the effect and implications of reinforcement corrosion on these properties - a literature review.

Experimental investigation of the effects of reinforcement corrosion on the structural performance of reinforced concrete beams - series two

Comparison of results with those from other investigators, and guidelines for the development of a possible analytical model to predict the effects of reinforcement corrosion on the load carrying capacity of reinforced concrete beams

List of Figures

List of Tables

Page

List of Symbols

a/d ratio	Shear span to section depth ratio.
b	Section breadth.
d	Depth to tension reinforcing.
f_b	Bond strength.
f_c	Stress in concrete.
f_{cu}	Cube strength.
h	Section depth.
t	Time under corrosion current.
t_1	Time to first crack.
t_p	Time to propagate crack to width of 0,3-0,4 mm.
x	Depth to neutral axis
A	Surface area of steel.
A_s	cross-sectional area of steel.
C	Corrosion percentage.
D	Bar diameter.

D_r Deflection ratio.

D_o Original bar diameter.

E_s Elastic modulus of steel.

E_c Elastic modulus of concrete.

E_{corr} Corrosion potential.

F Faraday's constant.

f_t Tensile strength of uncorroded bar.

f_t^{corr} Tensile strength of corroded bar.

I_{corr} Corrosion current.

M_{cr} Moment at appearance of first hairline cracks.

M_u Ultimate moment capacity.

M_y Moment at yield of steel.

P_{max} Maximum load carrying capacity.

P_{max}^{corr} Maximum load carrying capacity of corroded specimens.

P_y Yield load.

P^* Remaining load carrying capacity

U_{Pmax} Work done to maximum load in uncorroded beams.

U_{Pmax}^{corr}	Work done to the maximum load for corroded specimens.
W_a	Atomic weight.
W_t	Estimated weight loss.
X_c	Critical depth beyond which the moisture content remains constant.
Z	Metal valency.
α_b	Alpha factor for bond strength
α_c	Alpha factor for compression area
α_s	Alpha factor for steel area
ϵ_c	Strain in concrete.
$\epsilon_{strain\ hardening}$	Strain at which strain hardening starts.
ϵ_y	Yield strain in steel.
θ_y	Elastic end rotation at design moment.
θ_p	Plastic end rotation at design moment.
ψ_c	Curvature ductility factor.
$\psi_{failure}$	Failure ductility factor.
ψ_{Pmax}	Ductility ratio using maximum load.
$\psi_{graphic}$	Ductility ratio using graphic method.

ψ_r Rotation ductility factor.

κ_m Curvature at end of plastic range.

κ_y Curvature at steel yield.

$\Delta_{failure}$ Deflection at failure load.

ΔF_t % reduction in tensile strength of steel.

Δ_{Py} Deflection at yield load.

Δ_{Pmax} Deflection at maximum load.

Δ_{Pmax}^{Corr} Deflection of corroded specimens at maximum load.

$\Delta_{80\%Pmax}$ Deflection corresponding to 80% of P_{max} along the descending branch of the load deflection curve.

Δ_{Py} Deflection at yield load.

ρ_s Density of steel.

Introduction

The corrosion of reinforcing steel in concrete can cause cracking, spalling and staining of the concrete surface which presents aesthetic and structural problems that can have severe economic implications. The aesthetic deterioration of reinforced concrete due to corrosion usually requires that the concrete be repaired if aesthetics is of prime importance for the concrete structure concerned. The effect that reinforcement corrosion has on the structural performance of reinforced concrete elements is still poorly defined. Repairs are usually undertaken because 'spalling and cracking is occurring and therefore the structural performance must be affected.' No rational decision process is used to decide whether repairs from a structural viewpoint are in fact necessary. Research is therefore needed to establish when the structural integrity of a structure is impaired to such an extent that safety becomes an important consideration. Information of this kind will help eliminate unnecessary repairs which could make the use of concrete uneconomical compared with other materials.

Aim of this project

To examine the effect that reinforcement corrosion has on the structural performance of reinforced concrete beams.

To achieve this aim, this dissertation deals with the following topics :
Chapter one introduces the topic of corrosion of steel in concrete and how the corrosion rate is affected by various factors. Corrosion monitoring and protection techniques are also reviewed. Chapter two reviews the behaviour of reinforced concrete beams under load and the effects of reinforcement corrosion on the structural properties of beams. The implications of corrosion for safety and serviceability of structures is reviewed to highlight the need to be able to accurately predict the effects of corrosion on the structural performance of structures. Chapters three and four present the experimental work done to investigate the effect of corrosion on the structural performance of reinforced

concrete beams. Chapter three deals with series one beams which were corroded galvanostatically and chapter four deals with series two beams which were corroded by subjecting them to a series of wetting and drying cycles. Chapter five compares the results of this investigation with the results of other researchers and suggests guidelines for the development of an analytical model to predict the effects of reinforcement corrosion on the load carrying capacity of reinforced concrete beams. Chapter six is the concluding chapter.

Chapter One

Corrosion of steel in concrete, corrosion monitoring techniques and corrosion protection - a literature review

1.0 Introduction

The concrete in a reinforced concrete member serves two basic functions. The first is a structural function in which the concrete provides compressive resistance, bond and bulk physical shape. The second function of the concrete is to provide protection to the reinforcing steel and, in the case of a building, protection to the inside of the building from the elements. The protection that the concrete offers to the steel is, however, not only due to the concrete acting as a physical barrier, but also due to the material creating a highly alkaline environment, thus producing steel passivity and resistance to corrosion. It is the very presence of the elements oxygen and water in the concrete that results in the steel's passivity. However, under unfavourable environmental conditions, concrete can permit steel corrosion to occur. Once corrosion is initiated, cracking and spalling can create major safety and serviceability problems. These problems are becoming increasingly common today as refined design methods result in more slender structures that are sensitive to design and construction errors as well as being more sensitive to the consequences of corrosion of the reinforcing steel. An understanding of corrosion of steel in concrete is needed if one wants to study the effects of corrosion on the performance of reinforced concrete beams. This chapter aims at providing a basic understanding of the corrosion process, some corrosion monitoring techniques and some corrosion prevention techniques.

1.1 Corrosion of Steel in Concrete

1.1.1 Electrochemistry of corrosion[1.1]

Corrosion of steel in concrete is an electrochemical process that arises when there is a potential difference between two parts of the metal. The surface of the corroding metal functions as a mixed electrode, upon which coupled anodic and cathodic reactions take place. At anodic sites metal atoms pass into solution as positively charged, hydrated ions (anodic oxidation) and the excess free electrons flow through the metal to cathodic sites where an electron acceptor, such as a hydrogen ion or dissolved oxygen is available to consume them (cathodic reaction). The process is completed by migration of ions through the aqueous phase, leading to the formation of a corrosion product which may be soluble (e.g. ferrous chloride) or insoluble (e.g. rust, hydrated ferric oxide). Essential features of the process in each case are as follows[1.1] :

- a reactive metal which will oxidise anodically to form soluble ions,
- a reducible substance which provides the cathodic reactant,
- an electrolyte which allows ions to move between anodic and cathodic sites.

These different sites may be adjacent to one another on a particular reinforcing bar or may occur remotely in different parts of the member or structure. **Figure 1.1.1** shows a typical corrosion cell that may develop in reinforced concrete.

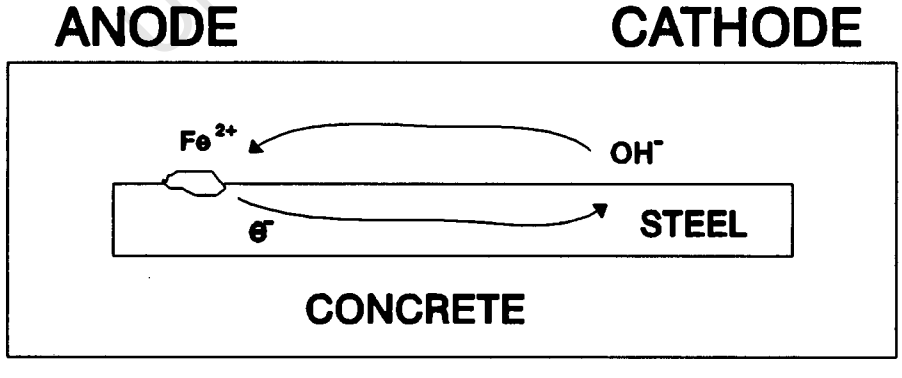

Figure 1.1.1 A corrosion cell that may develop in reinforced concrete.

Dense concrete, which has not become carbonated by reaction with acidic constituents of the atmosphere or penetrated by chlorides, contains a highly

alkaline solution (pH >13) within the pores of the hardened cement matrix surrounding the reinforcement. This alkalinity is due to the presence of sodium, potassium and calcium hydroxides, derived from the reactions between the mix water and the Portland cement. In this environment the steel is maintained in a passive condition and the corrosion rate is insignificantly low because of the protective oxide film surrounding the metal. The existence of a crack or a highly permeable region in the concrete may allow the ingress of acidic reactants or chlorides which lower the pH of the pore solution and result in depassivation of a small area of the reinforcing bar allowing corrosion to proceed freely. The depassivated part of the steel becomes the anode of the corrosion cell. The portions of the bar still protected by sound concrete become the cathode in the reaction.

The rate at which corrosion proceeds depends on many factors, most of which are influenced by the environment[1.1]. The ratio between the anode and cathode sizes plays an important part in determining the initiation of the reaction. Thereafter the rate of corrosion depends on the electrical resistivity of the concrete between the anode and the cathode and the availability of oxygen at the cathode. In humid environments the degree of saturation is high resulting in a low electrical resistivity of the concrete and usually resulting in high rates of corrosion. For structures completely immersed in water, it is the availability of oxygen at the cathode that determines the rate of corrosion.

The anodic and cathodic reactions are as follows[1.1] :

The Primary anodic reaction

(1.1.1)

$$Fe \rightarrow Fe^{++} + 2e^{-}$$

Secondary anodic reactions

$$Fe^{++} + 2OH^- \rightarrow Fe(OH)_2 \rightarrow Fe(OH)_3 \quad (1.1.2)$$

$$2Fe(OH)_3 + Fe(OH)_2 \rightarrow Fe_3O_4 + 4H_2O \quad (1.1.3)$$

$$2Fe(OH)_3 \rightarrow Fe_2O_3 + 3H_2O \quad (1.1.4)$$

The Cathodic reaction

$$O_2 + 2H_2O + 4e^- \rightarrow 4OH^- \quad (1.1.5)$$

Figure 1.1.2 is a diagrammatic summary of the corrosion reactions

1.1.2 States of corrosion of steel in concrete

Steel embedded in concrete can be classified into one of a number of states of corrosion, depending on the nature of the corrosion[1.1] :

The Passive State

Concrete that has not been carbonated or been penetrated by chlorides has a naturally high alkalinity with a pH greater than 13. In this environment the protective oxide film is in a stable form and protects the steel from corrosion. The steel is then said to be in the passive state and the probability of corrosion occurring is very low.

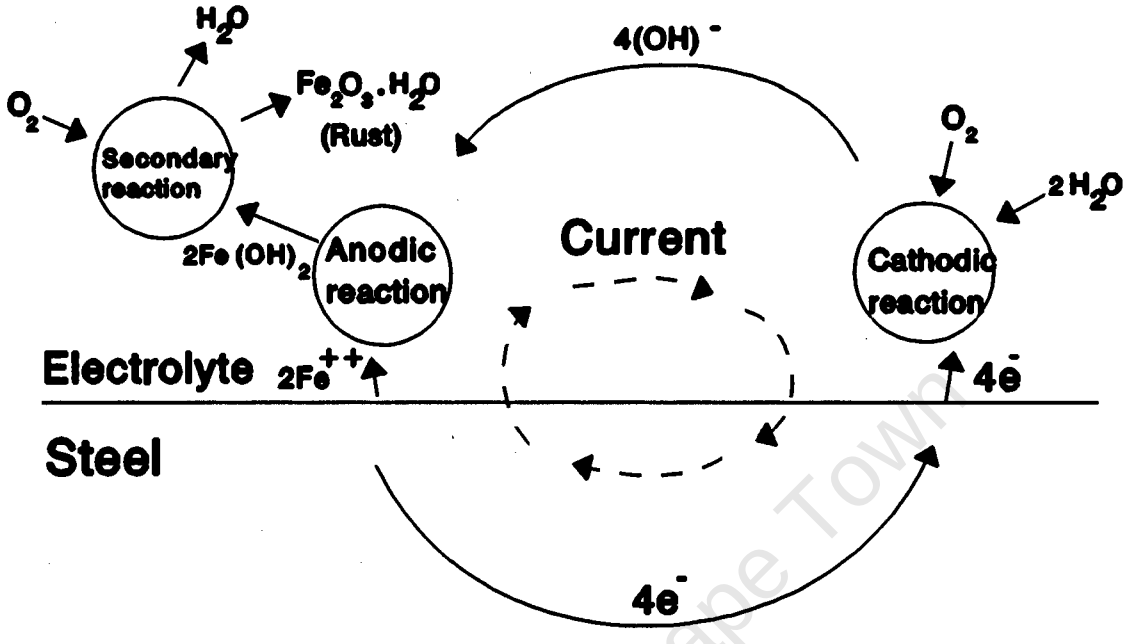

Figure 1.1.2 Diagrammatic representation of the corrosion reactions.[1.1]

The State of General Corrosion

General loss of the steel passivity can arise if the pH value of the pore water at the level of the reinforcement is substantially reduced from its initial level of approximately 13 to below 11,5. This can happen as a result of carbonation or sulphation which generally involves penetration of acidic gases from the external environment, or from the ingress of chlorides. The penetration of these gases causes a change in the chemical structure of the concrete resulting in a lower pH of the pore water. A higher level of corrosion may occur if the reinforcement has become contaminated with chloride ions to such an extent that the entire passive film is destroyed. Electrical potential gradients in structures undergoing general corrosion are relatively small, unlike steel undergoing pitting corrosion (see below) where there are very large potential gradients in the region of the pits.

The State of Pitting Corrosion

Pitting corrosion is most likely to occur in reinforced concrete that has very high levels of chloride ions at isolated spots. These can either come from the external environment or from contaminants in the mix materials. This corrosion state is characterized by galvanic action between relatively large areas of passive steel acting as the cathode and the pits acting as anodic regions where there is a local concentration of chlorides, causing a local suppression of the pH. In the regions of the pits a very high potential gradient is thus formed between the pits and the passive steel.

The State of Active, Low Potential Corrosion

In environments where the availability of oxygen is extremely limited, such as in concrete that is fully submerged in sea water, the passive film may not be maintained and the steel becomes active despite being in a very alkaline environment. The steel undergoes uniform dissolution to form $Fe(OH)_2$. The rate of metal dissolution is extremely low due to the limited oxygen availability and for practical purposes this type of corrosion can be assumed to have no negative effects on the steel or concrete.

1.1.3 Time Dependence of Corrosion States

The state of corrosion of steel in concrete is often a time dependant function as the external environment slowly influences the internal controlling environment of the concrete surrounding the steel. **Figure 1.1.3**[1.1] shows a schematic representation of when the various states occur during the service life of a structure. The initiation period is the period during which the metal, having been embedded in the concrete remains in a passive state within the concrete. The corrosion period begins at the time that depassivation starts and involves the propagation of corrosion at a significant rate until a final state is reached when the structure is no longer considered to be acceptable on the grounds of structural integrity, serviceability or appearance.

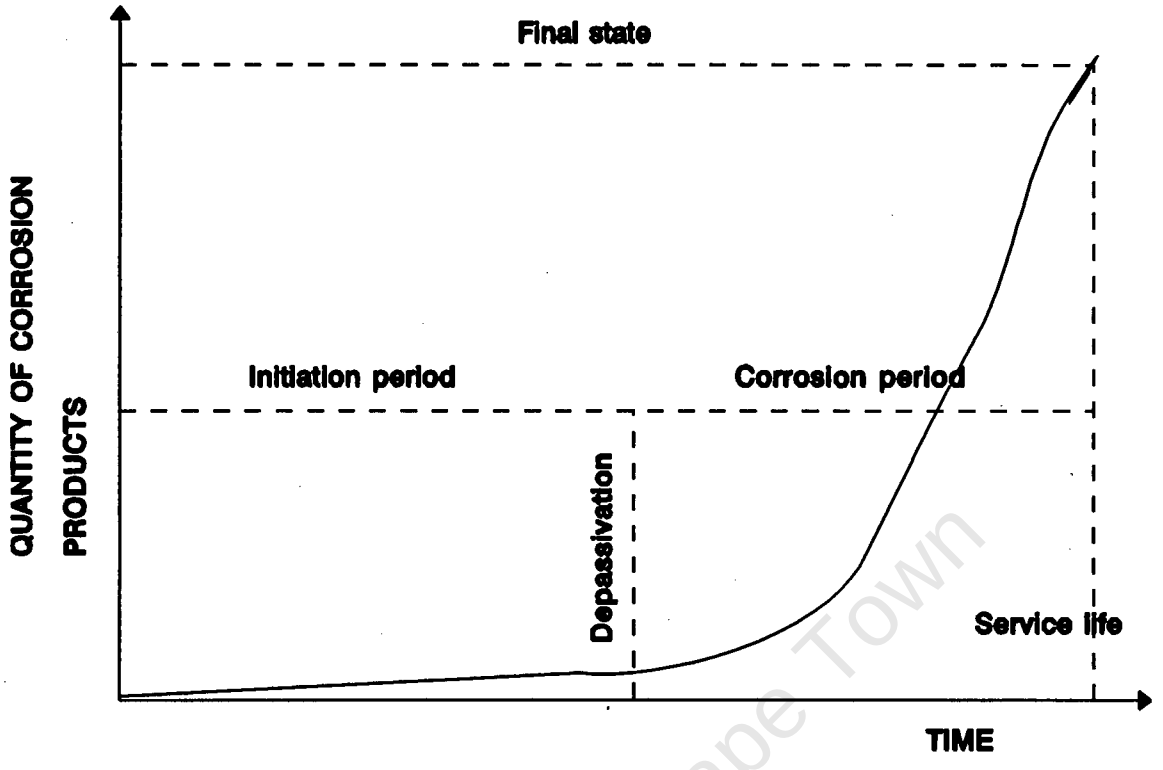

Figure 1.1.3 Schematic representation of the components of service life[1.1]

1.1.4 Penetration of Chlorides

Chlorides can be introduced into the concrete either by contaminants in the mix materials or as a result of post-setting exposure to de-icing salts, sea water or other chloride-bearing liquids. If there were chlorides in the mix materials then corrosion will be initiated immediately. In the case of the concrete being exposed to a chloride-bearing environment, the concentration of chlorides will slowly increase with time until the steel loses its passivity and corrosion begins.

The rate of chloride penetration is dependant on several parameters. The following have been identified[1.1] :

The composition of the cement

The cement type and its composition determine the chloride-binding capacity of the concrete. The higher the chloride-binding capacity of the concrete, the higher the concentration of chlorides will need to be to allow free chlorides to be present in

the pore water which can then play a part in the depassivation of the steel.

The amount of cement per cubic metre of concrete

The higher the cement content in the concrete the higher will be the chloride-binding capacity of the concrete and consequently there will be less probability of corrosion occurring.

The composition of the concrete

The water/cement ratio of the concrete determines the potential quality of the concrete. The lower the ratio the lower the permeability of the concrete will be, resulting in a reduced diffusion of chloride ions and oxygen and a longer time before depassivation begins.

The compaction of the concrete

Effective compaction reduces the permeability of the concrete and consequently the rate of chloride penetration.

The curing conditions of the concrete

Better curing results in more cement hydration and therefore a lower permeability.

External environmental conditions of the concrete

The transportation of chloride ions can only take place in an electrolyte. The transport of ions in concrete can take place in two ways. The first is by diffusion of the ions in a stationary electrolyte. In the second case, ions are transported by capillary suction of chloride-containing water into pores that are dry. This occurs when concrete is alternately wetted by a chloride-containing solution and dried, as is the case with marine concrete that is within the intertidal zone. The depth to which this capillary action will have an influence will depend on the periods of wetting and drying and on the permeability of the surface layers of concrete. At the depth where the concrete never dries out there is merely diffusion of the chloride ions.

There have been many attempts to predict the rate of ingress of chlorides into concrete where the concrete is in constant contact with a salt solution. These

prediction formulas are of the form $x = A\sqrt{(t)}$, where t is the length of time in contact with the solution and x the depth of penetration of chlorides at time t. The accuracy of the various formulas varies greatly, although they usually give a rough indication of the time to depassivation. Concrete that is in contact with a chloride-containing solution alternating with dry periods has a depth beyond which the moisture content is constant for practical purposes. If the steel is beyond this depth and the moisture content is sufficiently high then negligible corrosion will occur. **Figure 1.1.4**[1.1] shows this depth schematically. The complexity of alternating cycles of wetting and drying leads to models that are too complex to be applied and often do not provide any meaningful prediction of the time required for chlorides to reach a particular depth in the concrete. Predictions about the service life of structures within the intertidal zone therefore should be viewed with caution.

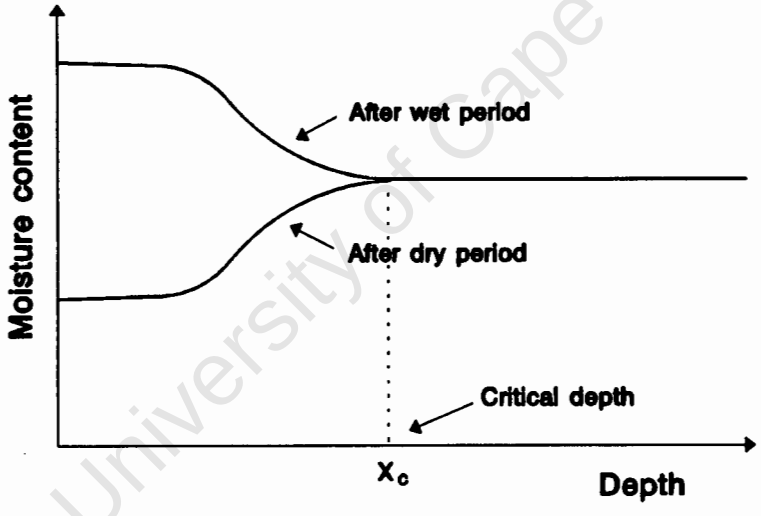

Figure 1.1.4 Schematic representation of depth beyond which the moisture content never varies.[1.1]

The influence of cracks

The diffusion resistance within a crack is substantially less than through sound concrete.[1.1,1.2] Therefore the chloride concentration along a crack will reach a higher concentration sooner than the surrounding concrete, leading to a faster depassivation of the steel and consequent corrosion in the region of the crack. Certain small cracks may become blocked and thus slow down the ingress of chlorides to a rate that is similar to that of sound concrete. Cracks also influence

the oxygen diffusion to the cathode which is the rate determining factor after depassivation.[1.1] The more cracks there are and the bigger they are, the greater is the amount of oxygen diffusion and the faster the corrosion proceeds.

1.1.5 Effect of the external environment on the corrosion rate

Corrosion of steel in concrete can be initiated by many different factors. The initiation of corrosion however does not necessarily result in active corrosion because the corrosion rate can be insignificantly low. That is, the factors controlling the rate of corrosion are different from the factors controlling the initiation of corrosion. Parameters that have been found to influence the rate of corrosion are[1.2, 1.3] :

electrical resistivity of the concrete
relative humidity of the concrete
temperature of the concrete
availability of oxygen at the cathode
presence of chloride ions
pH of the pore solution

In order to maintain a corrosion current, charge transfer through the concrete is necessary. Thus the electrical resistivity will be the rate determining factor. Under normal conditions oxygen reduction occurs in the corrosion process and hence the rate at which oxygen can be transported to the site of the corrosion will also be a rate determining step in the overall corrosion process. Of importance when it comes to oxygen diffusion is the moisture content of the capillary pores because oxygen has been found to diffuse up to four orders of magnitude more slowly in the dissolved form than it does in the gaseous form.[1.3] A change in moisture content of the concrete will change the salinity of the pore solution thereby also changing the solubility of oxygen and the electrical resistivity of the concrete.

Enevoldsen and Hansson[1.2] found that by increasing the relative humidity, the electrical resistivity of the concrete reduces, making the transfer of charge easier

and therefore increasing the corrosion rate. It was also found[1.2] that 85% relative humidity in the pores is the threshold level below which a corrosion current cannot be maintained. In contrast Lopez and Gonzalez[1.3] found 45-50% pore relative humidity is the limit below which the risks of corrosion are negligible. Lopez and Gonzalez[1.3] monitored the corrosion current and found that the maximum corrosion current occurred at 60-70% relative humidity in the pores.

Corrosion is an electrochemical process, and temperature therefore plays a role in determining the rate of the chemical reaction. In low humidity environments the effects of increasing temperature do not influence the corrosion rate as much as in high relative humidity environments. This has been explained by Lopez et al[1.4] as follows : at a given relative humidity, increasing the temperature decreases the pore radius at the wetting/drying equilibrium with the atmosphere facilitating the emptying of the pores. The concrete is thus desiccated, losing the electrolyte and thus the corrosion potential as the resistance of the concrete increases. Therefore provided enough electrolyte is available, such as in pores with a high relative humidity, the accelerating effect of temperature prevails over the inhibiting effect of an electrolyte being lost to the atmosphere and the corrosion process is speeded up. Therefore temperature plays an active role in speeding up the corrosion process provided the relative humidity is high and there is ample supply of electrolyte available to replace lost electrolyte.

1.2 Corrosion monitoring techniques

The presence of corrosion of reinforcing steel is often only detected in the advanced stages of corrosion when spalling and cracking start to affect the serviceability of the concrete element. Non-destructive early detection methods therefore can be usefully applied to concrete elements before it is too late and cracking has necessitated repairs. The majority of the monitoring techniques used today are electrochemical techniques. There are however also a few physical methods such as the gravimetric weight loss method.

1.2.1 Potential mapping

The corrosion potential in reinforced concrete can be determined by measuring the voltage difference between the reinforcing steel and a reference electrode in contact with the concrete. The probabilities of corrosion occurring at any point in concrete based on the voltage difference (E_{corr}) between the steel and the reference electrode is given in **Table 1.2.1** for various measured voltages.[1.5]

Table 1.2.1 Probabilities of corrosion occurring

Probability of corrosion	E_{corr} (vs $Cu/CuSo_4$)
> 95%	< -0,35
< 5%	> -0,20
50%	-0,2 to -0,35

By plotting potential contours over the entire surface of the concrete element it is possible to determine possible areas of corrosion or areas where preventative or remedial action should be taken.

1.2.2 Concrete resistivity measurements

This method is based on the Wenner method of measuring soil resistivity using four electrodes to measure the resistance resistivity of the concrete.[1.3,1.5] By making the assumption that the concrete's resistivity is proportional to the corrosion rate it is possible to determine areas where corrosion is probable.

The accuracy of measurements is affected by local inhomogeneities in the material. Reinforcement embedded in the concrete also affects readings taken, especially when the steel is at a relatively low cover. Millard and Gowers[1.6] have reported several influences that can severely affect the accuracy of resistivity measurements : the effect of member size is usually negligible provided that the

breadth and depth of the section are at least four times the electrode spacing, and provided that the spacing of the probe from the edge is at least twice the electrode spacing. For sections smaller than this the resistivity measurement obtained will be greater than the actual resistivity. Surface layers of differing properties such as saturation or chloride content can severely affect the accuracy of the resistivity measurements. If the surface layer is of a lower resistance than the underlying layers then the apparent resistivity measured will be substantially higher than the actual resistivity of the concrete.

A further refinement can be made when concrete resistivity measurements are combined with potential mapping, the potential mapping defining the areas with high potential gradients. If these occur in regions of low concrete resistivity it can be assumed that there will be a high corrosion rate at this point in the concrete.

1.2.3 Electrical resistance measurements of the reinforcing steel

By measuring the resistance change of the reinforcing steel with time as corrosion proceeds it is possible to measure an extent of corrosion in the steel. The resistance of steel changes as its cross-sectional area changes, the resistance being inversely proportional to the cross-sectional area of the steel. This method is however extremely difficult to apply in practice as it is difficult to monitor the very small changes in resistance that occur as the corrosion products start to disrupt the concrete.[1.1,1.5]

1.2.4 Polarization curves

Changes in corrosion potential due to changes in the applied current produce a polarization of the potential in the region of the actual corrosion current. By applying a range of currents to a specimen and then plotting the potential versus the applied current it is possible to identify the actual corrosion current in the steel by identifying the polarization potential of the steel. This is usually a graphic method called the Tafel plot method.[1.7] However, there are also mathematical

methods of identifying the actual corrosion current from the current and potential readings taken.[1.7]

By applying Faraday's law it is then possible to determine the weight loss of steel per surface area if the corrosion current and the time for which this current flows is known.

$$W_t = \frac{I_{corr} W_a}{ZF} \qquad (1.2.1)$$

Where W_t is the weight loss at time t [g/cm^2]
W_a is the molecular weight of the metal
Z is the metal valence
F is Faraday's constant [96500 Amp.sec]

1.2.5 Gravimetric techniques

This technique is widely regarded as one of the easiest and most accurate methods of monitoring corrosion of metals in electrolytes. Its application to steel imbedded in concrete is however not so successful due to the difficulty of removing the reinforcing from the concrete and the destructive nature thereof. The technique consists of weighing the steel before and after it has been embedded in the concrete, the difference being the amount of metal that has been lost by corrosion. An extent of corrosion can be established by expressing the weight loss as a percentage of the original weight.

1.3 Protection of Reinforced Concrete from Reinforcement Corrosion

Reinforcement corrosion can be prevented either by designing the concrete and the structure in such a way as to ensure a durable concrete in which reinforcement corrosion does not occur during the design life of the structure, or by using protective measures such as cathodic protection or surface layer protection. Both cathodic protection and surface coatings can be used as preventative measures on new structures or as curative measures on structures that are already corroding. A fourth type of protection is also coming into use, that is coating the reinforcing bars themselves with an epoxy coating thus electrically isolating the steel from the elements. Problems have been experienced in creating a durable coating that will not be damaged during the construction phase while still providing adequate bond between the reinforcing bar and the concrete. Galvanizing the reinforcing bars is also used as a means of protecting the steel.[1.5]

1.3.1 Cathodic Protection[1.5]

Cathodic protection is suitable for corrosion whenever moisture is present. For structures with reinforcement corrosion caused by gaseous diffusion, a protective surface layer to the concrete would be a more effective means of protection.

Surface inhomogenieties on a piece of reinforcing steel may set up local corrosion cells, or on a larger scale, macro-corrosion cells can be set up due to stray currents or differential environmental conditions (e.g. partially submerged marine structures). Cathodic protection works on the principle of neutralizing the potential difference so that a current is unable to flow and therefore the corrosion reactions will not occur. By connecting the reinforcing steel to an anode (external to or internal to the structure) and applying a potential difference such that the reinforcing bar becomes the cathode and the sacrificial metal the anode, corrosion of the reinforcing bars is prevented. The potential difference can either be applied in the form of a direct current or by connecting the rebar to a metal which is higher in the electrochemical series of metals than steel e.g. magnesium, aluminium or zinc.

The relatively small current required to neutralize the corrosion cells, makes cathodic protection an economically viable choice, using only 60-150 W for a highway bridge structure. The sacrificial anode can be incorporated into the structure at the construction phase, or as is usually the case with existing structures, it can be applied to the surface of the structure in the form of a metal conductor which is then coated with gunite. The use of conducting ceramics fixed to the surface of the concrete is also becoming popular[1.5].

1.3.2 Surface treatments[1.5]

Surface treatments are applied to a concrete structure to improve its appearance or to protect it from potentially aggressive agents. Surface treatments therefore either enhance the durability of the concrete on a new structure or extend the service life of an existing structure. Surface coatings used in this way to halt the progress of corrosion also provide protection to the concrete from freeze thaw and other environmental problems that may be experienced with concrete structures.

Surface treatments essentially enhance the protection of the steel by the concrete by limiting the ingress of environmental influences such as water, gases or chlorides through the concrete to the steel. This can be done by either creating a physical barrier (e.g. by creating an impermeable surface layer, or by blocking the pores) or by chemically lining the pores and surfaces with a hydrophobic layer.

If the entire structure is not coated with the protective surface layer or if it is damaged in one area, water may enter the concrete but then not be able to exit causing the concrete to become water-logged and hence causing the peeling off of the protective surface layer. It is therefore essential for a surface layer to allow water to exit the concrete but not enter it if the surface coating is to be effective.[1.5] Coating with an impermeable surface layer is therefore not suitable and the pores should rather be chemically lined with a hydrophobic layer.

1.4 Closure

A basic review of the corrosion process of steel and in particular of steel in concrete has been presented. The different states of corrosion and the influences of the external environment on the corrosion rate have been highlighted. The intention has been to provide a basic understanding of the process of corrosion of steel in concrete. This understanding is necessary if a study of the effects of corrosion of steel in concrete on the structural performance of reinforced concrete beams is to be made. The last section covered two methods of protecting reinforced concrete from reinforcement corrosion. Thus, there are methods available to prevent corrosion which is always better than trying to manage the consequences of corrosion.

1.5 References

1.1) Schiessl, P., *Corrosion of Steel in Concrete*, RILEM, Report of technical committee 60-CSC, New York: Chapman & Hall 1988, pp. 3-22.

1.2) Enevoldsen, J.N. and Hansson, C.M., The influence of relative humidity on the corrosion rates of steel embedded in mortar and concrete, *3rd Canadian Symposium on Cement and Concrete*, NRC, Canada, August 1993, pp. 342-350.

1.3) Lopez,W. and Gonzalez, J.A., Influence of the degree of pore saturation on the resistivity of concrete and the corrosion rate of steel reinforcement, *Cement and Concrete Research*, Vol 23, No 2, 1993, pp. 368-376.

1.4) Lopez,W., Gonzalez, J.A. and Andrade C., Influence of temperature on the service life of rebars, *Cement and Concrete Research*, Vol 23, No 2, 1993, pp. 1130-1135.

1.5) Mays,G. (ed), *Durability of Concrete Structures: Investigation, Repair & Protection*, London: E & FN Spon, 1992, pp. 45-58.

1.6) Millard, S.G. and Gowers, K.R., Resistivity assessment of in-situ concrete :The influence of conductive and resistive surface layers, *Proc.Instn Civ. Engr Conf. on Structs & Bldgs*, No 94, 1992, pp. 389-396.

1.7) Abdul-Hamid Al-Tayyib and Mohammad Shamim Khan, Corrosion rate measurements of reinforcing steel in concrete by electrochemical techniques, *ACI Materials Journal*, May-June, 1988, pp. 172-177.

Chapter Two

Structural properties, behaviour of reinforced concrete beams under load, and the effect and implications of reinforcement corrosion on these properties - a literature review.

2.0 Introduction

The behaviour of reinforced concrete beams under load is a complex interaction of several factors. The size of the compression zone, the amount of tension reinforcing, the bond strength and the shear resistance all play a part in the way that a reinforced concrete beam responds under load. It is therefore essential to try and understand the behaviour under uncorroded conditions first before attempting to establish what the effects of reinforcement corrosion are on the structural behaviour of reinforced concrete beams. Ductility in reinforced concrete elements also needs to be understood as it is of great importance, both from a safety point of view and from an economic point of view. Structural elements that behave in a ductile manner display large deformations at near-maximum load. This allows evacuation of the building or preventative actions to be taken before total collapse occurs. If the level of ductility of reinforced concrete structures can be ensured and predicted, it is possible to allow for moment redistribution in design, thereby achieving greater economy. The accurate quantification of the effect that reinforcement corrosion has on the ductility of reinforced concrete elements reduces risk and allows for safer design. By being able to predict the effect of reinforcement corrosion on the structural performance of reinforced concrete beams one is able to make better estimates of the service life of structures which also improves safety. The aim of this chapter is to provide a basic review of the behaviour of reinforced concrete beams under load and the concept of ductility. A literature review of the effects of corrosion on the structural properties and performance of reinforced concrete beams follows.

2.1 Behaviour of reinforced concrete beams under load[2.1]

The behaviour of reinforced concrete beams under load in the elastic range is relatively easy to predict and to understand. It is the behaviour beyond the elastic range that is complicated and needs to be understood if the concept of ductility is to be grasped.

Stress-strain relationship for reinforcing steel

This well known curve (**Figure 2.1.1**[2.1]) for mild steel displays an initial elastic portion, where the stress is directly proportional to the strain, a yield point (ϵ_y) beyond which strain increases with little or no increase in stress, and a strain-hardening range in which stress increases again with increase in strain. The last portion of the curve displays a decreasing stress for increasing levels of strain.

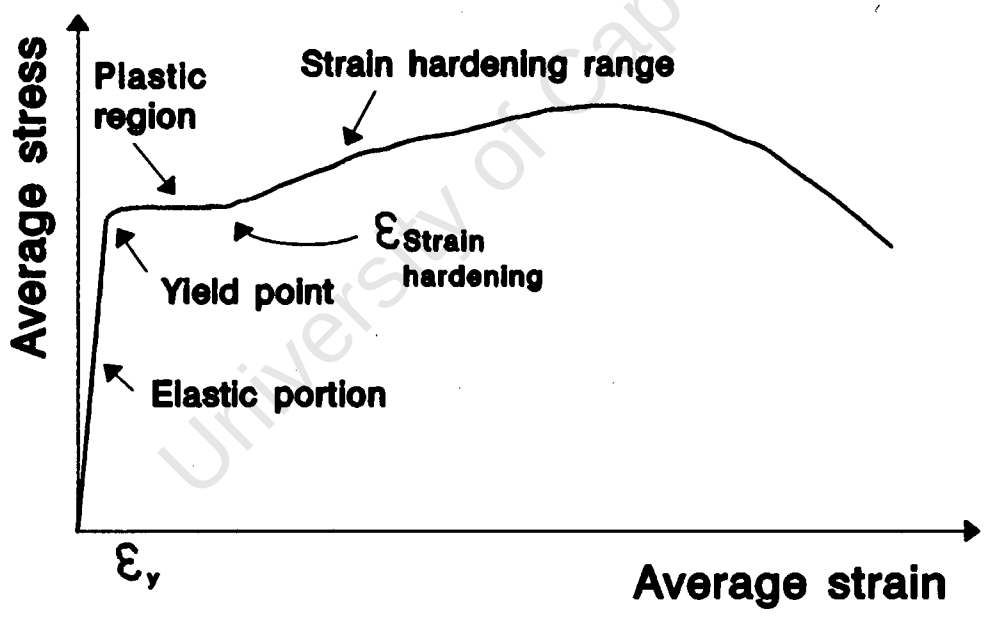

Figure 2.1.1 Stress-strain diagram for mild steel.

For a typical mild steel the proportions of the graph are approximately as follows; the plastic portion between ϵ_y and $\epsilon_{\text{strain hardening}}$ is about 10 to 20 times the elastic range. The portion of the curve beyond $\epsilon_{\text{strain hardening}}$ is about 8 times the plastic range, and over 100 times the elastic range. For reinforced concrete beams of ordinary proportions a strain of up to $2.\epsilon_{\text{strain hardening}}$ is the significant portion that needs to be considered for ductility.[2.1] Consequently the stress-strain curve is

usually idealized to two straight lines, one for the elastic range and another for the plastic range. A more accurate idealization would be to use two lines instead of one for the plastic range. The first line would represent the initial plateau and the second the strain hardening portion, thus taking account of the increase in the stress in the strain hardening range.

Stress-strain relationship for concrete

Concrete displays very different stress-strain characteristics depending on whether it is confined or not. The behaviour of confined concrete will only be considered here. It is important to note that both strength and ductility of concrete increase dramatically when the concrete is confined. Concrete is termed 'confined' when the concrete is stressed in all directions and not only uniaxially. This condition arises when spiral reinforcement, hoops, or stirrups are provided to restrain it in directions perpendicular to the applied stress.

A typical stress-strain diagram for spirally confined concrete in compression is given in **Figure 2.1.2**[2.1]. This curve is usually idealized[2.1] by the three dashed straight lines in the Figure. The first line represents unconfined concrete behaviour and the second confined behaviour. The transition from unconfined to confined behaviour occurs when the spiral reinforcement is first stressed by the concrete straining perpendicular to the applied load. The transition from the second to third lines occurs when the spiral reinforcement first yields.

Reinforced concrete sections subject to bending only

The behaviour of a reinforced concrete section under an applied bending moment can conveniently be described by the relationship between moment and curvature. This relationship depends upon the material and geometric properties of the cross-section. The useful limit of strain for concrete is approximately 0,004, and for tension steel between 0,03 and 0,06 for mild steel. Depending on the design of the section, the ultimate flexural capacity of a reinforced concrete member may correspond to :

1) reaching the useful limit of strain of the concrete before yielding of the tension steel,
2) reaching the useful limit of strain of the concrete after yielding of the tension steel,
3) reaching the useful limit of strain of the tension steel before the useful limit of strain in the concrete is reached.

The design of flexural elements in most codes ensures that moderately reinforced members will fall into category 2 (above) thus avoiding catastrophic failure which would occur if they were in category 1 or 3.

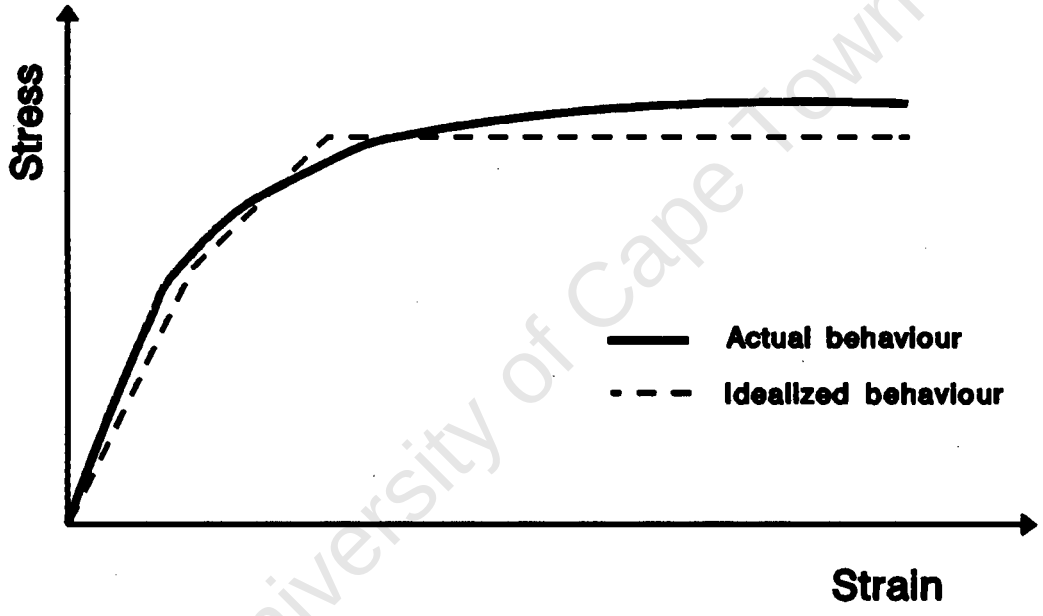

Figure 2.1.2 Stress-strain diagram for spirally confined concrete in compression.

The idealized moment-curvature relationship

The moment-curvature curve (M-ϕ) for a moderately reinforced cross-section exhibits four distinctly different stages as shown in **Figure 2.1.3**[2.1]. The first stage corresponds to an uncracked section and the M-ϕ curve is essentially linear. The appearance of the first hairline cracks initiates the second stage at M_{cr}. The third stage begins at the yielding of the tension steel (at M_y) and ends when the useful limit of strain is reached in the concrete at M_u. The fourth stage begins at the point of ultimate load P_{max}, corresponding to the ultimate moment M_u. The moment starts to reduce again after the useful limit of concrete strain has been reached. In most cases the point M_{cr} can be ignored as it has little significance and the M-ϕ

curve can be approximated by the two straight dashed lines shown in Figure 2.1.3.

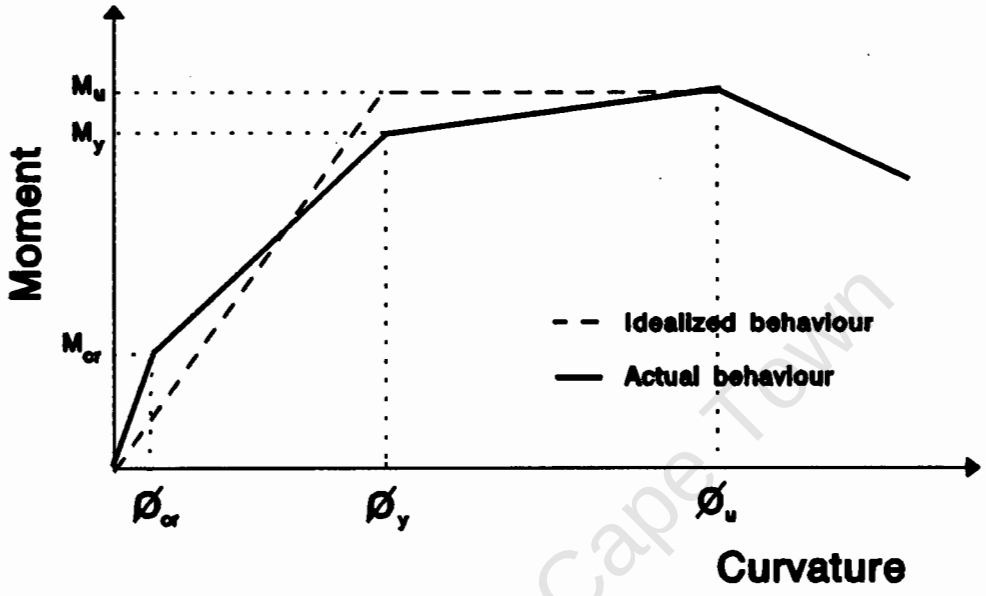

Figure 2.1.3 Moment-curvature diagram for beam in flexure only.[2.1]

Changes in the stress-strain curves under increasing load

Beams resist applied moments by equal and opposite internal couples that are the result of a stress distribution that varies from zero at the neutral axis to some stress level at the extreme fibre of the beam. Initially both the concrete and the reinforcing steel share the tension force, increasing linearly as the applied moment increases until the stress reaches the rupture stress of the concrete in tension. At this point the concrete cracks, and the steel carries all the tension force. This sudden increase in steel stress causes an increase in the steel strain which causes a reduction in the neutral axis depth. As a result of this the depth of the compressive zone decreases and therefore the compressive stress must increase to maintain equilibrium. This process then continues until one of the following types of failure occurs : shear, bond, tension or compression failure.

If the shear force anywhere in a beam exceeds the combined shear resistance of the concrete and the steel (longitudinal and hoop) shear cracks will develop. If the load is increased further, these cracks will widen reducing the effective

compression zone of the section, possibly to such an extent that a compression failure is possible. For relatively short spans (compared with the section depth) the middle portion of the beam's span may be punched out, similar to punching shear failures in thin slabs and collapse may then occur.

Bond failures occur when the change in tensile force in the reinforcing steel per unit length exceeds the bond strength. When this occurs, the beam deflects rapidly, unable to maintain the applied load level until collapse occurs.

If the tension steel content is small, the steel will reach its yield strength before the concrete reaches its maximum capacity. After yield small increases in applied moment will cause significant plastic elongation of the steel resulting in a widening of the concrete tension cracks and a reduction of the neutral axis depth. The increased stress in the compressive zone causes the concrete to crush and the beam no longer can resist an increase in the applied load.

If the tension steel content is large, the concrete may reach its compressive yield stress before the tension steel yields. As the tension steel has not yet yielded there will be little or no tension cracks that will give warning that the concrete in the compression zone is about to crush and cause a sudden failure of the member. This type of failure is known as a compression failure.

2.2 Ductility

2.2.1 Describing ductility

Ductility has been defined[2.2] as the ability of a material or structure to sustain post elastic deformations without significant loss of resistance capacity. Material and member ductility are both influenced by several factors, and sometimes those that increase the one type of ductility decrease the other type. For example; low strength concrete has more material ductility than high strength concrete, but beams with low strength concrete exhibit less member ductility than similar beams

with high strength concrete.[2.2]

Ductility of structural members is usually measured in terms of rotation or curvature. The rotation ductility factor ψ_r of a simply supported beam is defined as[2.2] :

$$\psi_r = \frac{\theta_p}{\theta_y} \qquad (2.2.1)$$

where : θ_p is the plastic end rotation at the design moment M_p
θ_y is the elastic end rotation at design moment.

The curvature ductility factor ψ_c is defined as[2.2] :

$$\psi_c = \frac{\kappa_m}{\kappa_y} \qquad (2.2.2)$$

where : κ_m is the curvature at the end of the plastic range
κ_y is the curvature when the steel reaches its yield stress.

Blume et al[2.1] give a theoretical method of calculating the ductility factor :

$$\psi_c = \frac{\epsilon_{cu}}{\epsilon_y} \cdot \frac{(1-k)}{k_u} \qquad (2.2.3)$$

substituting :

$$k = \sqrt{(p.n)^2+2.p.n} - (p.n) \qquad (2.2.4)$$

$$k_u = \frac{p.f_y}{f_{cu}} \qquad (2.2.5)$$

where : p is the tensile steel ratio

$$p = \frac{A_s}{bd} \tag{2.2.6}$$

n is the long term modular ratio

$$n = \frac{E_s}{E_c} \tag{2.2.7}$$

ϵ_{cu} is the ultimate strain in the concrete
ϵ_y is the yield strain in the steel

It can be seen that the smaller the tensile steel and modular ratios are, the greater the ductility will be. The ACI committee 363[2.3] defines an additional way of expressing the flexural ductility of a member, the deflection ductility index:

$$\psi_{failure} = \frac{\Delta_{failure}}{\Delta_{Py}} \tag{2.2.8}$$

where: $\Delta_{failure}$ is the member deflection at failure
Δ_{Py} is the member deflection at yielding of the tension reinforcement.

To say that a structure or member fails when it can no longer support the maximum load it is capable of carrying is the least arbitrary of the definitions of failure. Using this definition ductility could be defined as follows :

$$\psi_{Pmax} = \frac{\Delta_{Pmax}}{\Delta_{Py}} \tag{2.2.9}$$

where : Δ_{Pmax} is the member deflection corresponding to the maximum load the member can carry.

This definition is usually also inadequate as members often sustain substantial load well beyond the peaks of the load deflection diagrams. The following definition has therefore been suggested by Sung-woo Shin et al[2.4]

$$\psi_{80\%Pmax} = \frac{\Delta_{80\%Pmax}}{\Delta_{Py}} \qquad (2.2.10)$$

where : $\Delta_{80\%Pmax}$ is the final deflection corresponding to 80 % of P_{max} along the descending branch of the load-deflection curve.

Since the concept of ductility has to do with the ability to sustain inelastic deformations without substantial decreases in the load carrying capacity, this definition of ductility is logical and practical.

2.2.2 Factors affecting ductility in reinforced concrete beams[2.2]

Material strengths: Ductility increases with increasing concrete strength and decreasing tension reinforcement strength. Higher concrete strengths at the same applied load will strain less, while lower steel tensile strengths at the same applied load will strain more resulting in a smaller ratio of maximum strain in the concrete to the strain in the steel.

Bond: Ductility improves for sections with increasing bond strength.

Amount of reinforcement: Ductility decreases with increasing amounts of tension reinforcement.

Confinement of the compression zone: Confinement provides a triaxial constraint to the concrete in compression, thus affording the section greater ductility if smaller spacing between the stirrups is used.

2.3 Concrete/Steel bond

Loads are usually applied to structural elements and not directly to the reinforcing steel. The steel therefore is stressed by the concrete surrounding the steel. The shear stress that develops between the steel and the concrete is known as the bond stress. Provided the bond stress is sufficiently developed, it is the bond

stress that ensures strain compatibility between the steel and the concrete and ensures the steel and concrete act as a composite whole. Bond therefore plays an important role in the load carrying process and any disruption of it, by for example corrosion, will cause an alteration of the load-deflection response of the element.

Four components of bond are usually recognized[2.5] as playing a part in the shear transfer process if ribbed bars are used :

1) Bearing resistance
2) Friction
3) Chemical adhesion
4) Shear induced dilation.

The smooth portions between ribs have microscopic undulations that in addition to the ribs provide bearing surfaces against which the concrete can bear as the shear stress increases. The second component, frictional resistance, can be derived from the microscopic undulations as well as the ribs. The frictional resistance is enhanced when the concrete compressive stress around the steel is increased, for example by concrete shrinkage or by the confining stress offered by shear steel. The chemical adhesion between concrete and steel was always thought to make a significant contribution to the bond strength, especially with plain round bars. Rehm[2.5] discredited most of this theory as chemical adhesion can only exist before any slip occurs at the steel-concrete interface. Once slip has occurred bond can only be developed by friction and shear-induced dilation of the concrete surrounding the bar. The relative movement between the ribs and the concrete causes a dilating strain in the concrete. This strain is prevented from occurring by the sound concrete surrounding the portion that wants to dilate. The compressive stress in this region of the concrete is therefore increased, maintaining the bond strength.

2.4 Implications of reinforcement corrosion for safety and serviceability

Safety and risk are closely related and to ensure economic construction a satisfactory balance between the two must be found in order to make the structure safe and also to be perceived as being safe.[2.6] Safety and risk are therefore also closely related to serviceability and safety factors. Corrosion of reinforcing steel affects the serviceability and therefore also the safety of concrete structures. The extent to which the effects of corrosion of steel are allowed for in the design of elements will depend on the perception of risk and the monetary valuation of safety. Risk categories for structures are based on the consequences of failure. There are three main categories[2.6] :

- Risk to life or concern for public reaction to possible failures.

- Economic consequences due to :
  - -loss of use of structure and all ancillary costs
  - -need for replacement and repair.

- Environmental damage.

The balance between risk and safety will determine the cost of the structure. The more accurately the risk can be assessed the smaller can the safety factors used in the design be and the more economical the structure.

The safety of a structure depends on several factors[2.6]:

The type of structural system. In a series system one failure leads to the next, while in a parallel system the load is able to be redistributed and complete collapse may not occur. An example of a series system would be a structure where continuous beams, columns and frames are connected and dependant on each other for support. A parallel system would be one where 'simply supported' beams connect isolated columns, not forming continuous frames.

The manner of failure. Ductile elements maintain load levels at large deflections providing warning of possible failure, making the structure safer. Brittle elements progressively lose load-carrying capacity with increasing deflections, resulting in a sudden unpredictable failure.

Structural continuity. Continuous structures are more prone to progressive collapse (domino effect) than structures that have several isolated members which do not depend on other members for support or load sharing.

The effects of reinforcement corrosion on the structural properties of reinforced concrete elements will be described in section 2.7. The effects described all have a negative effect on the structural performance of the elements, namely: a reduced load carrying capacity, increased deflections, cracking and disruption of the concrete, and a loss of shear strength and bond. If the amount by which each of these affect the structural performance, for a given amount of corrosion, is not known then they cannot be allowed for in the design. By not allowing for the effects of reinforcement corrosion in the design, structural elements will be less safe as smaller margins will exist between the actual load and the load carrying capacity of the element.

Reinforcement corrosion usually presents itself in the form of rust staining, before any significant structural damage is done giving ample warning of deterioration. There are however instances[2.6,2.7] where reinforcement corrosion advances to critical levels unnoticed. Instances like these have severe safety implications. If general reinforcement corrosion is present in a structure, serviceability problems usually present themselves well before the safety of the structure is affected. With localized (pitting) corrosion, which usually results when chlorides are included in the mix or penetrate to the level of the reinforcement through cracks or construction joints, the reinforcement cross-sectional area can be reduced drastically by a pit, causing safety problems while still not displaying any visible signs of distress. The type of corrosion present therefore often determines the type of distress. If localised reduction of the reinforcement cross-sectional area occurs then a sudden catastrophic collapse is possible, or if the sectional geometry is altered by cracking and spalling the member stiffness may be reduced.

Reinforcement corrosion may only affect isolated members in a structure, but failure of or a change in the properties of one member may have structural or safety implications for the structure as a whole. Assessing the implications of reinforcement corrosion on the structure as a whole would require a study of the structure's susceptibility to progressive collapse.[2.6] Local failure may reduce the structure's redundancy, and this together with the corrosion-altered member properties may reduce the moment redistribution possible and hence cause further structural problems. This emphasises the importance of understanding what effects reinforcement corrosion has on member ductility. Once the effects on member properties and ductility are better understood the effects on the overall structural stability will be able to be assessed.

Reinforcement corrosion causes staining, cracking and spalling of the concrete cover thus affecting the aesthetics and serviceability of the concrete element. From a structural point of view, reinforcement corrosion also affects the serviceability of elements by increasing the deflections.

2.5 Service life predictions for structures

2.5.1 Structural investigations for service life predictions

The general method of structural investigations has been well documented by several sources and the CEB has published[2.8] their recommendations on how to undertake structural investigations of structures affected by reinforcement corrosion. The first step is to collect as much background information on the structure as possible and then, based on the particular structure under consideration, the most appropriate test method or technique can be decided on.

The wide variety of tests and test methods that exist can be classified broadly into the following categories[2.9]:

-Those dealing with structural integrity or location of reinforcement or voidage.
e.g. visual surveys, tapping surveys, covermeter surveys, thermography, acoustic emission, dynamic response, radar, load testing of structures and elements.

-Those dealing with concrete quality and composition.
Core sampling for permeability, sorptivity, and crushing strength tests; powder drilled samples for chloride contents, determination of the depth of carbonation, non-destructive assessment of in situ strength, surface hardness, surface density and porosity, petrographic examination of concrete.

-Those dealing with reinforcing steel serviceability and condition.
Half cell potential mapping, resistivity of concrete, cross-sectional area/diameter loss of steel, weight loss of steel, loss of tensile strength, loss of bond strength.

The vast array of tests that is available highlights the fact that careful consideration must be given to which tests should be used to give the best and most useful results. The interpretation of test results needs careful study, usually by a team of specialists in each type of test method. The interpretation of the results must be done considering the results of all the tests used in conjunction as one test result cannot be taken as definitive and may under certain circumstances be misleading.

2.5.2 Service life prediction

Service life predictions play an important part in determining the time period over which a structure meets its safety and serviceability requirements. Today it is more generally accepted that concrete structures only have a finite service life and that concrete cannot be considered as a 'maintenance-free' material. This is an important understanding as many of the older structures were designed and built, expecting unrealistic service lives. Accurate service life predictions ensure that at the end of the service life of the structure, the structure is still in a fit state and still meets the safety requirements. The more accurate the service life predictions are and the more is understood about how the behaviour of a reinforced element is

affected by reinforcement corrosion, the smaller can be the safety factors used in the design. This translates into safer structures while at the same time allowing for more economical design.

Structures are often designed from a structural viewpoint independently from the conceptual design which may be done by an architect. This type of independent design can lead to problems affecting the safety of the structure while still not affecting the serviceability of the structure. Poor communication between the parties involved could for example lead to ponding or penetration of water into construction joints leading to reinforcement corrosion. Service life predictions therefore have to be made considering the overall design of the structure and not just considering the structural element under consideration.

Despite the great technological and economic significance of service life predictions for reinforced concrete structures, there is no specific methodology for calculating the residual life of a reinforced concrete structure reliably. Most of the methods that have been suggested[2.7] also do not combine the consequences of the corrosion with both the serviceability limit state and the ultimate limit state. Thus the appearance of cracks may signal the end of the service life even though the ultimate limit state has not been reached yet. The visual signs of reinforcement corrosion usually only become apparent on the surface of the concrete once severe reinforcement corrosion has already started. Thus either early detection of corrosion or accurate service life prediction is essential to ensure a safe and economic structure.

The CEB has published the most comprehensive overview of the various methods for predicting service life[2.8] by classifying structures according to different extents of deterioration based on the appearance of external signs: rust stains, cracks, delaminations and thinner reinforcements. The damage levels are then used as the basis for recommendations on the need for the urgency of repairs. Tuutti's model is one such model.

2.5.3 Tuutti's model

The most widely used model for predicting the service lives of reinforced concrete structures is that developed by Tuutti[2.10], which establishes a maximum acceptable corrosion level related to the appearance of cracks and divides the service life of structures into two parts; an initiation and a propagation period. The length of the initiation period can be estimated from the time required for aggressive agents to reach the reinforcement and trigger active corrosion, while the propagation period can be taken as the time elapsed until visible cracks appear (0,05-0,1 mm) or repair becomes necessary. **Figure 2.5.1**[2.10] shows the components of Tuutti's model for the service life of reinforced concrete structures.

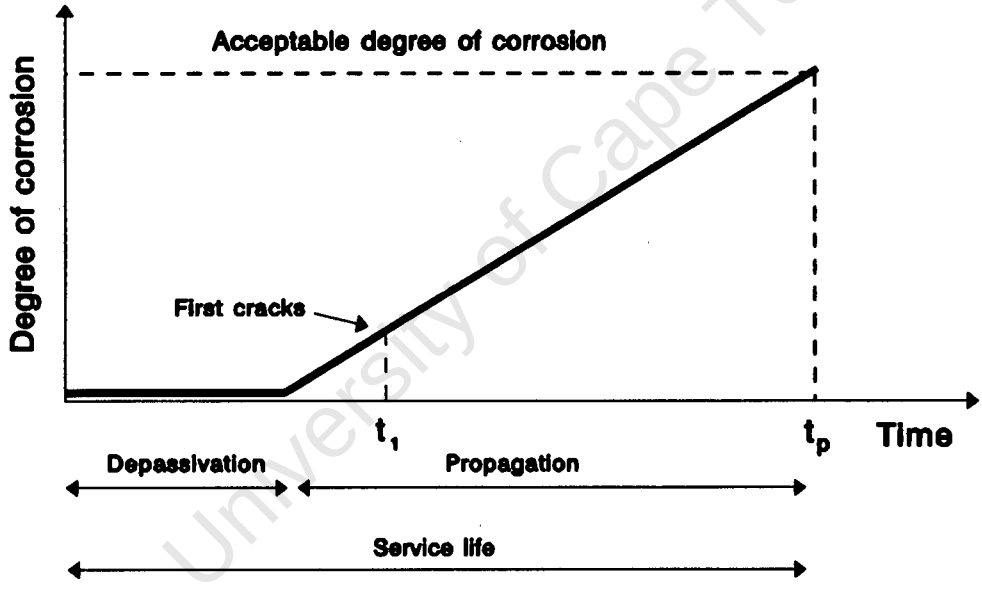

Figure 2.5.1 Tuutti's model for service life of reinforced concrete structures.[2.10]

On the basis of Tuutti's conceptual model, Andrade et al.[2.11] developed a methodology for estimating the residual life of corroded reinforced structures, as well as various procedures for implementing the model. The residual life of a structure can be estimated provided its corrosion rate is known or can be calculated and the knowledge of an unacceptable level of deterioration that will vary with the element's intended use and function in the structure. In order to obtain a quantitative prediction, the effects of corrosion must be transformed into some numerical index, for example the decrease in reinforcement cross-section

arising from corrosion or the time to produce concrete cover cracking or delamination. An estimate of the influence of these effects on the structural behaviour is then needed to complete the prediction of the remaining service life of the structure. The work undertaken in this investigation is aimed at quantifying the effects on the structural properties and is presented in Chapters three and four.

Many authors [2.7,2.12] link the service life of the structure to the time until depassivation of the steel occurs. This can be too conservative an estimation, especially when the depassivation period is relatively short. A better way is to identify the service life of the structure with the time taken to cause surface cracking.[2.13,2.14] Cracking of the concrete cover represents a serviceability limit state. Using this to determine the remaining service life of a structure can however be hazardous as in certain local conditions reinforcement corrosion may not induce cover cracking until substantial loss of the bar diameter has already taken place and a potentially catastrophic failure could result. Serviceability states can therefore not be used on their own in predicting the remaining service life of a structure. The ultimate limit states also need to be checked, since often the strength of the structure can be significantly reduced even though the structure displays no visual signs of distress.

Andrade and Molina[2.15] did work on crack widths and the time to propagate the cracks and adapted this to be used with Tuutti's model. Their results indicate that at the appearance of the first visible cracks (i.e. the end of the service life) the bar diameter needs only to be reduced by 40 μm (for a cover/bar ratio of 3) which clearly represents an insignificant reduction in the tensile capacity of the bar (1,6% reduction in cross-sectional area for a 10 mm bar). Lopez et al.[2.16] consider a 10% loss in area as the critical level for damage in terms of structural safety. Therefore in this case the appearance of cracks only has serviceability significance and not ultimate limit state significance. Andrade and Molina[2.15] identified a reduction of bar diameter so as to cause a crack of 0,3-0,4 mm wide as the level at which the serviceability is affected and the end of the service life of the structure is reached. They found that for most cover to bar size ratios the first crack appeared when the bar diameter had been reduced by 2 percent. Using this Andrade and Molina[2.15] proposed a time to first crack as follows:

$$t_1 = \frac{(0,02).D}{Corrosion\ rate\ (mm/year)} \qquad (2.5.1)$$

Where: t_1 is the time to first crack
D is the bar diameter.

The time to enlarge the crack to a width of 0,3-0,4 mm is given by:

$$t_p = \frac{Loss\ of\ diameter}{Corrosion\ rate\ (mm/year)} \qquad (2.5.2)$$

where: t_p is the time to propagate the crack to a width of 0,3-0,4 mm and is taken as being equal to the service life of the structure.

The consideration of the propagation period (t_p) as part of the service life could be easily accepted in the case of corrosion induced by carbonation, in which a generalized attack is produced, and the bar cross-section loss is gradual and more or less uniform. However when the corrosion is induced by chlorides it can be too risky to apply the same principle, due to the localized attack which chlorides induce, since under such conditions higher local penetration rates can develop invalidating Andrade and Molina's equation (2.5.2).

2.6 Effect of corrosion of reinforcing steel on structural properties and performance

The following section is a review of the work done on laboratory-accelerated corroded specimens. In most instances the specimens were corroded by the galvanostatic method (see Chapter three for details). Some of the differences between accelerated corrosion and 'natural' corrosion are discussed in Chapter four.

2.6.1 Cover cracking due to accelerated corrosion of reinforcement in laboratory specimens

Andrade et al[2.15] investigated the evolution of cracks with respect to the loss in bar diameter in specimens that were corroded galvanostatically. They highlighted the implicit assumptions and weaknesses that are made when using galvanostatic corrosion and assuming uniform corrosion of the reinforcing bars: all the current is assumed to be spent in the dissolution of iron, no losses due to heat or other factors are considered and the dissolution of iron is only caused by the impressed current and is not occurring spontaneously. These factors emphasize the need to recognize that accelerated corrosion specimens may perform differently to those naturally corroded. Long term tests are therefore necessary to establish how different the two are.

The process of cracking is initiated when a passive reinforcing bar starts to corrode, a gradual decrease in its diameter (assuming generalized corrosion) is produced together with the generation of an oxide of a higher volume (2 to 3 times that of the parent metal). This increase in the volume is enough to induce the formation of cracks when the concrete's tensile strength is exceeded. The cracks are formed at the bar/concrete interface and then propagate radially until they reach the concrete surface.

The conversion of the corrosion rate or applied current to a loss in bar diameter was done using the equation derived from Faraday's equation :

$$D_t = D_o - (0{,}023).I_{corr}.t \qquad (2.6.1)$$

where D_t is the bar diameter (mm) at time t
I_{corr} is the corrosion intensity (μAmp/cm^2)
t is the time under impressed current (years)
0,023 is a conversion factor (μAmp/cm^2 to mm/year)

In all the specimens (16 mm bars with 20-30 mm cover) that they studied the first

visible cracks appeared at a reduction of about 40 μm of bar diameter. The evolution of cracks was as follows: a series of small discontinuous cracks forming that get wider and longer with time until they become one continuous crack. The final crack usually still displays its widest part in the region were the crack first appeared. It was also observed that the time until the first crack appeared was relatively fast and once the crack had appeared it widened relatively slowly. This is because when the crack reaches the surface the energy is liberated and the rate of extension of its width becomes a lot slower. The slowing of the crack growth is due to the fact that the corrosion products can now easily diffuse through the crack, no longer contributing as much to the cracking stress as is the case before the crack reached the surface. This provides an explanation for Misra and Uomota's[2.17] observation that almost all of the cracking was within the first 10 hours of the accelerated corrosion process.

Another significant result obtained is that the current density used to corrode the steel seems to have little effect as to when the first visible cracks appear. For a current density 10 times higher than another specimen, both displayed the first visible cracks at a reduction of about 40 μm of the bar diameter.

Andrade et al[2.15] also found experimentally and analytically using a numerical model that the cover/bar diameter ratio had very little influence on the time needed for the crack to appear at the concrete surface (for cover/bar diameter ratios of 1,25 and 1,875). The cover/bar diameter ratio does however have an influence on the probability of cracks occuring. Beeby[2.18] established that a ratio of less than 3 is needed in order to result in cracks. Above 6 the effect of increasing the ratio seems to have little effect on the likelihood of cracks forming.

2.6.2 Loss of compression zone

If compression reinforcement corrosion is allowed to proceed to such an extent that cracking and spalling causes a loss of the compression zone then it is obvious that there will be a corresponding decrease in the load carrying capacity of the element as the available internal resisting moment is reduced.

2.6.3 Loss of tension zone

Cracking and the loss of concrete in the tension zone by reinforcement corrosion-induced spalling reduces the section and therefore the section stiffness. The loss in cross-sectional area of the tension reinforcement will have a similar negative effect on the load carrying capacity of the section as that of reducing the compression zone of the member.

2.6.4 Loss of bond and its effects on deflection

Corrosion of reinforcing steel causes unsightly cracking and spalling as well as a reduction in the bond strength at the steel concrete interface.[2.19] The products of corrosion occupy up to three times the volume of the parent material causing a disruption of the bond strength at relatively low levels of corrosion. It has been reported[2.21] that the corrosion of only 5 μm of parent material is sufficient to cause a disruption of the concrete and consequently the bond strength.

The effect of reinforcement corrosion on the steel concrete bond was investigated by Cabrera and Ghoddoussi[2.19]. They performed pull-out tests on reinforcing bars embedded in 150 mm cubes as well as deflection tests on beams. The effect of corrosion was assessed by performing the tests on specimens with varying degrees of corrosion.

The results of the investigation into the effects on bond in the pull out tests revealed that bond strength increases with corrosion up to a maximum after which increasing corrosion causes a significant reduction of bond strength (see section 5.3 for the graph). It was found that at 12,6% corrosion (percentage mass loss) the bond strength had reduced to only 23,8% of the original bond strength. The initial increase in bond strength was attributed to the expansion which results from the precipitation of iron oxides which occupy a larger volume than the parent material and therefore increases the hoop-stress and radial compression so that the friction bond increases. With increasing amounts of corrosion, a layer of loose

material builds up between the steel and the concrete, facilitating relative longitudinal movement between them. At higher levels of corrosion the ribs of bars are destroyed, and loss of bond strength becomes substantial. The initial increase and then decrease in bond strength was confirmed by Tachibana et al[2.20]. They did not measure the corrosion mass loss but they found the point after which bond strength starts to decrease was between 3 and 6 days galvanostatic corrosion at a current density of 0,5 mAmp/cm^2.

A mathematical relation to describe the loss of bond, ignoring the initial effect of increasing bond strength, associated with the level of corrosion was found by regression analysis[2.20]:

(2.6.2)

$$f_b = 23{,}478-(1{,}313).C$$

Where: f_b = Bond strength [MPa]
C = Corrosion % [percentage mass loss]

The effects of corrosion on the deflection of the beams, one of the most important effects from a serviceability point of view, were obtained by Tachibana et al[2.20]. It was found that at increasing levels of corrosion the midspan deflection of beams increased under service load. The effect on the deflection was expressed as a ratio of the deflection of the corroded beam divided by the deflection of the uncorroded beams loaded to the service load. By linear regression the following relationship was found;

(2.6.3)

$$D_r = 1{,}002+(0{,}05).C$$

Where D_r is the deflection ratio (corroded/uncorroded)
C is the corrosion % (percentage mass loss)

2.6.5 Effect of corrosion on load carrying capacity of reinforced concrete beams

Misra and Uomoto[2.17] recognized the need to try and quantify the implications of steel corrosion on the load carrying capacity of reinforced concrete beams. They performed loading tests on corroded beams with and without stirrups. Both types of corroded beams showed very much more brittle failure after showing an increased central deflection relative to the uncorroded beams.

The effect of corrosion on the load carrying capacity of the beams was found to be largely dependant on the shear span to section depth (a/d) ratio. For beams corroded to the same extent it was found that the load carrying capacity was reduced by 33% when the a/d ratio was 1,6 while for an a/d ratio of 2,5 the reduction in load carrying capacity was only 17 %. Work by other authors[2.19,2.21,2.22] supports this trend of increasing amounts of reduction in the load carrying capacity of beams which have lower shear span to depth ratios. From this trend it can be concluded that reinforcement corrosion has a greater effect on the shear capacities of beams than their flexural capacities.

Misra and Uomoto's[2.17] results also indicated that at a corrosion mass loss of 3-5 % (which is sufficient to cause a reduction of 22% in the load carrying capacity of the beams) the tensile strength of the reinforcing bars was only about 5% less than for uncorroded bars. This result suggests that steel corrosion is more likely to affect the load carrying capacity in other ways than by reduced bar cross-section that could cause a tension failure. The appreciable reduction in the load carrying capacity of the beams on account of the reinforcement corrosion therefore cannot be explained by the reduction in tensile strength of the bars alone. A disruption of the compression zone by corrosion cracking results in a smaller compression zone. A smaller compression zone means that the beam has a smaller internal resistance capacity and this translates into a lower load carrying capacity.

Cabrera and Ghoddoussi[2.19] also found that with increasing amounts of corrosion, the load carrying capacity of the beams increased up to a point. The tied-arch phenomenon experienced in uncorroded beams can be used to explain this behaviour. Kani[2.23] found that beams with poor bond had a higher load carrying

capacity than the ones with better bond. It has already been shown above that corrosion reduces the bond strength in beams. Kani's tied arch theory can therefore be applied to corroded beams to provide an explanation for the initial increase in the load carrying capacity. Tachibana et al [2.20] have also suggested that the corroded specimens acted as a tied arch. **Figure 2.6.1** is a diagramatic representation of Kani's tied arch.

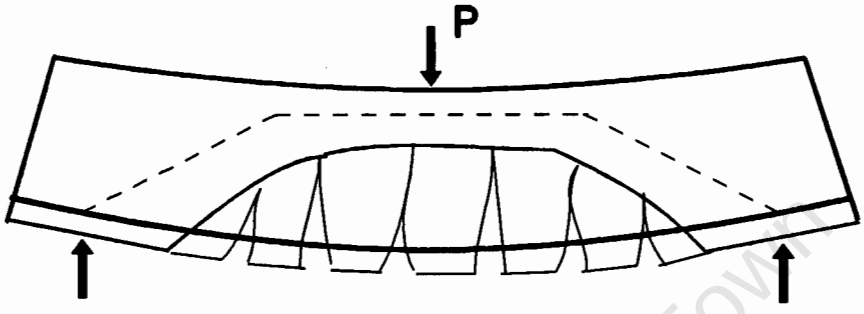

Figure 2.6.1 Diagramatic representation of remaining arch[2.23]

An important point to note is that the galvanostatic corrosion, in all the above cases, was carried out while no load was applied to the beams, which is quite different from the corrosion in actual structures. The relatively short period that was involved in the corrosion process also makes no allowance for possible time related effects (similar to creep) that corrosion may have on the load carrying capacity of reinforced concrete beams. These differences may be sufficient to cause a totally different behaviour to the behaviour of naturally corroded elements.

2.6.6 Loss of member ductility

It was show in section 2.2.2 that ductility increases with increasing amounts of confinement of the concrete in the compression zone. The products of corrosion cause cracking and spalling, reducing the confinement to the compression zone and thus reducing the ductility of the element. This problem is further aggravated by the fact that using a larger bar diameter increases spalling as well as decreasing the ductility as a greater percentage steel is used.

2.6.7 Loss of puching shear strength

Tachibana et al[2.21] found that reinforced concrete slabs damaged by reinforcement corrosion had a reduced punching shear strength. They explained this reduction in the punching shear strength as follows : orthogonally reinforced concrete slabs cause horizontal cleavage planes at the level between the two layers of steel when corroded. These horizontal cleavage planes reduce the influence of dowel action on the punching shear strength of the slab. In sound uncorroded concrete tensile stress is introduced into the concrete by the dowel action of the reinforcement thus generating cracks and horizontal cleavage planes. However in the case of corroded reinforced concrete slabs there already exists a horizontal cleavage plane generated by the swelling of the corrosion products. The dowel action therefore becomes ineffective and is no longer able to contribute to the load carrying capacity. The generation of a horizontal cleavage plane is seen as the turning point where the mechanical behaviour of the slab is changed and is therefore the point where the shear strength is reduced.

If the horizontal spacing between bars in beams is less than twice the cover, horizontal cleavage planes are likely to result.[2.21] The presence of cleavage planes is likely to cause a reduced shear capacity in reinforced concrete beams as was found to be the case in orthogonally reinforced slabs. The reduced load carrying capacity at small shear span to depth ratios found by Misra and Uomoto[2.17] could be a similar type of failure as the low shear span to depth ratio approximates the conditions normally associated with punching shear failure.

2.7 Closure

The corrosion of reinforcing steel has significant effects on the performance of reinforced concrete. Corrosion results in cracking of the concrete between the steel and the surface, a reduction in the load carrying capacity, a loss of bond and shear strength. Each effect has been reviewed here independently. Knowledge of these general trends in isolation is essential if the behaviour of corrosion affected reinforced concrete beams under more than one influence is to be understood.

2.8 References

2.1) Blume, J.A., Newmark, N.M. and Corning, L.H., *Design of Multistorey Reinforced Concrete Buildings for Earthquake Motions*, Skokie, Illinois : Portland Cement Association, 1961, pp. 92-113.

2.2) Rankine, R.G.D., *Appropriate Properties for a New Corrosion Resisting Reinforcing Steel,* MSc dissertation, University of the Witwatersrand, Johannesburg, 1990.

2.3) ACI Committe 363, State-of-the-art report on high strength concrete, ACI 363R-84, *American Concrete Institute*, Detroit, 1984, pp. 48.

2.4) Sung-woo Shin, Satyendra K Ghosh and Moreno, J., Flexural ductility of ultra-high strength concrete members, *ACI Structural Journal*, 86-S35, July-August 1989, pp. 394-400.

2.5) Rehm, G., *The Basic Principles of the Bond Between Steel and Concrete,* Berlin : Wilhelm Ernst & Sohn, Cement and Concrete Association, No 134, 1961.

2.6) Marshall, A.L., *Marine Concrete*, London : Blackie, 1990, pp. 291-301.

2.7) Brown, R.D., Geoghegan, M.P. and Baker, A.F., *Corrosion of Reinforcement in Concrete Construction*, London : A.P. Crane, 1983, ch. 13.

2.8) CEB Bulletin No 162, *Assessment of Concrete Structures and Design Procedures for Upgrading*, August 1983.

2.9) Mays, G.(Ed), *Durability of Concrete Structures : Investigation, Repair & Protection*, London : E & FN Spon, 1992.

2.10) Tuutti, K., Service life of structures with regard to reinforcement corrosion of embedded steel, SP65-13, *Performance of Concrete in the Marine Environment*, Detroit : ACI, 1980.

2.11) Andrade, C., Alonso, C. and Gonzalez, J.A., Approach to the calculation of the residual life in corroding concrete reinforcements based on corrosion intensity values, *9th European Congress on Corrosion,* Utrecht, The Netherlands, October 1989.

2.12) Funhashi, M., Predicting corrosion free service life of a concrete structure in a chloride environment, *ACI Materials Journal*, Nov-Dec 1990, pp. 581-588.

2.13) Sygula, S. and Riz, K., Longitudinal cracking and its relation to service life of reinforced concrete bridges, *Proc. of ACI-RILEM International Symposium on Long Term Observation of Concrete Structures*, Budapest, 1984, pp. 182-192.

2.14) Braun, K., Prediction and Evaluation of Durability of Reinforced concrete element and structures, *Proc. 4th Conf. on Durability of Building Materials and Components*, Singapore, 1987, pp. 383-388.

2.15) Andrade, C. and Molina, F.J., Cover cracking as a function of bar corrosion: Part I-experimental tests, *Materials and Structures*, No 26, 1993, pp. 453-464.

2.16) Lopez, W., Gonzalez, J.A. and Andrade, C., Influence of temperature on service life of rebars, *Cement and Concrete Research*, Vol 23, No 2, 1993, pp. 1130-1140.

2.17) Misra, S. and Uomoto, T., Effect of corrosion of reinforcement on the load carrying capacity of reinforced concrete beams, *Proc. of Japanese Conc. Inst.*, Vol 9, No 2, 1987, pp. 675-680.

2.18) Beeby, A.W., Corrosion of reinforcing steel in concrete and its relation to cracking, *The Structural Engineer*, No 3,Vol 56A, March 1978, pp. 77-81.

2.19) Cabrera, J.G. and Ghoddoussi, P., The effect of reinforcement corrosion on the strength of the steel/concrete bond, *Proceedings of the Conference on Bond in Concrete*, Latvia, CEB, October 1992, pp. 11-24.

2.20) Tachibana, Y., Kajikawa, Y. and Kawamura, M., The mechanical behaviour of RC beams damaged by corrosion of reinforcement, *Concrete library of Japanese Society of Civil Engineers No 14*, March 1990.

2.21) Tachibana, Y., Kajikawa, Y. and Kawamura, M., Behaviour and punching strength of RC slabs damaged by corrosion of reinforcement, *Concrete Library of Japanese Society of Civil Engineers,* No. 18, December 1991.

2.22) Al-Sulaimani, G.J., Kaleemullah, M., Basunbul, I.A., and Rasheeduzzafar, Influence of corrosion and cracking on bond behaviour and strength of reinforced concrete members, *ACI Structural Journal*, March-April 1990, pp. 220-231.

2.23) Kani, G.N.J., The riddle of shear failure and its solution., *Journal of the American Concrete Institute*, Vol 61, pp. 441-447, April 1964.

Chapter Three

Experimental investigation of the effects of reinforcement corrosion on the structural performance of reinforced concrete beams - series one

3.0 Introduction

For this project flexural tests were conducted on simply supported beams which had varying degrees of corrosion. The beams were subjected to a concentrated static load at midspan. If this loading is inverted, it closely approximates the portion of a beam between an internal support of a continuous beam and the adjacent point of contraflexure. The results can therefore be used to asses the ductility of the beams if hinges were to form over a support in a continuous beam. The beams were designed to fail in flexure by providing adequate shear reinforcement and anchorage, taking account of the added loss that corrosion would cause for a shear or bond failure to occur. Two series of tests were conducted. The work done on the series one beams, which were corroded electrostatically using an impressed current, is presented in this chapter. The series two beams, which were corroded by subjecting them to alternate wetting and drying cycles with saline water and then using an impressed current on some of the specimens, is presented in Chapter four.

3.1 Test set-up

The test method adopted was similar to that used by other investigators[3.1,3.2]. The beams were supported on half round bearers, the round part facing down and

bearing on a steel plate. This allowed free rotation without the effects of a knife edge cutting into the concrete at the support. At midspan the beams were loaded by means of a hydraulic jack which had its own ball swivel joint to allow for any out of plane loading by the jack. A 5x155x155 mm steel loading plate was used between the load cell and the beam. This spread the load sufficiently to prevent local crushing of the concrete, which would be the case if a knife edge load point was used, while still approximating a concentrated load at midspan.(see **Figure 3.1.1** and **Photograph 1** on page 51.)

The load and the deflections were recorded by means of a data acquisition facility with a load cell recording the applied load and Linear Variable Displacement Transducers (LVDT) the deflections. Deflections were measured at the following locations using LVDTs : at midspan on either side of the beam and at the supports. The midspan deflection was measured on each side of the beam to be a able to measure the amount that the beam twisted by (if at all). The support LVDT was used to measure any support settlement. In addition to these a 50 mm dial gauge was used on the one side of the load cell at midspan and a 100 mm plunger on the other side at midspan. The dial gauge was used as a precautionary measure in case the LVDTs did not record any deflections. The 100 mm plunger was used to record the deflections after the LVDTs and the 50 mm dial gauge had run out of travel.

The load cell was calibrated by applying incremental loads from 0 to 100 kN by means of an Amsler cube crushing machine. The linear range of the LVDTs was established by applying increments of 0,25 mm to the LVDTs by means of a screw micrometer and a clamping bracket to hold the LVDT and the micrometer. The LVDTs were then also calibrated in the same way. Linear regression of the data yielded slope constants of the straight lines for the load cell and the LVDTs in terms of (computer) bits as given by the data acquisition facility. The zero points in terms of bits was then recorded before each beam test was started. These zero points together with the slope constants obtained in the calibration procedure gave a linear expression that could be applied to the data (bits) recorded during the test to convert the data into loads in kN and deflections in mm.

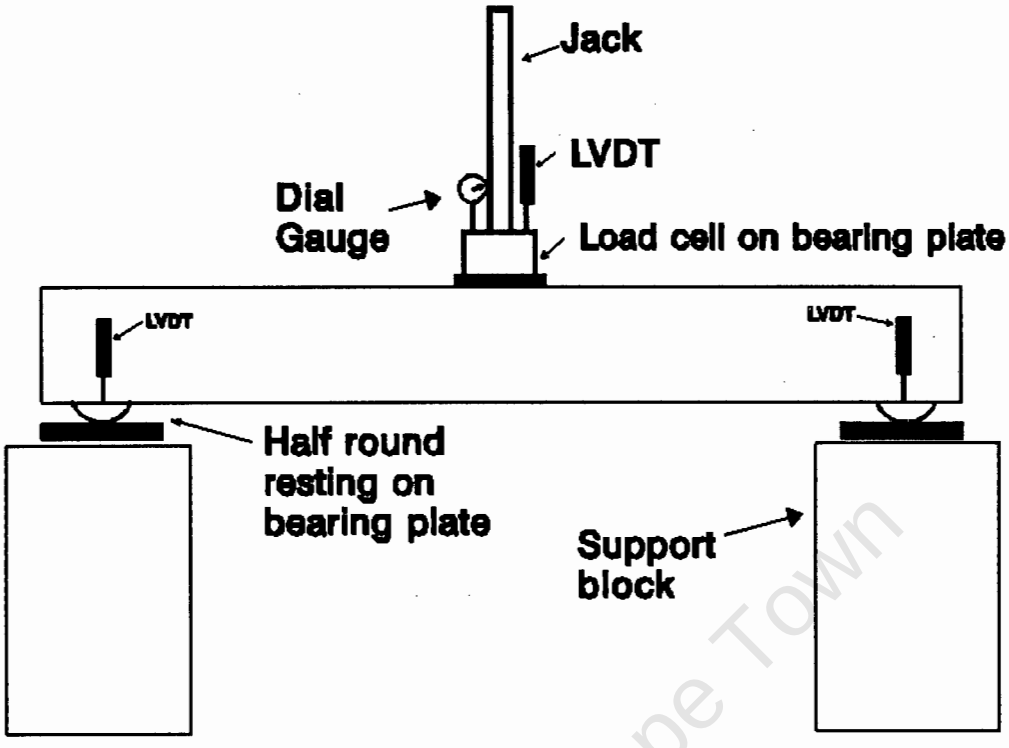

Figure 3.1.1 Schematic representation of test set-up.

Before testing, each beam was loaded to 2 kN to allow the supports and the load plate to bed-in. The beams were then unloaded and all recording instruments were zeroed. The load was applied at a rate of approximately 2 kN per minute. The data acquisition device was set up to record the load and the deflections every 1 second. The readings on the dial gauge and the plunger were recorded every 2 kN in the elastic range. Once the plastic range was reached, the readings were taken every 30 seconds. Each beam took approximately 25 minutes to load until its load carrying capacity started to decrease substantially or the jack reached the end of its travel (approximately 100 mm).

3.2 Series one results

Series one beams were corroded galvanostatically by impressing a current through the beams for a specified time period (see Table 3.2.3) as illustrated in **Figure 3.2.1** (see also **Photograph 2** on page 51). The electrolyte used was a 5 % sodium

chloride solution. The beams were soaked in the solution for 24 hours before connecting the current source. The voltage applied by the current source was adjusted to deliver the currents given in Table 3.2.3. After disconnecting the current source the beams were allowed to air dry for 5 days and then immediately tested. The current was delivered to the reinforcing bars by 2 mm^2 copper wire which was fixed to both ends of the reinforcing bars by means of insulation tape. The insulation tape was then sealed off with epoxy resin. The wires were marked with the top bars being A and B and the bottom bars C and D. A 2x30x1800 mm mild steel flat was used as the cathode

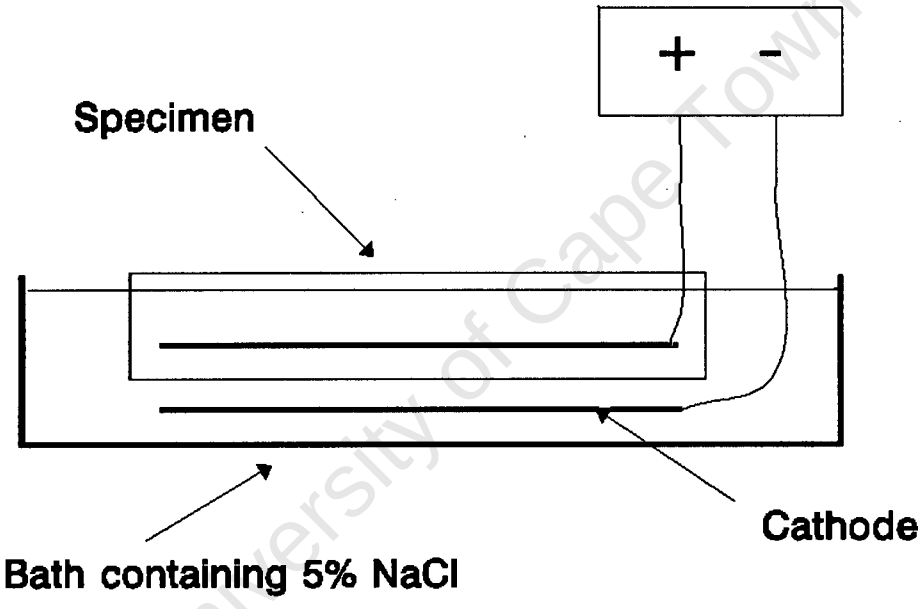

Figure 3.2.1 Schematic representation of galvanostatic corrosion set-up.

The beams were 155x220x2200 mm long reinforced with two ribbed high tensile Y10 bars in both the tension and compression zones. The beams were designed and manufactured in such a way that no shear steel (or supporting steel for the top steel) was required. The beams were designed to have a flexural capacity greater than the shear and bond strength capacities thus ensuring a flexural (bending failure) would dominate. The side, top and bottom cover to the steel was 20 mm. The proportions used in the mix (per m^3) are given in **Table 3.2.1.**

Photograph 1 Test set-up

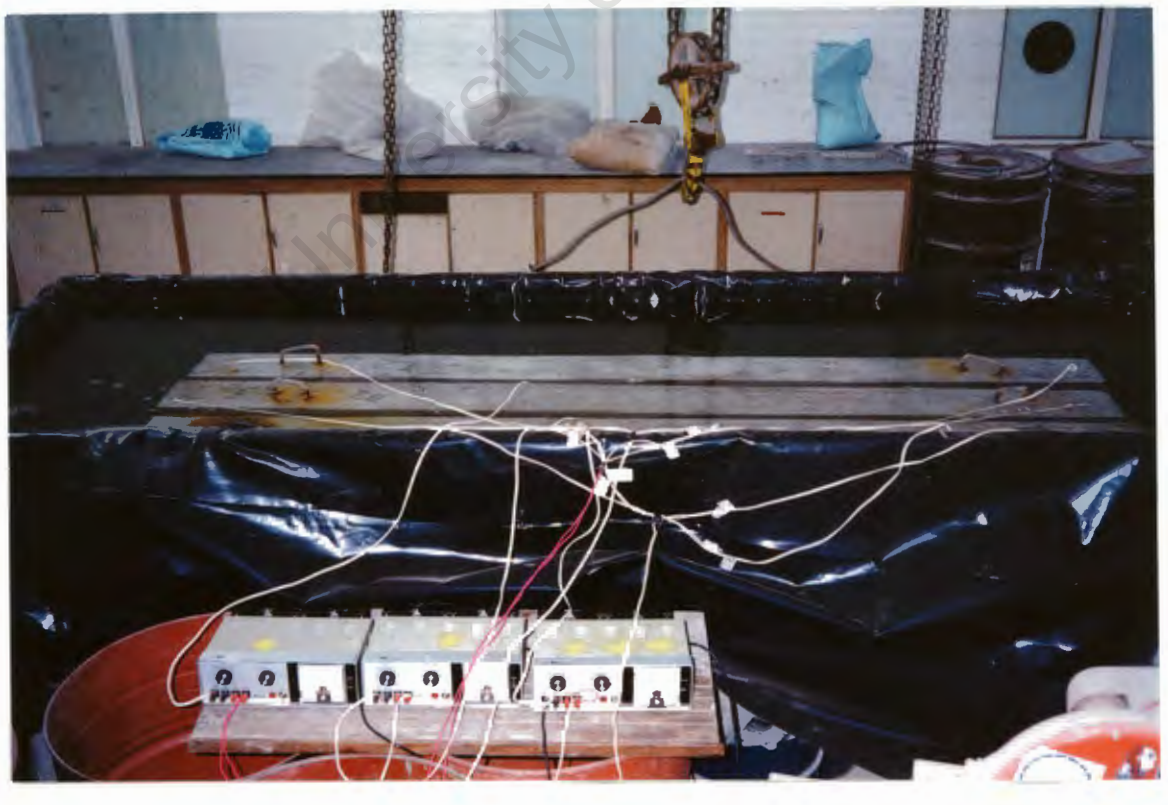

Photograph 2 The galvanic corrosion set-up

Table 3.2.1 Concrete mix proportions per m^3 used in series one beams.

Water	190 l
Ordinary portland cement	317 kg
Cape Flats dune sand	785 kg
19 mm Greywacke stone	1000 kg
Water/cement ratio	0,6

The specimens that were cast are given in **Table 3.2.2.** The following abbreviations are used in the table : C-Control specimen, T-Top steel corrosion only, B-Bottom steel corrosion only, TB-Top and bottom steel corrosion specimen.

Table 3.2.2 Series one specimens.

Control beams (no corrosion)	Corrosion extent 1	Corrosion extent 2
C1	T1	T2
C2	B1	B2
	TB1	TB2

A corrosion current density of 0,38 mA/cm^2 was used, the current and the time period used is summarized in **Table 3.2.3.**

Table 3.2.3 Summary of corrosion currents and times.

Corrosion extent 1	Current Time	Corrosion extent 2	Current Time
B1	,5A 7 Days	B2	,5A 14 Days
T1	,5A 7 Days	T2	,5A 14 Days
TB1	1A 7 Days	TB2	1A 14 Days

The specimens were cast in two batches :

Batch 1 : beams T1,T2,B1 and B2 and cubes 1/1, 1/2, 1/3, 1/4,1/5, 1/6, 1/7, 1/8 and 1/9.

Batch 2 : beams TB1,TB2,C1 and C2 and cubes 2/1, 2/2, 2/3, 2/4, 2/5, 2/6, 2/7, 2/8 and 2/9.

The 28 day cube strengths are given in **Table 3.2.4** and the cube strengths at the time of the beam tests (86 days) are given in **Table 3.2.5.** Both sets of cubes and the all beams were cured by wrapping them in plastic. All the beams were treated the same way so that comparisons could be made between the control beams and the corroded ones.

Table 3.2.4 28 day cube strengths.

Batch 1	MPa	Batch 2	MPa
1/1	30,9	2/1	33,7
1/2	31,4	2/2	32,9
1/3	32,3	2/3	30,1
1/4	30,0	2/4	30,8
Average	31,2	Average	31,8

Table 3.2.5 Cube strengths at time of beam tests.

Batch 1	MPa	Batch 2	MPa
1/5	35,2	2/5	37,3
1/6	36,5	2/6	37,8
1/7	36,7	2/7	36,2
1/8	37,1	2/8	33,0
1/9	37,1	2/9	33,5
Average	36,5	Average	35,6

Chloride concentrations at the depth of the bottom steel at time of beam tests are given in **Table 3.2.6.** The chloride concentrations by mass of cement were measured by means of a silver/silver nitrate titration. The 0,06 % given for the control specimens reflect the inherent salt content of the mix materials. (See section 3.3 for a discussion of the results)

Table 3.2.6 Chloride concentrations by mass of cement at the depth of the bottom steel.

Beams	% Cl^-
C1 C2	0,06
T1 B1 TB1	4,23
T2 B2 TB2	4,25

3.2.1 Classifying corrosion extent

The classification of corroded elements into meaningful categories is extremely difficult since under differing conditions, the same 'amount' of corrosion will present itself as a different amount of distress. The same 'amount' of corrosion is also likely to present itself differently in different elements. The following factors will have an influence on the amount of distress displayed by any element:

Material ductility[3.1]-The greater the material ductility the greater will be the expansive forces due to corrosion that the material will be able to absorb before cracks develop. Concrete material ductility decreases with increasing concrete strength, therefore high strength concretes will display cracks at lower amounts of corrosion.

Cover/bar diameter ratio[3.3]-With ratios greater than 6 the likelihood of cracks forming is small, while a ratio smaller than 3 usually leads to spalling.

Environmental influences[3.4]-Depending on the environmental conditions different corrosion products may form. Each corrosion product has a different relative volume. Therefore depending on what corrosion products form different amounts of cracking or distress may be displayed. The relative volumes of corrosion products are as follows[3.4] :

Fe	1,0
FeO	1,8
Fe_3O_4	2,1

Fe_2O_3	2,2
$Fe(OH)_2$	3,6
$Fe(OH)_3$	4,2
$Fe(OH)_3.3H_2O$	6,4

In this investigation two types of classification were used; classifying the deterioration visually, and secondly quantitatively. Both of these can be applied either to the concrete or to the reinforcing bars.

Classification of the concrete appearance

1) Corrosion crack pattern, crack size and continuity

Corrosion cracks form along the length of reinforcing bars. Cracks tend to start from the sites of the rust sources and spread out along the length of the reinforcing bar. Several cracks therefore begin simultaneously and eventually link up to form one continuous crack at higher extents of corrosion. The total length of the crack and how continuous the crack is can therefore be used to classify corroded specimens into common groups. This method is obviously greatly influenced by any local variations in concrete quality and the position of the crack relative to the corner edge of the specimen. The method can only therefore be used on specimens of the same concrete quality, same cover to bar diameter ratio and the same reinforcing pattern. **Table 3.2.7** classifies the various specimens according to crack length, size and continuity. Limits of total crack length and width are also given. The crack length given in the table is sum of all the longitudinal crack lengths for any particular bar in the beam.

2) General structural condition classification

The following classification system (**Table 3.2.8**) is used by the South African Department of Transport for bridge inspections.[3.5] This method of classification is only really useful for the broad categorization of structures (not individual elements). It is useful for structures that show great variations in distress, but its lack of detail makes it inappropriate for structures where a detailed classification needs to be made to determine the structural integrity. It is also not correctly

ordered in its descriptions of the various categories e.g. allowing for spalling before moderate rust stains are present.

Table 3.2.7 Classification according to crack appearance.

Specimen	Crack location, Crack width and length. Extent of rust staining.
C1 C2	No corrosion cracks. No rust staining.
T1 B1 TB1	40% < Crack length < 80% of bar length. Crack not continuous. Average crack width 0,24 mm. Rust stain sources limited, spaced > 150 mm apart.
T2 B2 TB2	Crack length > 90% of bar length. Crack is continuous. Average crack width 0,29 mm. Rust stain sources more frequent, spaced <100 mm apart. Rust stain sources tend to spread out along the crack length, although staining between the original sources is still limited.

Table 3.2.8 DOT classification system[3.5].

	Rating	Description
9	Excellent	New condition
8	Very Good	Minor shrinkage or temperature cracks
7	Good	Non-structural cracks, light spalling, no rust stains through cracks
6	Satisfactory	More significant non-structural cracks, moderate spalling, no rust stains visible
5	Fair	Some section loss due to spalling, structural cracks with light rust staining
4	Marginal	More general section loss due to deterioration, spalling, structural cracks with moderate rust staining visible
3	Poor	Advanced deterioration, spalling exposing reinforcing steel, structural cracks with severe rust staining
2	Very poor	Significant structural cracks, rebar exposed & rusted
1	Critical	Study required to repair or replace
0	Beyond repair	Replace only option

Table 3.2.9 Categorization of series one beams according to the DOT system.

Beam	Description	Category number
C1 C2	New condition. No rust stains. No cracks. No signs of distress.	9
T1 B1 TB1	Light rust staining. Small cracks. No spalling.	5
T2 B2 TB2	Moderate to heavy rust stains. Moderate cracks. No spalling.	4 or 3 ?

Classification of the test specimens in this investigation demonstrated the inappropriateness of this system for detailed categorization. Specimens of both extents of corrosion displayed the following characteristics : Severe rust staining, minor non-structural cracks, no shrinkage cracks or exposed steel. The specimens cannot be confidently placed into any one category. **Table 3.2.9** shows the category into which each beam falls.

It should however be noted that the specimens under consideration have been corroded under accelerated conditions. In practice, corrosion would be over a much longer time period allowing for flushing and removal of rust stains etc.

Classification of the reinforcing appearance and properties

1) Visual classification of reinforcement appearance

The visual classification of corroded reinforcing bars is very subjective. Often bars that appear more severely corroded than others upon initial inspection appear similar to each other once the rust products have been removed. The local conditions surrounding the bar therefore have an effect on the type of corrosion formed and consequently the classification of the reinforcing bar. Examination of the bars upon removal from the concrete (before cleaning) aids the classification process as it is easier to identify corroded and uncorroded areas, firstly by the rust staining and secondly by the fact that the rust products occupy a much greater volume thus amplifying the location of corrosion pits etc. **Table 3.2.10** classifies the visual appearance of the bars, suggesting limits for the amount of corroded

area, the size, location and spacing of corrosion pits. Corrosion products were only found on the outside 270° of the circumference of reinforcing bars in the specimens (see **Figure 3.2.2**). As the corrosion increased so the corrosion products spread around the bar perimeter.

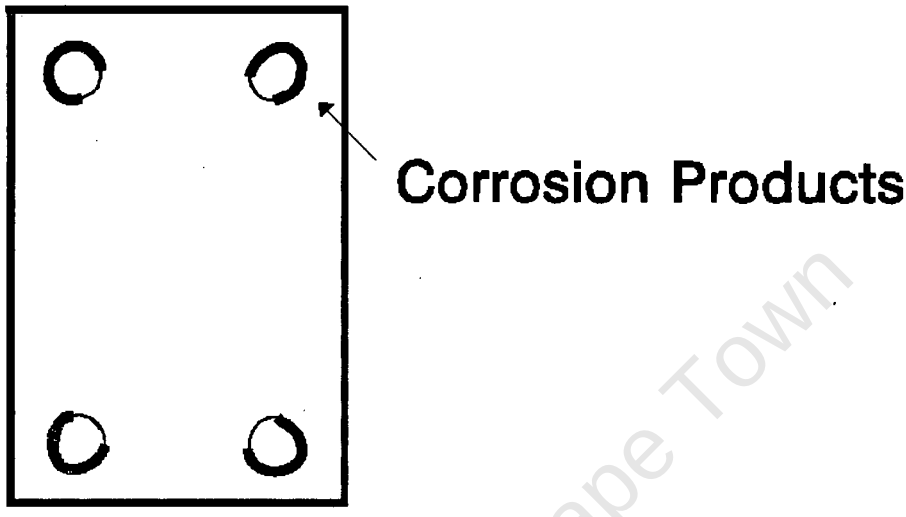

Figure 3.2.2 Location of corrosion products around bar perimeters.

Table 3.2.10 Classification of bar condition.

Specimen	Description of bar corrosion condition
C1 C2	Dull grey colour along entire length of bars and around the entire circumference of bar. No rust stains or pits.
T1 B1 TB1	Dull grey colour only along the inside 90^0 of the bars circumference. Grey area (uncorroded area) extends > 80% of bar length and is generally continuous. Pits < 10 mm long spaced > 50 mm apart. Pit depth < 0,5 mm. Pits distributed evenly around entire circumference of bar.
T2 B2 TB2	Dull grey areas only along inside 90^0 of the bars circumference. Grey area (uncorroded area) extends < 40% of bar length and is not continuous. Pits <30 mm long spaced 15-20 mm apart. Pit depth <1 mm. Pits distributed evenly around entire circumference of bar.

2) Percentage mass loss due to corrosion (see section 3.3 for discussion of results)
The percentage mass loss of the steel in column 2 of **Table 3.2.11** is calculated using **Equation 3.2.1** derived from Faraday's formula.[3.6] This is essentially a

laboratory technique although it could be used in the field if the corrosion current can be measured.

$$W_t = \frac{W_a.I.t}{Z.F} \qquad (3.2.1)$$

Where W_t is the estimated weight loss [g]
W_a is the atomic weight [g] (for steel 56 g)
F is Faraday's constant [Amp.seconds](96500 Amp.seconds)
Z is the metal valency (for steel 2)
I is the corrosion current [Amps]
t is the time under corrosion current. [seconds]

The percentage mass loss can then simply be calculated using **Equation 3.2.2**. The average total mass of bars for each specimen was used in the calculation of the values in the table.

$$\%Mass\ loss = \frac{W_t}{total\ mass\ of\ rebar}.(100) \qquad (3.2.2)$$

3) Percentage loss of bar diameter

This can either be physically measured or can be estimated using a formula derived from Faraday's equation. Measuring the diameter loss is not considered an accurate method at low amounts of corrosion where pitting and irregular bar ribs in the case of high yield steel make it difficult to measure. Physically measuring the diameter loss in the field can be done but this requires the removal of the rust products from the bars. The corrosion rate estimated according to Faraday's

equation is given by **Equation 3.2.3.**[3.6]

$$Corrosion\ rate = \frac{W_a \cdot I}{2(A.F.\rho_s)} \qquad (3.2.3)$$

Where The corrosion rate is the loss of
parent metal [cm of bar diameter/second]
W_a is the molecular weight of iron [g/mol] (55,85)
I is the corrosion current [amps]
F is Faraday's constant [96500 Amp.seconds]
A is the surface area of steel [cm^2]
ρ_s is the density of steel. [7,85 g/cm^2]

From this the percentage reduction in the diameter can be calculated using **Equation 3.2.4.**

$$\%reduction\ of\ diam = \left(\frac{2(corr\ rate.t)}{D_0}\right).100 \qquad (3.2.4)$$

Where D_0 is the original bar diameter
t is the time under the corrosion current.
(The 2 is to account for the reduction in the bar diameter from both sides.)

4) Percentage loss of tensile strength

Any loss in the cross-sectional area of the reinforcing bar will have a reducing effect on the tensile strength (rupture strength) of the bar. Changes in the tensile strength are easy to measure in a tension test and can be performed on real structures by taking a sample of the exposed steel. The percentage loss in tensile strength is then given by **Equation 3.2.5.** The average value of 16 bars was used for both f_t and f_{corr} in the calculations. The value used for f_t was 54,2 kN. The standard deviations for the tensile values were all below 1,24 kN.

$$\% \ Loss \ of \ f_t = \left(\frac{f_t - f_{corr}}{f_t}\right).100 \qquad (3.2.5)$$

Where f_t is the tensile strength for a particular bar size and type

f_{corr} is the tensile strength of the corroded bar.

Table 3.2.11 is a summary of the various percentage losses that were described above. The second and fourth columns are theoretical (predictive) while the third and fifth columns are measured percentage losses.

Table 3.2.11 Summary of percentage losses.

Specimen	% Mass loss (Faraday)	% Mass loss (Gravimetric)	% Diameter loss (Faraday)	% Tensile loss (measured)
C1 C2	0,00	0,00	0,00	0,00
T1 B1 TB1	3,56	-1,38 (mass gain)	1,61	5,55
T2 B2 TB2	7,11	1,85	3,23	12,47

3.2.2 Effects of corrosion on structural properties

The load-deflection graphs for each beam are given in **Appendix 1**. Various results were extracted from the graphs and have been summarized in this section. **Table 3.2.12** gives a description of the type of failure observed for each beam in series one (see also **Photographs 3-8** on pp.63). A failure described as a normal stepped flexural failure is a failure where deflections tend to occur in steps rather than gradually increasing. The smooth flexural failure mode observed in the corroded beams showed fewer large steps. **Table 3.2.13** gives the yield load, the maximum load carried by the beam and the deflections corresponding to these load points. The maximum load and deflection for beam C1 are the last values that were recorded before the instruments failed. See **Figure 3.2.3** for the location of these points. The failure load was taken as the point where the graph makes a sudden,

sharp downward turn and continues down. In most cases the load-deflection graphs display an initial vertical portion with no deflection being recorded until loaded to approximately 5 kN. The minimal deflection recorded here is because the beams were first pre-loaded and then unloaded to allow them to 'bed-in' before the actual test was started. Inaccuracies are also introduced when the linear regression lines derived in the calibration of the recording equipment are applied to the zero points for each beam that is tested.

Table 3.2.12 Type of failure observed in each beam in series one

Beam	Description of failure type
C1	Normal stepped flexural failure. Recordings stopped prematurely as dial gauge and LVDTs ran out of travel.
C2	Normal stepped flexural failure. Steps in graph suggest bond failure but no striations in concrete surrounding the steel could be found.
T1	Smooth flexural failure. Striations in concrete surrounding the steel indicate bond failure. Wide flexural cracks (up to 4 mm) led to chunks of concrete falling out resulting in the formation of shear cracks. Concrete crushing in the compression zone very limited.
B1	Normal flexural failure. Bending opened up the longitudinal corrosion cracks to 6 mm. Combination of corrosion cracks and flexural cracks caused large chunks of concrete to fall out in the tension zone.
TB1	Bond failure in left hand side of beam caused opening up of corrosion cracks only on this side of the beam. The graph however suggests normal flexural failure.
T2	Smooth flexural failure. Normal amount of concrete crushing in compression zone.
B2	Smooth flexural failure. Excessive widening of corrosion cracks (up to 12 mm). Large chunks of concrete fell out of tension zone.
TB2	Smooth flexural failure. Excessive widening of corrosion cracks (up to 9 mm). Large chunks of concrete fell out of tension zone.

Photograph 3 Beam T1

Photograph 4 Beam B1

Photograph 5 Beam TB1

Photograph 6 Beam T2

Photograph 7 Beam B2

Photograph 8 Beam TB2

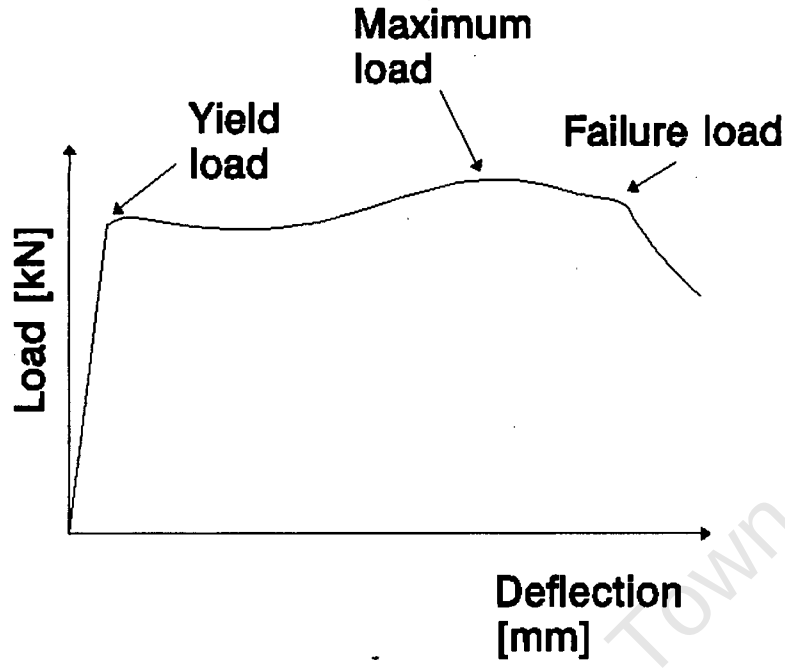

Figure 3.2.3 Generalized load-deflection graph.

Table 3.2.13 Summary of yield and maximum loads and deflections for series one.

Beam	P_y (kN)	Δ_{Py} (mm)	P_{max} (kN)	Δ_{Pmax} (mm)
C1	38,0	5,64	(41,0)	(34,5)
C2	34,0	8,33	39,1	37,0
T1	40,0	7,78	43,3	29,4
B1	36,0	6,29	39,1	27,0
TB1	36,0	6,10	40,8	30,5
T2	42,0	6,14	44,6	48,0
B2	36,0	5,49	40,0	16,5
TB2	36,0	6,65	39,7	24,3

Table 3.2.14 gives the work done to deflect the beam up to the maximum load P_{max}. The work done is calculated from the integral of the load-deflection graph up to the deflection corresponding to the maximum load. The ductility ψ_{Pmax} is the ratio of the deflection at the maximum load to the deflection at the yield load. A graphic method was also used to quantify the ductility $\psi_{graphic}$. This gives

essentially the same ratio as that given by ψ_{Pmax} and was used as a check for those beams where more than one possible maximum load peaks could be identified. It is the ratio of the deflection up to the maximum load to the deflection given by the intersection of a line drawn equal to the mean slope of the load-deflection curve, passing through the maximum load point and the line equal to the mean slope of the curve before yield. **Figure 3.2.4** shows the construction necessary to obtain $\psi_{graphic}$.

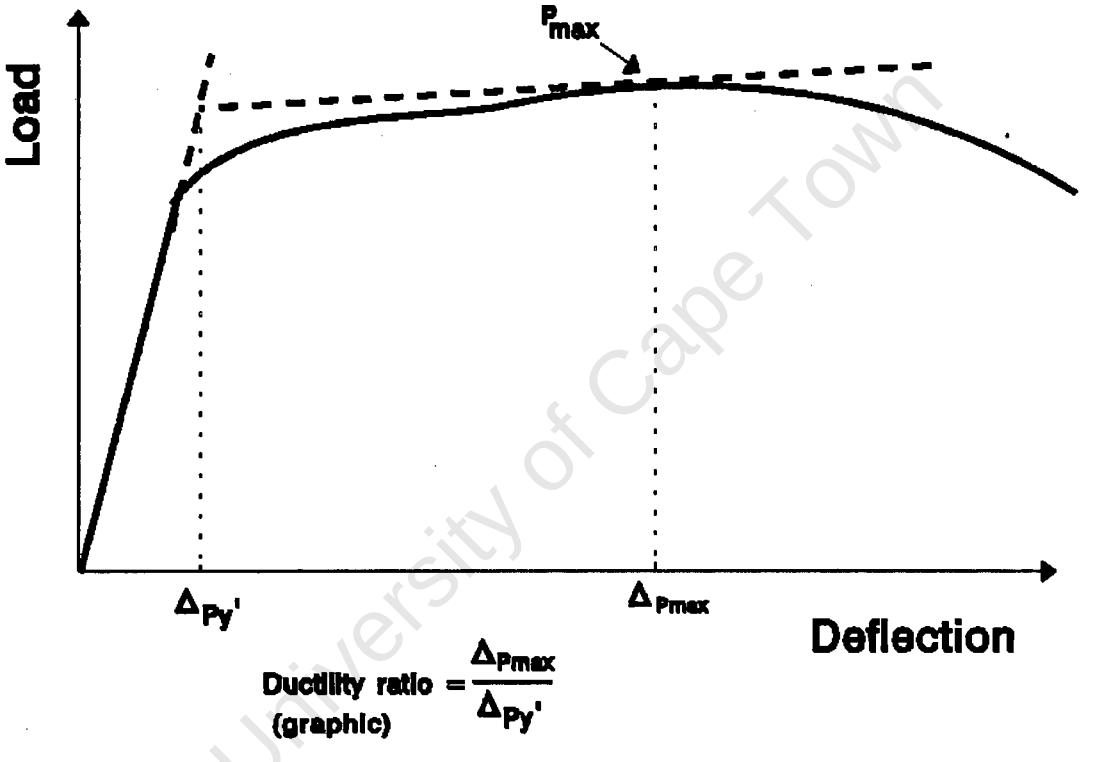

Figure 3.2.4 Derivation of $\psi_{graphic}$

Table 3.2.15 gives the load ratios for P_{max} and P_{yield} and the deflection ratios corresponding to P_{max}. The deflection ratio (column 4) is the ratio of the deflection of the corroded beams at maximum load to the average deflection at that load in the control beams. For each ratio the average load or deflection of beams C1 and C2 was used as the basis of comparison. **Table 3.2.16** gives the toughness indices for each beam using the maximum and failure loads as points for comparison. A toughness index is the ratio of the work done up to the deflection corresponding to the particular load under consideration to the work done up to the deflection corresponding to yield load.

Table 3.2.14 Summary of work done and ductility ratios, series one beams.

Beam	Work done to P_{MAX} (J)	Ductility ψ_{Pmax}	Ductility (Graphic) $\psi_{graphic}$
C1	(1232)	(6,1)	(5,0)
C2	1552	5,3	6,0
T1	1092	3,8	3,9
B1	1152	4,3	4,4
TB1	1158	5,0	5,0
T2	2125	7,8	7,5
B2	675	3,1	2,8
TB2	958	3,6	3,3

Table 3.2.15 Summary of load and deflection ratios, series one beams.

Beam	$\frac{P_{max}^{corr}}{P_{max}}$	$\frac{P_{y}^{corr}}{P_{y}}$	$\frac{\Delta_{Pmax}^{corr}}{\Delta_{Pmax}}$
C1	1,05	1,02	0,96
C2	0,94	0,97	1,03
T1	0,93	1,11	0,84
B1	0,96	1,00	0,95
TB1	1,07	1,00	0,89
T2	1,10	1,16	1,39
B2	0,87	1,00	2,42
TB2	0,98	1,00	1,61

Table 3.2.16 Toughness indices using the maximum and failure loads.

Beam	Toughness index using P_{max}	Toughness index using P_{fail}
C1	(5,38)	(5,38)
C2	8,21	14,73
T1	5,94	13,33
B1	8,36	23,39
TB1	8,57	26,45
T2	12,29	23,42
B2	11,72	13,25
TB2	11,65	14,34

3.3 Discussion of results

Concrete quality

A concrete grade of at least 30 MPa was chosen so that it would be representative of most structural reinforced concrete in practice. The results in Table 3.2.4 and Table 3.2.5 show very little increase in strength from 28 days to 70 days, as can be expected as the specimens were merely wrapped in plastic and not periodically wetted. The similar average cube strengths for batch 1 and batch 2 at the time of test allows for confident comparison between specimens made in different batches.

Chloride concentrations

The attraction effect of the positively charged reinforcing on the negatively charged chloride ions results in an increase in the concentration of the chloride ions in the region of the corroded reinforcing bars. The concentration of 0,06% for specimens C1 and C2 reflects the naturally occurring chloride concentration in the mix. A concentration of 0,90% would be the chloride concentration in the concrete when saturated with a 5% chloride solution (the porosity of the concrete was measured as 5,6%). Using this as a basis for comparison the concentrations of 4,23% and 4,25% for corrosion specimens 1 and 2 respectively shows a 4,7 times increase

(relative to the 0,9%) in the chloride concentration near the anode. The small difference in the concentration between specimens 1 and 2 may suggest that time plays a minor role in the concentration increase as specimens 2 had an impressed current for 2 weeks compared with 1 week for specimens 1. This occurrence can alternatively be explained by the concrete reaching a chloride saturation level beyond which the concentration can no longer increase.

Concrete appearance

The development of corrosion cracks seems to follow a definite pattern. At various points along the bar length local corrosion cells develop. Rust stains start appearing on the surface of the concrete nearest these corrosion cells. The sites where the rust stains first appear are in general the sites where cracking first starts. The cracks get wider at these points and spread outwards along the length of the bar.

Cracking is largely influenced by the local concrete quality (strength and permeability). In general if the crack surfaced closer to the top or bottom corner of the specimen, the crack tended to be wider, and with specimens T1, B1 and TB1 the crack tended to be more discontinuous as the crack would lead out to the corner rather than join up with the next crack along the length of the beam.

Rust staining also tends to spread out along the length of the bar as the crack opens up in un-stained concrete areas. This is substantiated by the fact that in specimens that were only corroded for a short period the rust stains in the concrete between the steel and the concrete surface tended to be discontinuous along the length of the bar. As the corrosion period increased the width of these rust stain planes become longer until all the individual cracks and rust stain surfaces became one continuous crack and rust plane.

In summary as corrosion proceeds :

- Crack length as a percentage of the bar length increases.
- Crack continuity increases.
- Crack width increases.
- Rust stain sources become more closely spaced and eventually become

continuous.

Reinforcing appearance

Galvanic corrosion is often described as being fairly uniform.[3.7,3.8] In this investigation this was found not to be entirely true. Local corrosion cells develop along the length of the bars as the corrosion process proceeds, and these local corrosion cells become more numerous and closely spaced until individual cells can no longer be identified and the bar appears to be corroding uniformly. At more advanced stages of corrosion the initial corrosion cells again become visible as deep pits start forming in these regions. Deep pits also occurred more frequently near the electrical connection to the reinforcing.(The reinforcing was electrically connected to the corroding current at both ends of the bars. Far deeper pits were found near the end of the bars near the electrical connection.)

Corrosion products would initially form only on approximately the outside 270° of the bar perimeter i.e. only on that part of the perimeter that had a concrete face immediately adjacent to it. Corrosion products would initially be in the form of red rust. As corrosion proceeded the corrosion products would be forming faster than oxygen was available for secondary oxidation and the corrosion products would therefore become darker in colour as more ferrous hydroxide was present in the products. The products also became more of a paste than powdery/flaky in texture.

In specimens that had more of a general corroded appearance, the occurrence and depth of pits was less. In specimens T2 B2 and TB2, if grey areas (uncorroded) were present the pits tended to be large and more closely spaced than if the specimens had little or no grey areas.(i.e. more of a general corroded appearance)

In summary as corrosion proceeds :

- The size of corroded areas increases and becomes more continuous.
- The corroded areas spread over the entire perimeter of the bar.
- The rust products formed change colour from red to dark black and become more of a paste.
- Pit occurrence becomes more frequent.

- Pit length increases.
- Pit depth increases.

Corrosion percentage losses

% Mass loss (Faraday)

The predicted percentage mass loss according to Faraday ignores exposed surface area and uses only the current and the time under current to calculate the loss. For bars of lower mass the percentage loss will therefore be larger.

% Mass loss (gravimetric)

In corrosion studies of metal (not embedded in concrete) gravimetric techniques are often used to quantify the amount of corrosion. The simplicity of this technique has made it a popular method to quickly classify the corrosion. It is however not so well suited for corrosion studies in reinforced concrete as it is often difficult to recover the entire length of reinforcing from the concrete. At low levels of corrosion there are often still chunks of concrete stuck to the reinforcing bars, these can be removed either mechanically or chemically. It was found that preparing and cleaning the bars according to ASTM G1-81[3,9] was not sufficient to remove all the concrete adhering to the steel. More extensive wire brushing was required, often to the level that could remove some of the parent material thus yielding an incorrect mass loss. This method was found to be very inaccurate at low levels of corrosion, where only small amounts of parent metal are lost. The decrease in mass due to loss of metal often cancelled out by the gain due to concrete adhesion. At higher levels of corrosion this effect would become less significant and could make this method of classification reliable.

% Diameter loss (Faraday)

This method of classification gives only a prediction of the average diameter loss of all the steel being corroded. As it is the maximum diameter loss along the length of a bar that will be the most critical for structural performance, this method is not a good way of classifying the corrosion extent.

% Tensile loss

The percentage reduction in tensile strength is a measured parameter on the steel in the beams used in the test. Using this as a means for comparison therefore has more validity than using a predictive classification system such as that of Faraday. The percentage loss in tensile strength is really a loss in rupture load and not of yield load. This method could be used on existing structures if it is possible to remove a section of the reinforcing without affecting the integrity of the structure. This method is quick and easy to perform. It provides results that have very little variance (less than 1,11 kN for an average load of 54,2 kN) and is extremely sensitive to changes in the corroded condition of the steel. A 5% reduction in tensile strength could be measured on steel that showed only a few patches of rust speckles, and which otherwise showed no other visual signs of corrosion. The sensitivity of the method is due to the stress raising effect that the pits have. Evidence of stress raising can be seen in the fact that the percentage tensile loss is greater than the percentage diameter loss (Faraday) squared. The stress raising effect therefore amplifies the changes in the bar condition.

Load deflection graphs

The data extracted from the load deflection graphs for each beam, summarised in Tables 3.2.13 to 3.2.16, is plotted in **Figures 3.3.1 to 3.3.10**, on pages 78 to 86. The values of the y axis for the loads and deflections are expressed as dimensionless ratios with the corroded value being the numerator and the control (uncorroded) value the denominator. In each case the values of the control beams have been plotted at 0% reduction in the tensile strength to provide an indication of the variation of the data. For each graph a separate curve has been plotted for top steel corrosion, bottom steel corrosion and for both top and bottom steel corrosion. The amount of corrosion induced in the beams was not enough to induce large spalls resulting in a loss of section in the compression zone. Corrosion of the top steel therefore should in theory have little effect on the beams' performance as only minor disruption of the compression zone occurred. Further the behaviour of the beams corroded only in the tension zone should be similar to the beams corroded in both the tension and compression zones.

General trends

The effects of steel corrosion on the shape of the load-deflection graph are as follows :

- Corresponding load points occur at greater deflections.
- The ratio of plastic to elastic deflections decreases.
- The final failure is more sudden (brittle) than for uncorroded specimens.

Maximum load ratio (Figure 3.3.1)(page 78)

The maximum load ratio is the ratio of the maximum load of the corroded beams to the average maximum load of the control beams. The maximum load ratios for bottom steel corrosion and for both top and bottom steel corrosion shows little change (considering the variation in the control specimens) with increasing amounts of corrosion. The ratio for the top steel corrosion shows an increase for the specimen at 12,5% reduction in tensile strength. Corrosion reduces the amount of steel available to resist load and therefore after some level of corrosion the load carrying capacity of the beams must decrease and therefore also the maximum load ratio. If the amount of steel lost is not sufficient, the maximum load ratio will not show a decrease. It is therefore possible that the results for this series of beams is in the initial stages of section loss which is still not enough to affect the maximum load ratio. The high ratio for the top steel corroded specimen at 12,5% loss in tensile strength could be due to a different position of the steel giving it a larger lever arm or because of a greater concrete strength. The high ratio is therefore probably not a reflection of the effects of corrosion.

Yield load ratio (Figure 3.3.2)(page 79)

The yield load ratio is the ratio of the yield load of the corroded beams to the average yield load of the control beams. The yield load ratio for the bottom steel corrosion and both the top and bottom steel corrosion shows no change with corrosion. The top steel corrosion shows an increase in the yield load for the specimen at 12,5% tensile loss. As for the maximum load ratio this increase could be due to a bigger lever arm or due to greater concrete strengths. The yield load should also show a reduction in the load level at higher levels of corrosion as loss of the steel section occurs.

Deflection ratio at maximum load (Figure 3.3.3)(page 80)

The deflection ratio is the ratio of the deflection of the corroded beams at maximum load to the average deflection at that load in the control beams.(**See Figure 3.3.5**) Corrosion reduces the steel cross-section. The amount of steel in a beam is one of many factors that controls the amount of deflection. A reduced steel section would result in an increase in the deflection if this effect is greater than the effects that could be reducing the deflection (e.g. improved bond). It has been reported in Chapter 2 that other workers found the deflection of corroded beams initially decreased and then increased at higher extents of corrosion. Initially the bond improved and then after a certain critical level was reached the bond rapidly decreased as corrosion products allowed more free movement between the steel and the concrete. The specimens appear to fall into this range below a 6% loss in tensile strength. Beyond that level, corrosion seems to increase the deflection significantly.

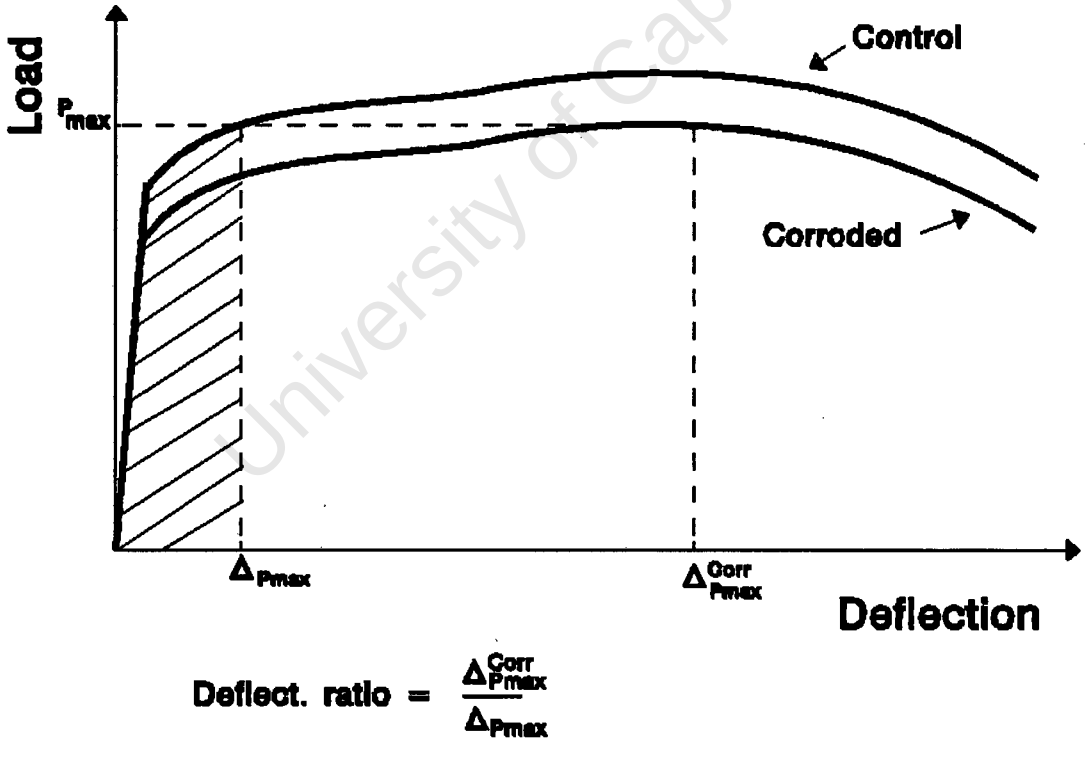

Figure 3.3.5 Schematic representation of the derivation of the deflection ratio.

Deflection ratio at service load (Figure 3.3.4)(page 81)

The service load is defined here as being 2/3 of the maximum load carried by the beam. The deflection ratio at the service load is the ratio of the deflection of the

corroded beam at the service load to the average deflection at that load in the control beams. For all three zones of corrosion there is a decrease in the deflection ratio (i.e. less deflection). At this level of corrosion, corrosion seems to have a beneficial effect on the service load deflections.

Ratio of work done to the maximum load (Figure 3.3.6)(page 82)

The integral of the load deflection graph represents the work done in deflecting the beam up to the load under consideration. The ratio of the work done to the maximum load is the ratio of the work done up to the maximum load in the corroded specimen to the average work done to that load level in the control specimens. (The shaded area in Figure 3.3.6 represents the work done in the control specimen up to the maximum load level in the corroded specimen.) The graph shows a decrease in the amount of work that has to be done. The top steel corrosion beam at 12,5% reduction in tensile strength again shows an increase which can be expected as it had a higher maximum load as has been explained above. A decrease in the amount of work done means that the rate by which the load is decreasing is faster than the rate by which the deflection is increasing as corrosion proceeds.

Ductility ratio using maximum load (Figure 3.3.7)(page 83)

The ductility ratio is the ratio of the deflection at maximum load to the deflection at the yield load for the beam under consideration. The top steel corrosion shows an increase (in contrast to the bottom steel and both top and bottom steel corrosion beams) in the ductility ratio after 6% reduction in the tensile strength. This is again most likely due to differences in the beam properties rather than a reflection of the actual trend.

Ductility ratio using maximum load (graphic method)(Figure 3.3.8)(page 84)

The graphic method essentially gives the same result as the numerical method (see section 3.2.2 for a description of the method). It provides slightly different results as it takes into account the shape of the load-deflection curve in determining the ratio between the plastic and elastic deflections.

Toughness index using the maximum load (Figure 3.3.9)(page 85)

The toughness index is the ratio of the area under the load deflection curve up to the maximum load to the area up to the yield load for the beam under consideration. The figure shows an increase in the toughness index with increasing amounts of corrosion for all the corrosion types.

Toughness index using the failure load (Figure 3.3.10)(page 86)

The toughness index using the failure load is simply the ratio of the area up to the failure load to the area up to the yield load. This form of toughness index, as can be expected, is not a reliable method of evaluating toughness as the failure load can vary greatly depending on any local aggregate locking around the bars causing a delay in the failure load and thus greatly affecting calculations made using this load. No clear trend can be identified considering the variation in the control beams.

3.4 Closure

This chapter has presented the experimental method of corroding the specimens galvanostatically and the method used in the flexural tests of the beams. A limited discussion of the general trends of the structural parameters studied was presented. A more detailed discussion, analysis and comparison with the results from series two will be presented in chapter 5.

MAXIMUM LOAD RATIO

FIGURE 3.3.1

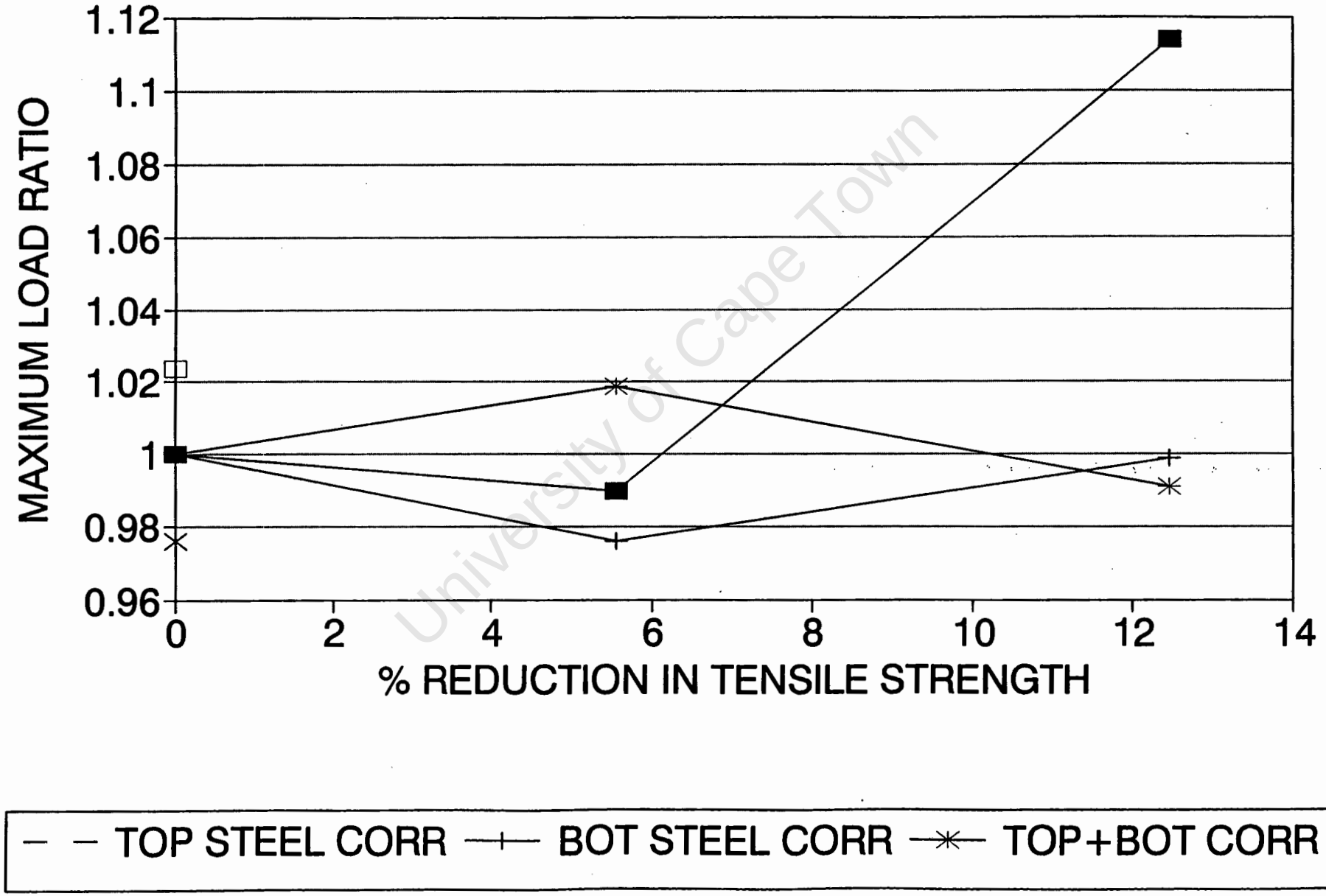

YIELD LOAD RATIO

FIGURE 3.3.2

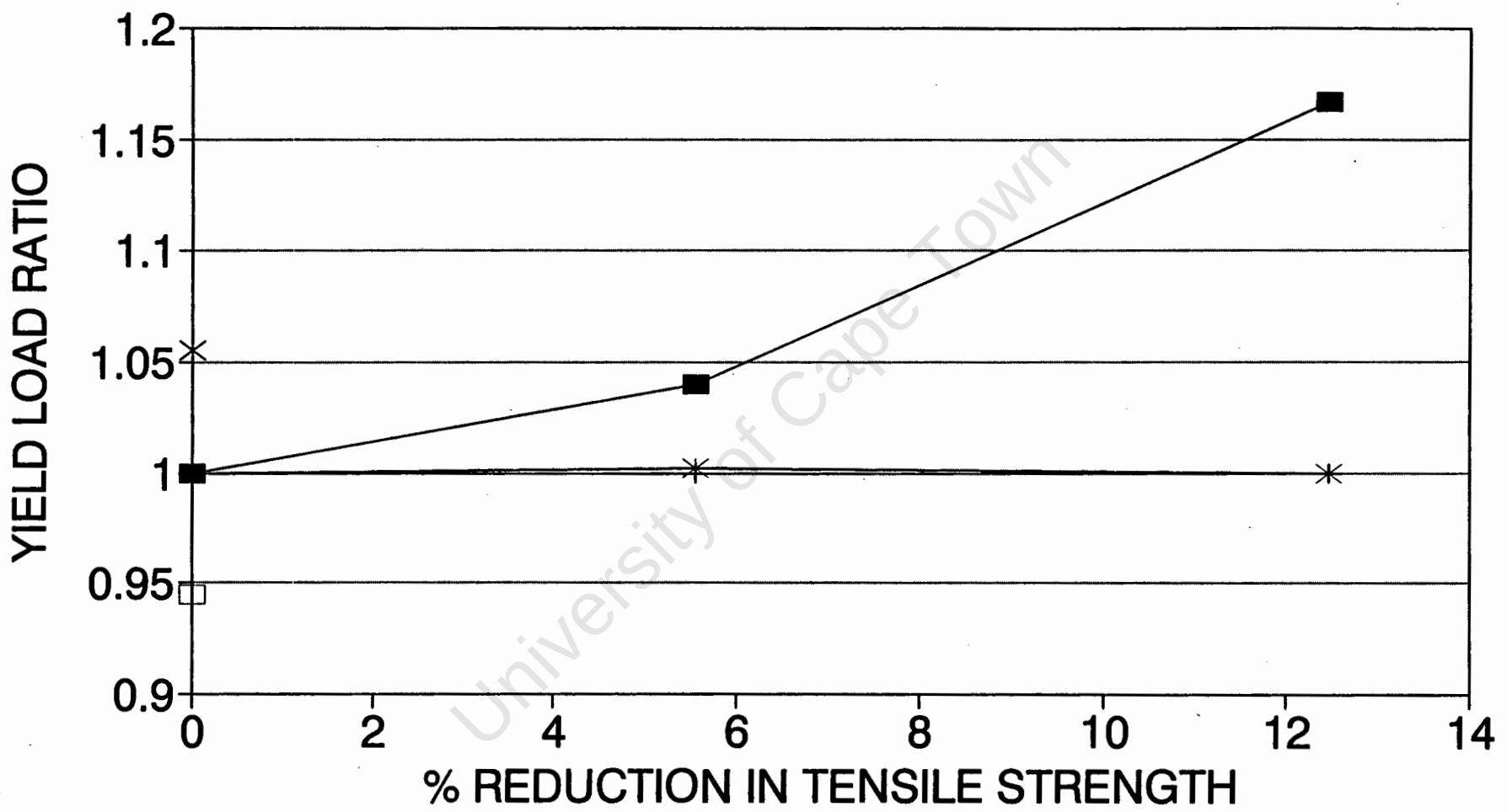

DEFLECTION RATIO (MAXIMUM LOAD)

FIGURE 3.3.3

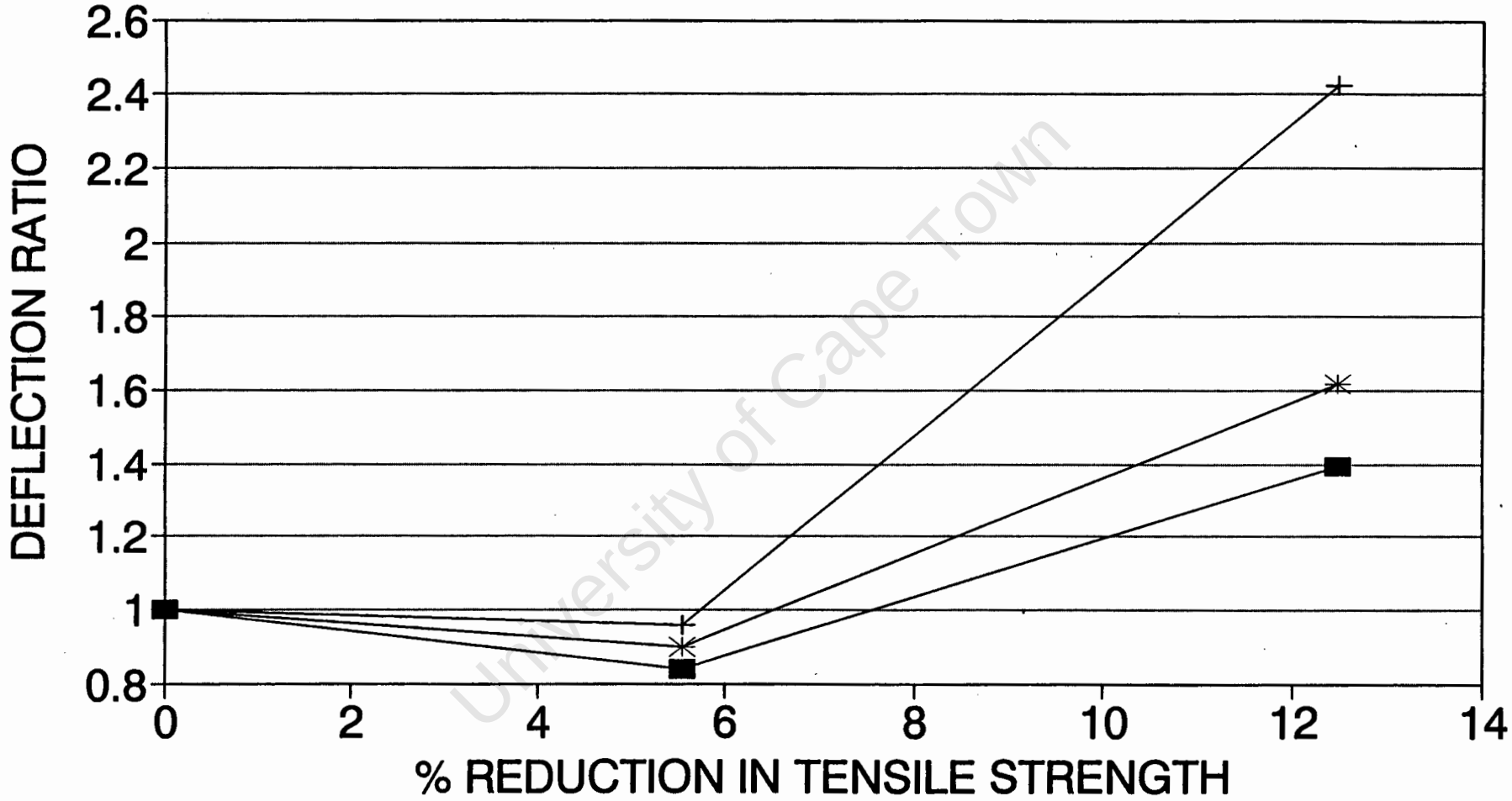

DEFLECTION RATIO (SERVICE LOAD)

FIGURE 3.3.4

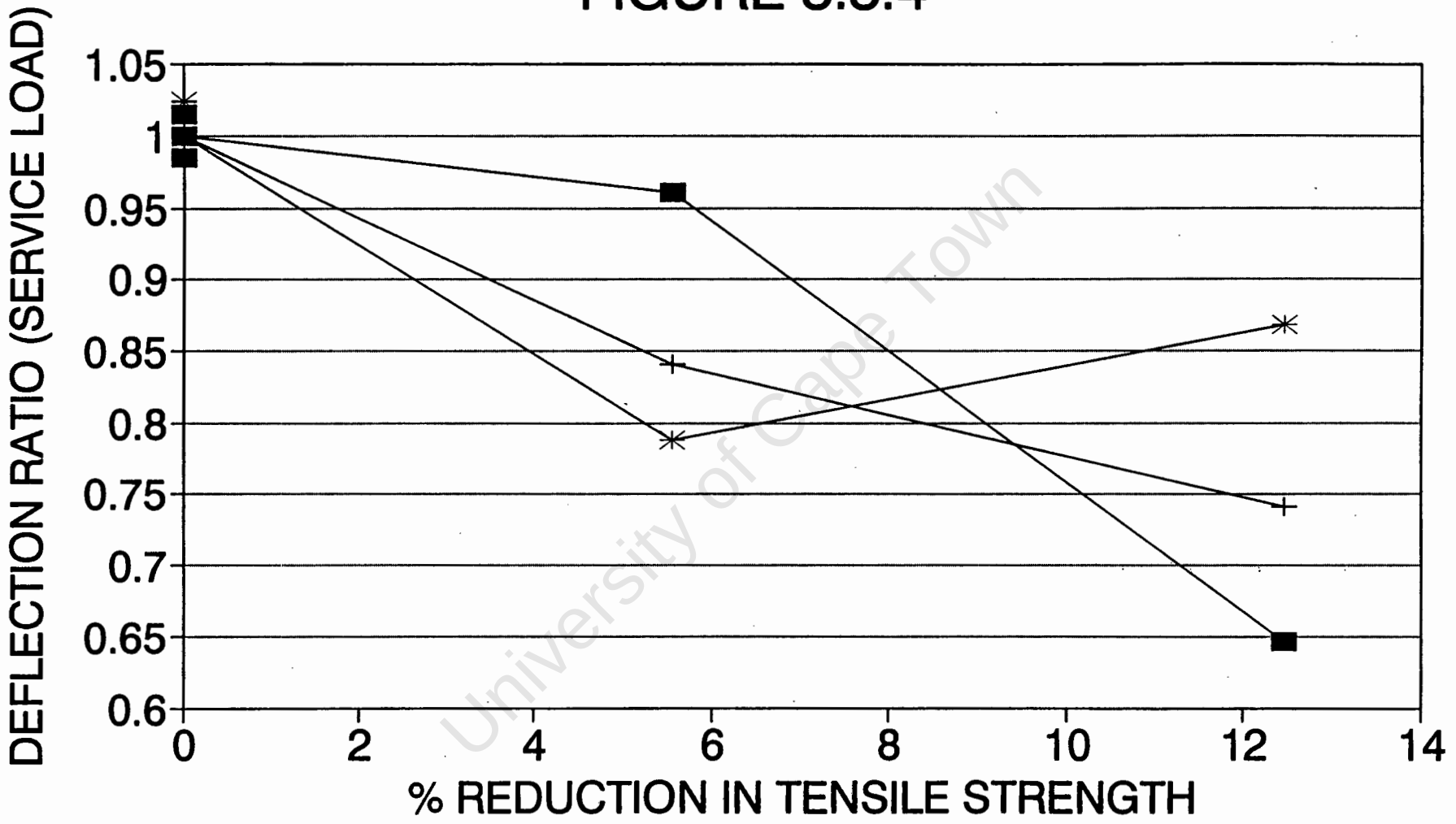

RATIO OF WORK DONE TO MAX LOAD

FIGURE 3.3.6

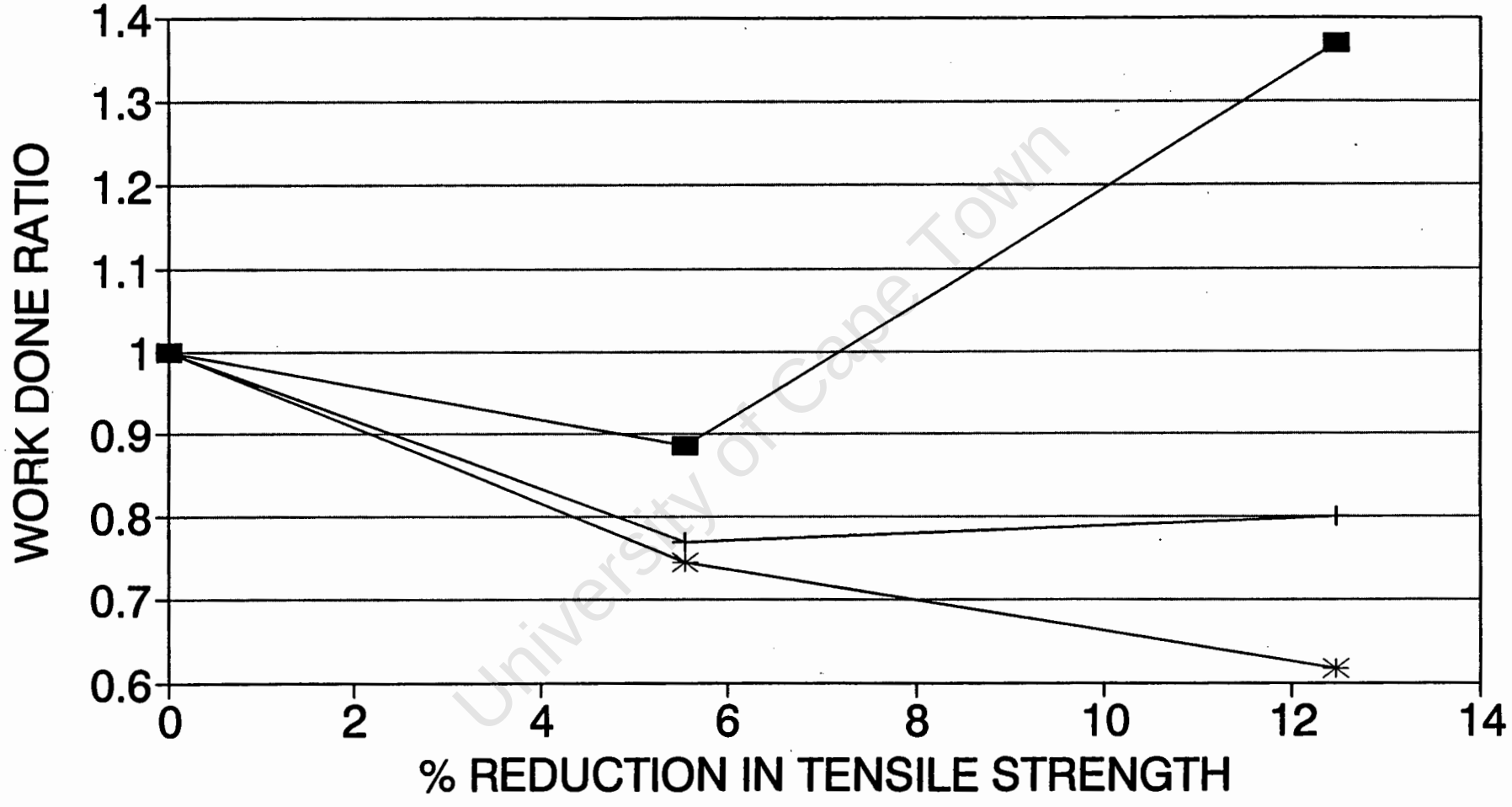

DUCTILITY RATIO

FIGURE 3.3.7

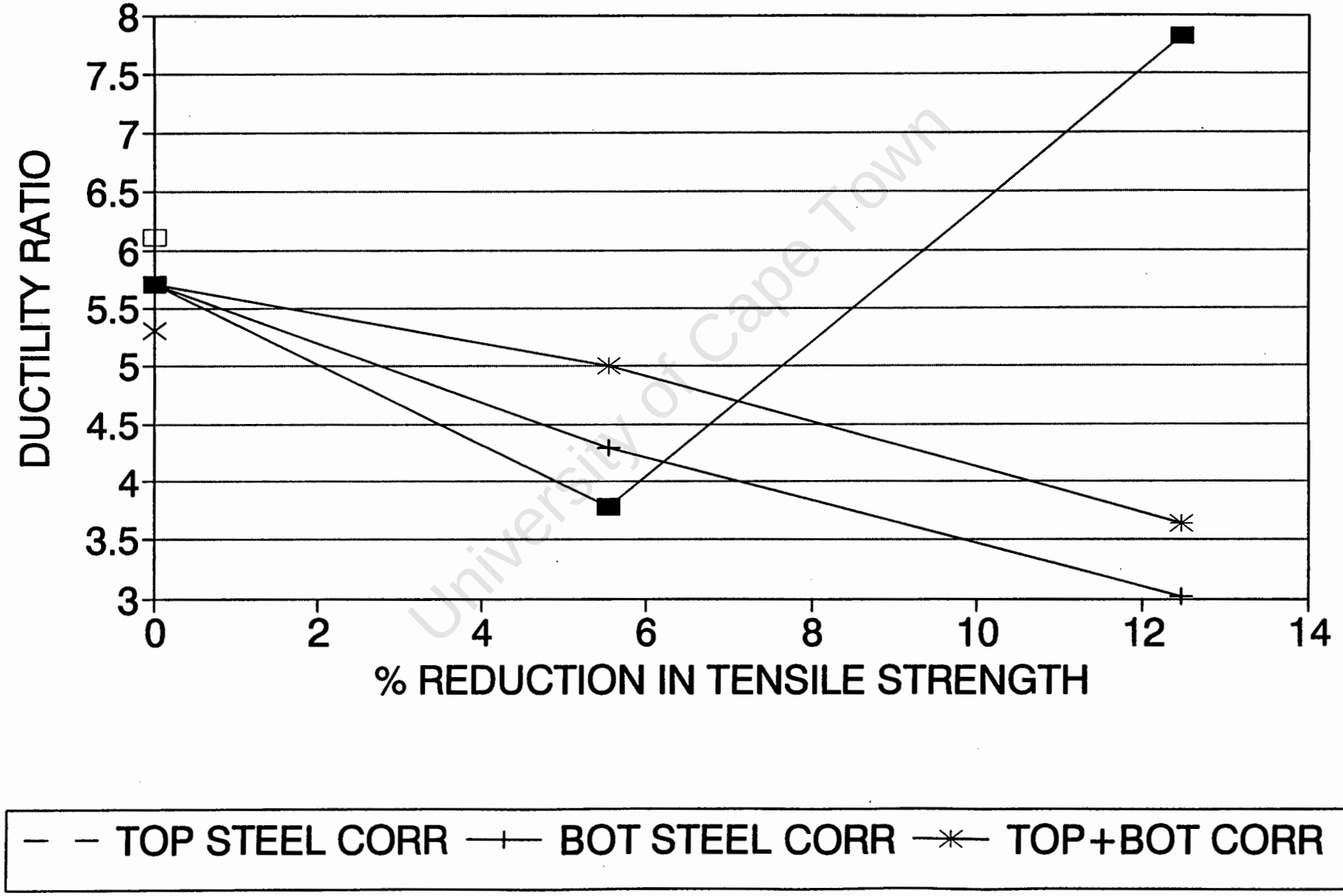

DUCTILITY RATIO (GRAPHIC METHOD)

FIGURE 3.3.8

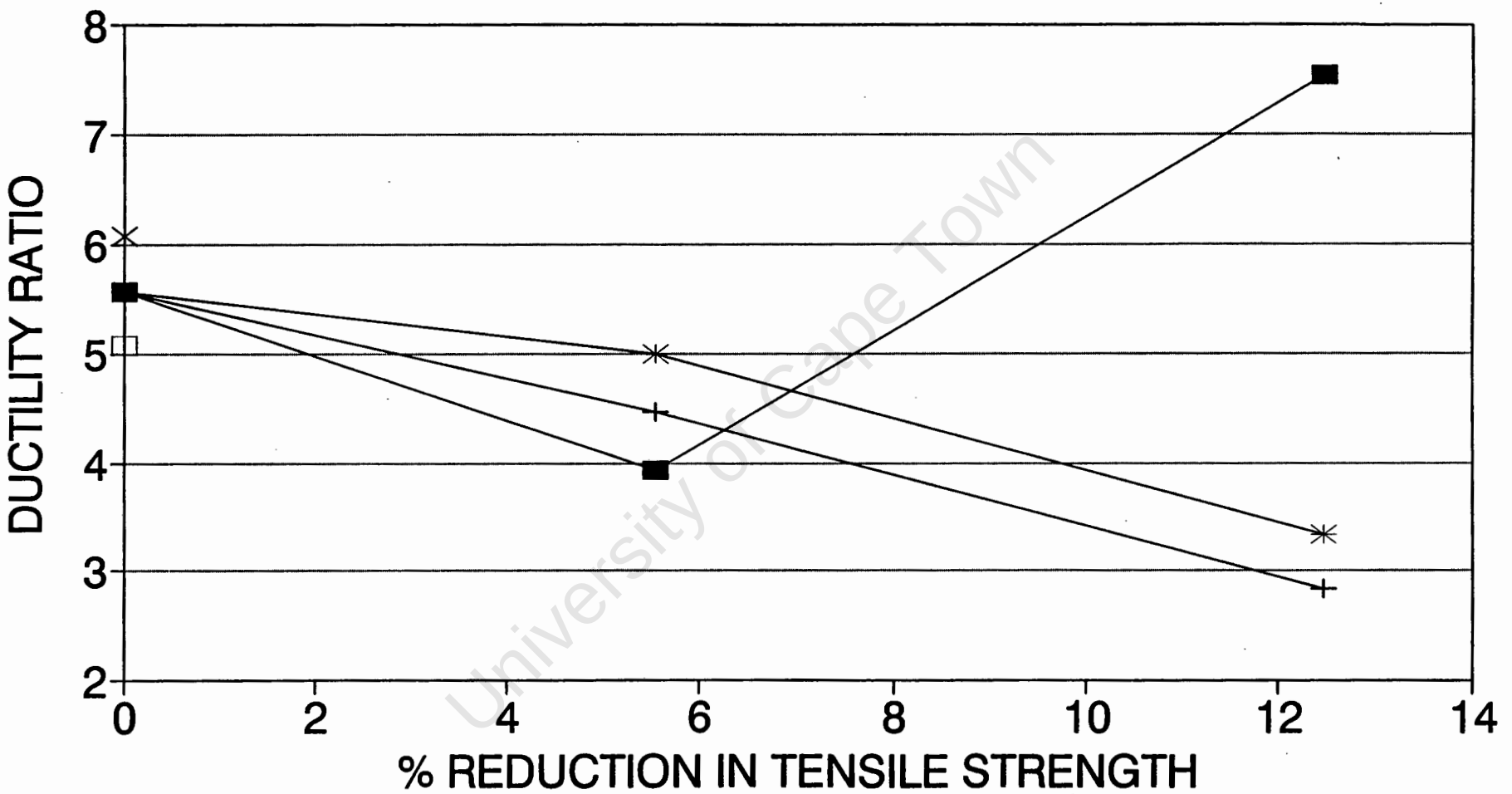

TOUGHNESS INDEX (MAXIMUM LOAD)

FIGURE 3.3.9

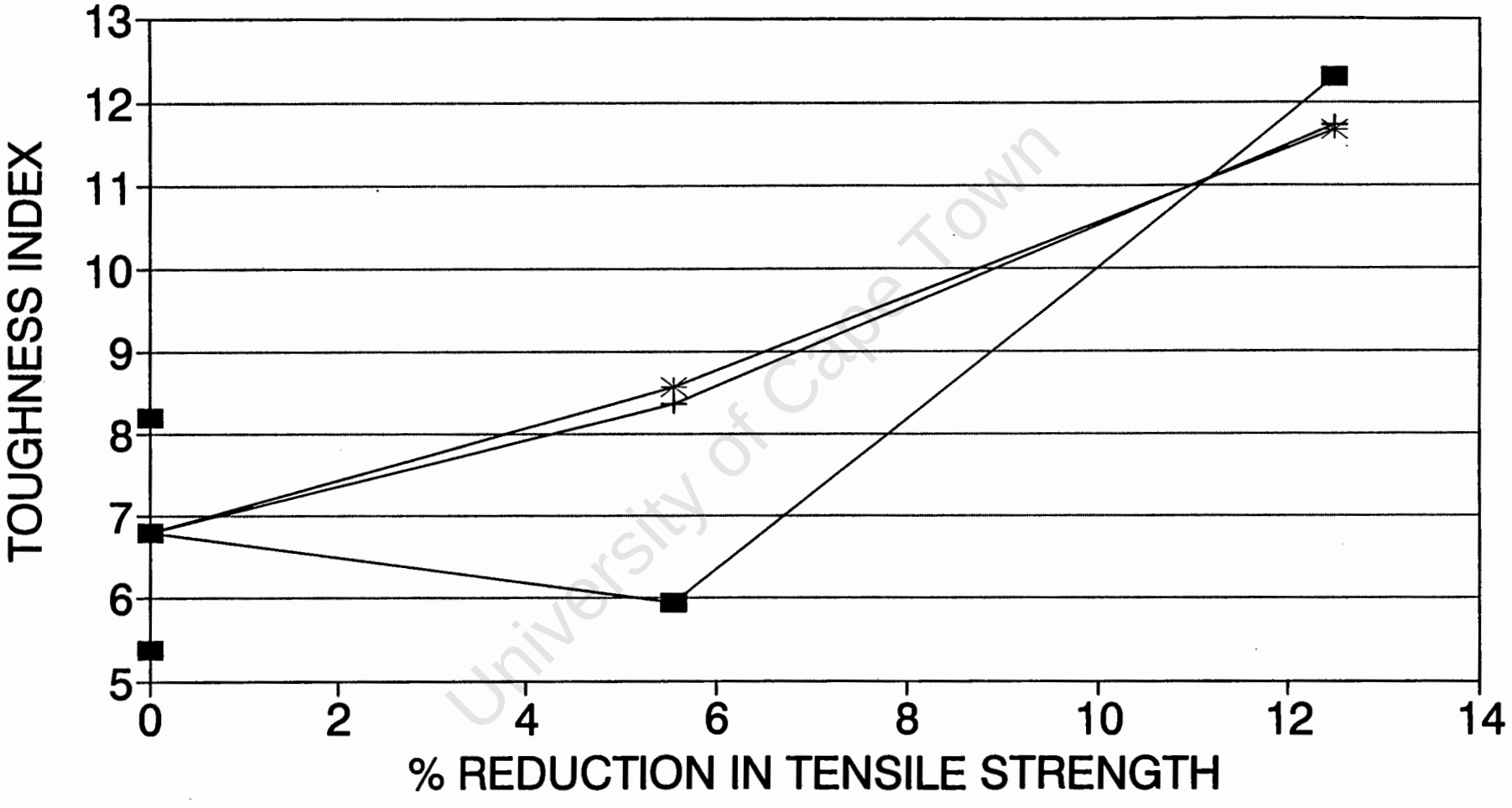

TOUGHNESS INDEX (FAILURE LOAD)

FIGURE 3.3.10

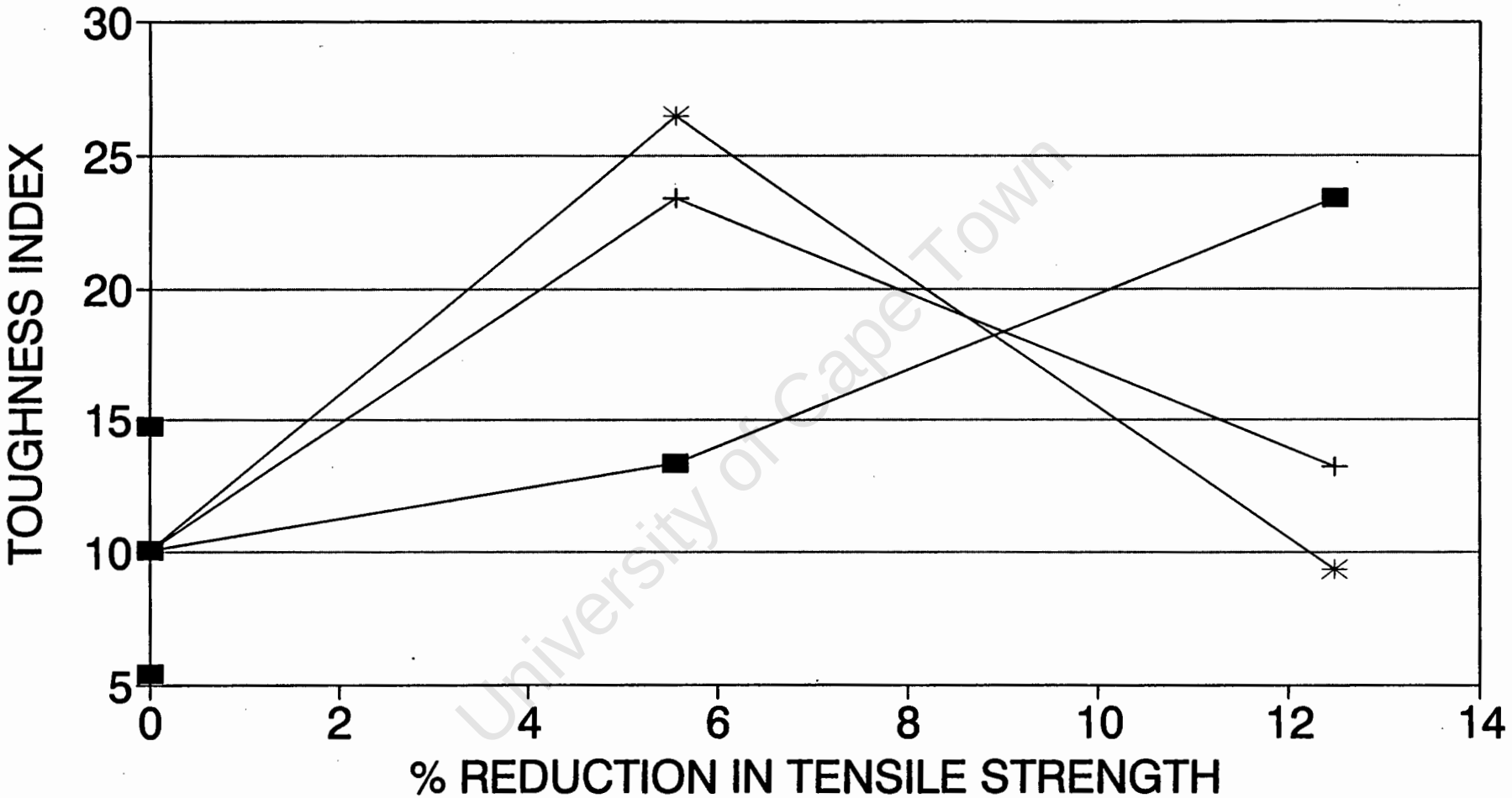

3.5 References

3.1) Rankine, R.G.D., *Appropriate Properties for a New Corrosion Resisting Reinforcing Steel,* MSc dissertation, University of the Wiwatersrand, Johannesburg, 1990.

3.2) Neveling, C.H., *A Critical Litrature Review and Limited Confirmatory Experimentation on the Ductility of Reinforced Concrete*, MSc dissertation, University of the Wiwatersrand, Johannesburg, 1992.

3.3) Beeby, A.W., Cracking, Cover, and corrosion of reinforcement, *Concrete International*, February, 1983, pp. 35-40.

3.4) Schiessl, P.(ed), *Corrosion of Steel in Concrete*, London :Chapman & Hall, 1988.

3.5) van Rensburg, J., *Van Wyk & Louw Consulting Engineers*, Personal communication, Pretoria, October, 1993.

3.6) Abdul-Hamid J. Al-Tayyib and Mohammad Shamim Khan, Corrosion rate measurements of reinforcing steel in concrete by electrochemical techniques, *ACI Materials Journal*, May-June, 1988, pp. 172-177.

3.7) Tachibana, Y., Kajikawa, Y. and Kawamura, M., The mechanical behaviour of RC beams damaged by corrosion of reinforcement, *Concrete Library of Japanese Society of Civil Engineers*, No 14, March, 1990, pp. 177-188.

3.8) Misra, S. and Uomoto, T., Effect of corrosion of reinforcement on the load carrying capacity of RC beams, *Procedings of the Japan Concrete Institute*, Vol. 9, No 2, pp. 675-680.

3.9) ASTM G1-81, Standard Practice for Preparing, Cleaning, and Evaluating Corrosion Test Specimens, July, 1981, pp. 89-94.

Chapter Four

Experimental investigation of the effects of reinforcement corrosion on the structural performance of reinforced concrete beams - series two

4.1 Corrosion method and results

Series two beams were corroded by the more realistic method of subjecting them to a series of wetting and drying cycles in a marine exposure chamber. The beams were wet with a 5% chloride solution (in the form of NaCl) by completely submerging them for 3 days and then drying them with industrial fans for 4 days. The cycle time was therefore one week long. Both the water and the air were at ambient summer temperature with the wetting and drying facility being in the shade for most of the day. **Figure 4.1.1** shows a schematic of the wetting and drying facility (see also **Photograph 9** on page 97). Some of the specimens were then in addition corroded galvanostatically in the same way as the specimens in series one. This was done so that these specimens could be used to establish the behaviour at higher extents of corrosion.

4.1.1 The beams

The model test beams were 2 metres in length and 165*220 mm in cross section. Two options existed in the design of the beams : they could either be heavily or lightly reinforced. If heavily reinforced beams were used (bars of large diameters) more spalling would be encouraged but the beams would have a lower ductility. This together with possible shear and anchorage problems may have made it difficult to achieve a bending failure and invalidated measurements to be made for the ductility tests. For this reason the beams were reinforced relatively lightly so that bending failure at a relatively low moment would be possible and ensure that

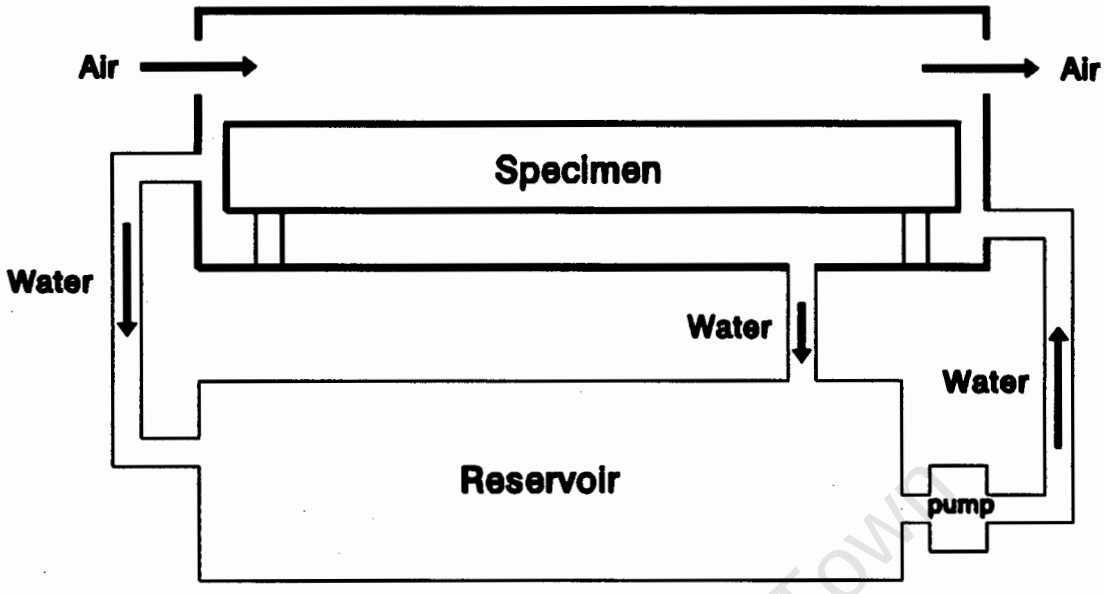

Figure 4.1.1 Schematic representation of wetting and drying facility.

anchorage or shear failures did not occur. The beams were reinforced with 2Y12 high tensile ribbed bars in the tension zone and 2R8 mild steel bars as link carriers. The stirrups were R8 mild steel bars spaced at 140 mm, the cover to the stirrups being 20 mm. All the beams and cubes (including the controls) had a 1,2% addition of chlorides (by weight of cement) in the mix, in the form of NaCl, to help speed up the time to initiate the corrosion. The concrete mix used to make the beams and cubes is given in **Table 4.1.1**. The specimens were cast in two batches as detailed in **Table 4.1.2**. The beams were tested in exactly the same way as the beams in series one.

Table 4.1.1 Mix design for series two beams.

Concrete mix design	Quantities per m^3
Water	190 l
Ordinary Portland Cement	317 kg
19 mm Greywacke stone	1100 kg
Cape Dune sand	785 kg
Sodium Chloride	6,25 kg

Table 4.1.2 Specimens cast

Specimens	Batch 1	Batch 2
Control beams	C1T	C2T
Test beams	T1T T2T	T3T T4T
28 Day Control Strength cubes	C1 C2 C3	C4 C5 C6
Control strength cubes	C7 C8 C9	C10 C11 C12
Test strength cubes	T1 T2 T3	T4 T5 T6

Test specimens

The beams were de-moulded at 3 days and then immediately wrapped in plastic and cured at the ambient laboratory temperature for 21 days. Thereafter they were placed in the marine exposure chamber and subjected to cyclical wetting and drying. This was decided upon as it approximates what happens to marine concrete. Six cubes (T1-T6) were cured in the same way as the test beams (in plastic and then in the exposure chamber) to be used for strength tests at the time that the beams were tested.

Control specimens

These were de-moulded at 3 days and wrapped in plastic to keep moist at ambient laboratory temperature. The reason for moist curing was to ensure that the control specimens have a strength that closely matches the strength of the test specimens which were subjected to partial (moist) curing in the marine exposure chamber. The C1-C6 cubes were used for 28 day strength tests and the C7-C12 cubes were used for strength tests at the time that the beams were tested.

The exposure (and corrosion conditions) are summarized in **Table 4.1.3**. All the reinforcement was corroded (including the stirrups) at the current densities given

in the table.

Table 4.1.3 Series two exposure times.

Beam	Exposure cycles (1 week long)	Current (Amp)	Current time (days)	Current density (mAmp/cm^2)
C1T	0	0	0	0
C2T	0	0	0	0
T1T	25	0	0	0
T2T	25	0,75	14	0,14
T3T	25	1,5	21	0,28
T4T	25	1,5 2,5	8 & 13 = 21	0,28 0,46

4.1.2 Material test results

The 28 day cube strengths are given in **Table 4.1.4**. The cube strengths at the time that the beams were tested (180 days) are given in **Table 4.1.5**. The results for both the control cubes (treated in exactly the same way as the control beams) and the results for the cubes that were subjected to the same wetting and drying cycles as the test beams are given.

Table 4.1.4 28-Day cube strengths.

Cube	Strength (MPa)
C1	26,8
C2	29,6
C3	30,1
Average	28,8
C4	29,0
C5	28,0
C6	26,4
Average	27,8

Table 4.1.5 Cube strengths at time of beam tests.

Control	Strength (MPa)	Test Chamber	Strength (MPa)
C7	50,3	T1	36,0
C8	43,0	T2	45,0
C9	42,7	T3	44,0
Average	45,3	Average	41,6
C10	43,9	T4	38,1
C11	43,3	T5	38,5
C12	44,8	T6	41,0
Average	44,0	Average	39,2

4.1.3 Classification of corrosion extent

The various methods used to classify the corrosion extent of the damaged beams for series two beams are identical to those used for the series one beams. **See Section 3.2.1** for definitions of equations and terms used.

Classification of the concrete appearance

1) Corrosion crack pattern, crack size and continuity

Table 4.1.6 classifies the concrete visual appearance according to the crack width, length and location.

Table 4.1.6 Visual classification of cracking.

Specimen	Crack location, Crack size and length. Extent of rust staining.
C1T C2T	Control specimens, no corrosion.
T1T	No corrosion cracks. Very limited rust stains. Stains < 20 mm long.
T2T	No corrosion cracks. Rust stains < 15 mm wide over entire height of stirrup. Rust stains on > 70% of stirrups.
T3T	Corrosion cracks only along longitudinal steel on side faces. Average crack width 0,06 mm. Cracks generally discontinuous along length. Total crack length < 60 % of bar length. Rust stains extensive and no longer limited to stains from stirrups only. Rust stain sources along length of cracks.
T4T	Corrosion cracks only along longitudinal steel on side faces. Average crack width 0,08 mm. Cracks generally discontinuous along length. Total crack length < 80 % of bar length. Rust stains very extensive covering > 50% of side faces.

2) General structural condition classification

Table 4.1.7 shows the classification of the beams according to the DOT system given in Table 3.2.8. The inappropriateness of this system is again shown by the fact that it does not make allowance for staining before cracking or spalling.

Table 4.1.7 DOT classification of beams.

Beam	Description	Category number
C1T C2T	New condition. No rust stains. No cracks.	9
T1T	New condition. Very minor rust stains. No cracking.	9
T2T	Minor rust stains. No cracks.	5
T3T	Moderate to heavy rust stains. Minor cracking. No spalling.	5
T4T	Very heavy rust staining. Minor to moderate cracking. No spalling.	5

Classification of the reinforcing appearance and properties

1) Visual classification of reinforcement appearance

Table 4.1.8 classifies the reinforcing bar appearance, pit size and location on the bars.

2) Percentage losses

The percentage losses as calculated by Equations 3.2.1 to 3.2.5 for each beam are summarized in **Table 4.1.9**. The third and fifth columns are measured values while the second and fourth are calculated values.

Table 4.1.8 Reinforcing bar condition classification.

Specimen	Description of bar corrosion condition
C1T C2T	Dull grey colour along most of the length of bars. General appearance still dull grey. Patches of rust speckles around the entire perimeter of bar. Rust patches 20-30 mm long. No rust stains in concrete surrounding the steel. No rust pits.
T1T	Dull grey colour along most of the length of bars. Patches of rust speckles more closely spaced (every 100 mm). Patches 20 mm long around entire perimeter of bar. No rust stains in the concrete surrounding the steel. No rust pits.
T2T	No dull grey areas. General rusty (red in colour) look as mill scale flakes off. Rusty over entire length of bar and perimeter, uniform colour appearance. Rust stains in concrete surrounding bar over entire length and perimeter of bar but rust stains reach the concrete surface only at certain points along bar length. Pits occur only along bar ends, spaced 30 mm apart, maximum size 2-3 mm long.
T3T	Black rust appearance of steel over entire length and perimeter of bar. Red rust stains with areas of black paste in concrete surrounding steel. Red rust stains reaching the surface of the steel along longer lengths but still not continuous. Areas of severe pitting (1-1,5 mm deep) up to 10 mm long alternating with smaller (1-2 mm long) more numerous areas of pits. Worst pitting occurred on bar ends near the wire connection. Stirrup contact near wire connection caused severe pitting (up to 2,5 mm deep and 10 mm long).

Specimen	Description of bar corrosion condition
T4T	Black rust appearance of steel over entire length and perimeter of bar. Black paste in concrete surrounding the steel. Red rust stains with areas with black rust forming a surface between the steel and the concrete surface. The surface was in general continuous along the length of the bar. Pits occurred along entire length and diameter up to 15 mm long and 1 mm deep. Where large pits do not occur numerous small pits less that 1 mm long occur. Loss of entire forming ridges parallel to the length of the bar common.

Table 4.1.9 Summary of percentage losses.

Specimen	% Mass loss (Faraday)	% Mass loss (Gravimetric)	% Diameter loss (Faraday)	% Tensile strength loss
C1T C2T	0,0	0,0	0,0	0,0
T1T	0,0	0,0	0,0	0,0
T2T	2,7	0,6	5,6	4,4
T3T	8,1	1,3	16,8	8,8
T4T	11,4	2,1	23,7	14,1

4.1.4 Effects on structural properties

The observed failure mode for each beam is given in **Table 4.1.10** (see also **Photographs 10-12** on page 97 & 98). **Table 4.1.11** gives the maximum and yield loads and the corresponding deflections for each beam. **Table 4.1.12** gives the work done and the ductility for each beam using the maximum load.

Table 4.1.10 Observed failure modes for each beam.

Beam	Description of failure mode
C1T	Normal stepped flexural failure.
C2T	Normal stepped flexural failure. Buckling of top steel on one side of beam under load point caused sudden final failure of beam. Large chunks of concrete popped sideways under load point.
T1T	Normal stepped flexural failure. Buckling of top bar near 1st stirrup from mid-span caused a loss of section here resulting in shear cracks.
T2T	Smooth flexural failure. Top steel buckled on one side only below the load point.
T3T	Smooth flexural failure. Excessive widening of corrosion cracks (up to 6 mm) as maximum load was reached.
T4T	Smooth flexural failure. Very wide opening of corrosion cracks caused many large chunks of concrete to fall out in tension zone.

Table 4.1.11 Summary of loads and deflections.

Beam	P_y (kN)	Δ_{Py} (mm)	P_{max} (kN)	Δ_{Pmax} (mm)
C1T	60,0	6,2	69,5	49,5
C2T	54,0	6,1	67,3	53,5
T1T	53,0	6,2	64,2	74,5
T2T	56,0	6,9	65,3	57,0
T3T	48,0	6,3	58,9	65,0
T4T	46,0	5,7	58,5	68,5

Table 4.1.12 Work done and ductility ratios.

Beam	Work done to P_{MAX} (J)	Ductility ψ_{Pmax}	Ductility (Graphic) $\psi_{graphic}$
C1T	3121	7,9	8,4
C2T	3150	8,7	9,0
T1T	4361	12,0	12,6
T2T	3334	8,2	7,7
T3T	3423	10,3	10,1
T4T	3621	11,9	10,8

Photograph 9 Wetting and drying facility

Photograph 10 Beam T2T

Photograph 11 Beam T3T

Photograph 12 Beam T4T

The load and deflection ratios for the maximum and yield loads are given in **Table 4.1.13.** The toughness indices for the maximum and failure loads are given in **Table 4.1.14.**

Table 4.1.13 Load and deflection ratios.

Beam	$\frac{P_{max}^{corr}}{P_{max}}$	$\frac{P_{y}^{corr}}{P_{y}}$	$\frac{\Delta_{Pmax}^{corr}}{\Delta_{Pmax}}$
C1T	1,01	1,05	0,96
C2T	0,98	0,94	1,04
T1T	0,93	0,92	1,44
T2T	0,95	0,98	1,12
T3T	0,86	0,84	1,26
T4T	0,85	0,80	1,33

Table 4.1.14 Toughness indices.

Beam	Toughness index using maximum load	Toughness index using failure load
C1T	14,4	27,8
C2T	17,4	25,3
T1T	22,1	22,1
T2T	14,8	18,8
T3T	18,6	28,3
T4T	22,6	30,7

It was observed that the top 15-20 mm of the concrete in the beams that were corroded galvanostatically, had a friable appearance. To establish whether the concrete in this layer had different properties to the rest of the beams, Schmidt hammer and ultrasonic pulse velocity measurements were taken on the concrete. The following Schmidt hammer numbers were found for the top surface layer of the beams. The readings in **Table 4.1.15** were all taken 15 mm from the top of

the beams. The ultrasonic pulse velocity measurements taken on the beams were measured with a Steinkamp BP-5 Ultrasonic Tester and are given in **Table 4.1.16**. The first and last readings were taken as close to the top and bottom surfaces respectively as was possible. The values in the table are the average of two readings.

Table 4.1.15 Schmidt hammer readings.

Beam	Average Schmidt hammer number	Standard deviation
C1T C2T	22,77	2,04
T1T	22,72	1,98
T2T	22,57	1,62
T3T	19,78	1,99
T4T	17,80	2,66

Table 4.1.16 Ultrasonic pulse velocity measurements.

Beam	Top [ms^{-1}]	Mid depth [ms^{-1}]	Bottom [ms^{-1}]
C1T C2T	4366	4538	4626
T1T	4441	4619	5032
T2T	4486	4640	4920
T3T	4492	4505	4626
T4T	4512	4696	4704

The chloride concentrations in the concrete (expressed as a percentage of the cement mass) at the depth of the steel in the top of the beam, mid-depth and in the bottom of the beam are given in **Table 4.1.17**.

Table 4.1.17 Chloride concentrations by percentage mass of cement at depth of the steel.

Beam	Top % Cl^-	Mid depth % Cl^-	Bottom % Cl^-
C1T C2T	1,72	1,38	1,40
Calculated	2,10	2,10	2,10
T2T	11,90	6,71	6,09
T3T	13,84	6,40	6,90
T4T	15,56	6,27	6,95

4.1.5 Discussion of results

Concrete quality

The cube strengths in Table 4.1.4 and Table 4.1.5 show the increase in cube strength from 28 days to 200 days. The cube strengths of the cubes that were cured in the same way as the test beams show a lower strength than those that were cured in the same way as the control beams. The initial moisture content in the control cubes that were cured in plastic was maintained in the initial stages after 28 days, explaining the higher cube strength (The control cubes were never wet once they were placed in plastic. They were therefore allowed to slowly dry out with time in the plastic.). The test cubes that were wet and dried therefore experienced more net drying than the control cubes that only experienced a very slow drying out period.

Concrete appearance

Series two beams showed the same crack development pattern as for series one beams. The greater cover to the main steel (8 mm more) explains why at the same level of corrosion series two beams showed less cracking and smaller crack widths. Beeby[4.1] identified a value of below 3 for the ratio of cover to bar diameter if cracking was to occur. For series one this ratio is 2,0 and for series two 2,33.

Series one therefore has a greater probability of cracking occurring. Cracking was limited to the longitudinal steel, despite the stirrups having less cover (and therefore a smaller ratio) they showed no signs of cracking. This could be due to the confining effect of the concrete adjacent to the stirrups that is not present on the one side of the longitudinal steel.

The excessive staining of the concrete in beams that were corroded to greater extents highlight the fact that the corrosion process and symptoms of distress are not the same as naturally induced corrosion. Firstly higher potential differences can result in different corrosion products forming than what would normally occur. Secondly the shorter time involved in accelerating the corrosion (at least 90 times shorter) does not allow for the flushing of corrosion products from the concrete, thus giving the concrete a far worse appearance.

Reinforcing appearance

The change in the appearance of the reinforcing with increasing amounts of corrosion followed a similar trend to the beams in series one. The inclusion of chlorides in the mix resulted in a more general appearance of corrosion. An increase in the occurrence and severity of pitting due to the presence of chlorides was not detected. All the beams with lower extents of corrosion (Table 4.1.8) showed more general patches of rust speckles around the entire perimeter of the bar (unlike for series one which only had rust patches on the outside 270° of the bar perimeter) this is probably due to presence of the chlorides in the mix.

The greater amount of pits and their severity near the electrical contact points suggests that the method of inducing corrosion is not as is often described as being uniform. The stirrup-longitudinal steel contact point near the electrical connections often resulted in very deep pits in the stirrups (up to 4 mm). As this tremendous loss of section of the stirrups only occurred near the ends of the beams beyond the support points, the shear capacity was not affected.

The summary of the percentage losses in Table 4.1.9 shows only small losses for the gravimetric mass loss. These measurements, if accurate and not affected by

the method, have a very small range thus making the method less accurate and not as sensitive to changes as the percentage loss of the tensile strength. The percentage mass loss and diameter loss as predicted by Faraday is questionable as it does not recognize different mass to surface area which will have an effect on the corrosion percentage predicted by the formula.

Integrity of concrete matrix structure

The friable texture of the top 10-15 mm of the beams that were corroded galvanostatically is supported by the Schmidt hammer results in Table 4.1.15 which show a 22% reduction in the hammer number for beam T4T. Both results indicate that the surface layer is less dense or that the surface layer's micro structure has been disturbed. This could be due to the casting position which usually results in a less dense surface layer as the aggregates settle after casting. The high levels of salt crystallisation in the top layer (see below) could also have disrupted the structure of the surface layer, or it could be as a result of a combination of these two factors.

Chloride concentrations

Table 4.1.17 clearly shows an increase in the chloride concentrations due to the positively charged reinforcing attracting the negatively charged chloride ions. The calculated concentration is the concentration in the concrete if it was saturated with a 5 % chloride electrolyte (the porosity of the concrete was measured as 5,6%) added to the concentration of chlorides already added to the mix. The chloride concentrations in the top of the beam show a much bigger increase in concentration with corrosion extent than at mid-depth and at the bottom steel. The top surface of the beams were exposed to air drying continuously while they were being corroded galvanostatically. The capillary action induced by this drying caused the chloride concentration to increase further in this layer as the salt started to crystallise in the concrete surface layer exposed to the air.

Load deflection graphs

The load deflection graph for each beam is given in **Appendix 2**. The summary of the data presented in Tables 4.1.11 to 4.1.14 is graphed in **Figures 4.1.2 to 4.1.10** on pages 108 to 116. The values for each of the control beams are plotted at 0% reduction in the tensile strength to give an indication of the variation of the data.

Maximum load ratio (Figure 4.1.2)(page 108)

The maximum load ratio is the ratio of the maximum load of the corroded beam to the average maximum load of the control beams. The figure shows a clear reduction in the maximum load supported by the beams. This can be explained by the reduction in the tensile capacity of the steel as the reinforcing section is being reduced by corrosion.

The reduction in the load ratio could be a straight line relationship with reduction in the tensile strength. Using linear regression the following equation was obtained with a correlation of 0,944.

$$\frac{P_{max}^{corr}}{P_{max}} = 1,0-(0,0112).\Delta f_T \qquad (4.3.1)$$

where Δf_t is the percentage reduction in the tensile strength of the steel.

Yield load ratio (Figure 4.1.3)(page 109)

The yield load ratio is the ratio of the yield load of the corroded beam to the average yield load of the control beams. The reduction in the yield load can also be explained as for the maximum load ratio. Linear regression of the data yielded the following equation with a correlation of 0,896.

$$\frac{P_y^{corr}}{P_y} = 1,0-(0,015).\Delta f_T \qquad (4.3.2)$$

Deflection ratio (Figure 4.1.4)(page 110)

The deflection ratio is the ratio of the deflection of the corroded beam at maximum load to the average deflection at that load in the control beams. The deflection ratio increases with an increasing percentage reduction in tensile strength. A reduced steel section would result in an increase in the deflection. It has been reported in Chapter 2 that the deflection of corroded beams initially decreased and then increased at higher extents of corrosion corresponding to changes in the bond strength. Initially the bond improved and then after a certain critical level was reached the bond rapidly decreased as corrosion products allowed free movement between the steel and the concrete. The superposition of both these effects leads to an increase in the deflection as the corrosion proceeds. Linear regression of the data yielded the following equation with a correlation of 0,967.

$$\frac{\Delta_{Pmax}^{corr}}{\Delta_{Pmax}} = 1,0+(0,434).\Delta f_t \qquad (4.3.3)$$

Deflection ratio at service load (Figure 4.1.5)(page 111)

The service load is defined as 2/3 of the maximum load carried by the beam. The deflection ratio at the service load is the ratio of the deflection in the corroded beam at the service load to the average deflection in the control beams at that load. The deflection at the service load increases with increasing amounts of corrosion which is in agreement with the deflections at the maximum load. Linear regression of the data yielded the following equation with a correlation of 0,896.

$$\frac{\Delta_{Pservice}^{corr}}{\Delta_{Pservice}} = 1,0+(0,029).\Delta_{ft} \qquad (4.3.5)$$

Where $\Delta_{Pservice}{}^{corr}$ is the service load deflection in the corroded specimens.

Ratio of work done to the maximum load (Figure 4.1.6)(page 112)

The integral of the load deflection graph represents the work done in deflecting the beam up to the load under consideration. The ratio of the work done is the ratio of the work done to the maximum load in the corroded specimen to the average

work done to that load level in the control specimens. The general trend of the load reducing and the deflection increasing has already been described above. The figure shows that the work required to deflect the beams to the maximum load decreases with increasing amounts of corrosion. As the work done is the integral of the product of the load and deflection, the deflection must be increasing at a slower rate than the load is decreasing. Linear regression of the data gives the following equation with a correlation of 0,866.

$$\frac{U_{Pmax}^{corr}}{U_{Pmax}} = 1,0-(0,016).\Delta f_T \qquad (4.3.5)$$

Where U^{corr}_{Pmax} is the work done to the maximum load for the corroded beams.

U_{Pmax} is the work done to that load in the control beams.

Δf_t is the percentage reduction in the tensile strength of the reinforcing bars.

Ductility Ratio using the maximum load (Figure 4.1.7)(page 113)
The ductility ratio is the ratio of the deflection at maximum load to the deflection at the yield load. As discussed above the deflection increases with increasing amounts of corrosion. For the ductility ratio to increase the plastic deflection must be increasing faster than the elastic deflection is.

Ductility ratio using the maximum load (graphic method)(Figure 4.1.8)(page 114)
The graphic method essentially gives the same result as the numerical method (see Section 3.2.2 for a description of the method). It provides slightly different results as it takes into account the shape of the load-deflection curve in determining the ratio between the plastic and elastic deflections. A similar trend to the numerical ductility ratio is evident, the initial decline is most likely due to the variation in the data.

Toughness index using the maximum load (Figure 4.1.9)(page 115)
The toughness index shows almost the identical trend to that of the ductility (ignoring the slight initial decline as it is within the range of the control specimens).

The increase in the toughness index suggest that corrosion affects the post yield work requirements more than the elastic work requirements.

Toughness index using the failure load (Figure 4.1.10)(page 116)
The figure shows an initial decline and then a increase in the toughness required to reach the failure load.

4.2 Closure

This chapter has presented the results of series two tests together with a limited discussion of the results. A more detailed discussion of the structural parameters studied, as well as a comparison with the results from series one, will be presented in Chapter 5.

MAXIMUM LOAD RATIO

FIGURE 4.1.2

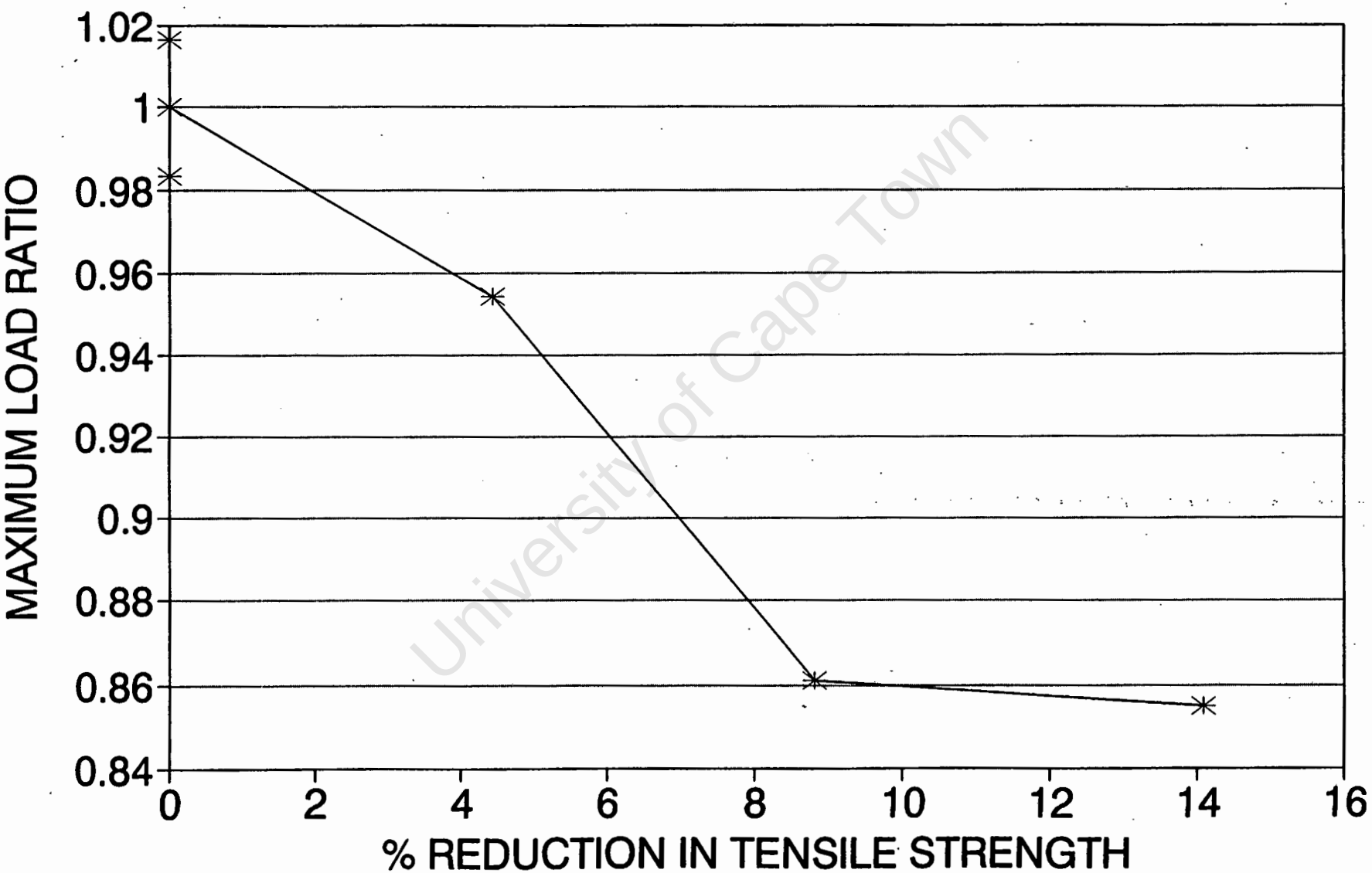

YIELD LOAD RATIO

FIGURE 4.1.3

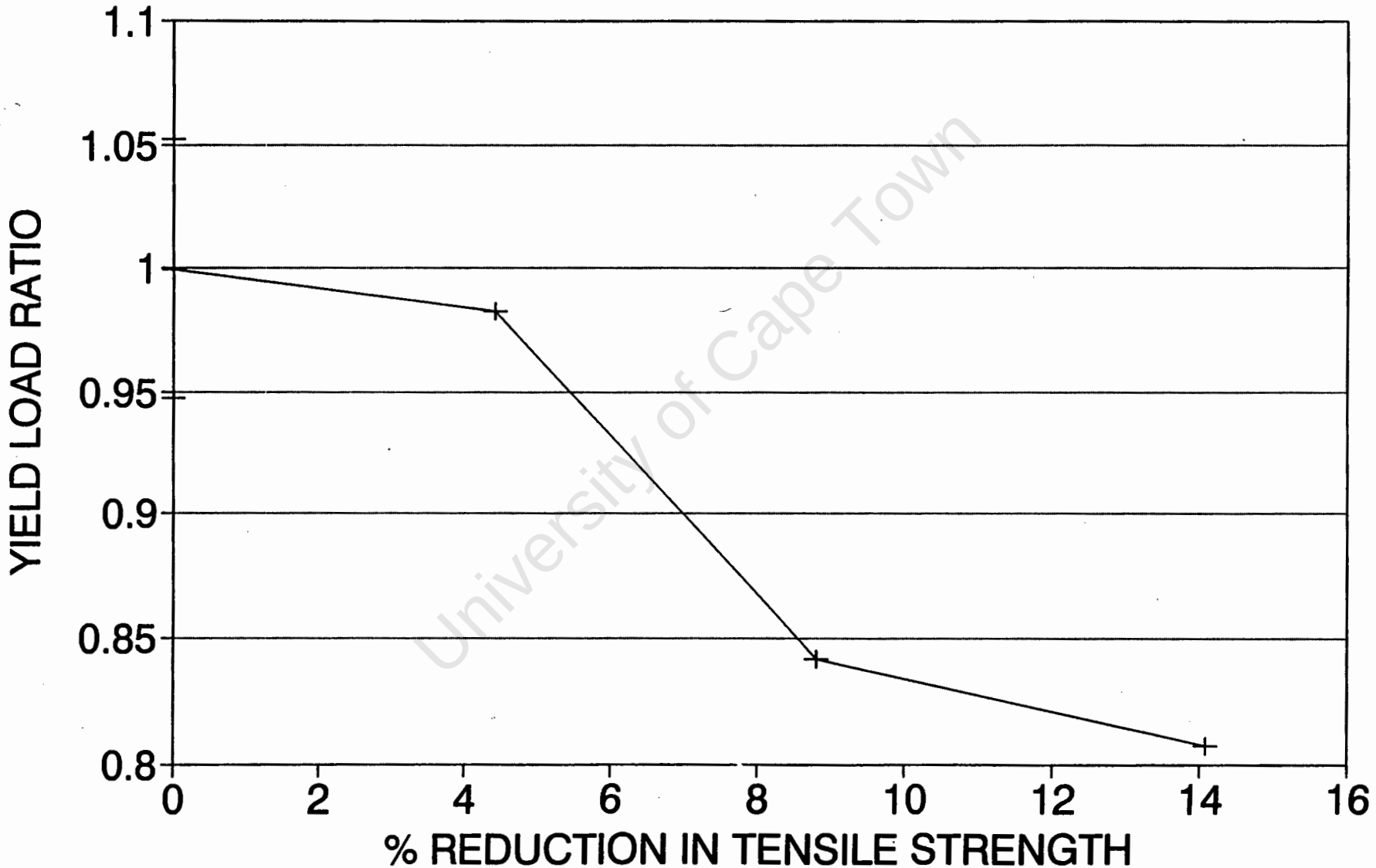

DEFLECTION RATIO (MAXIMUM LOAD)

FIGURE 4.1.4

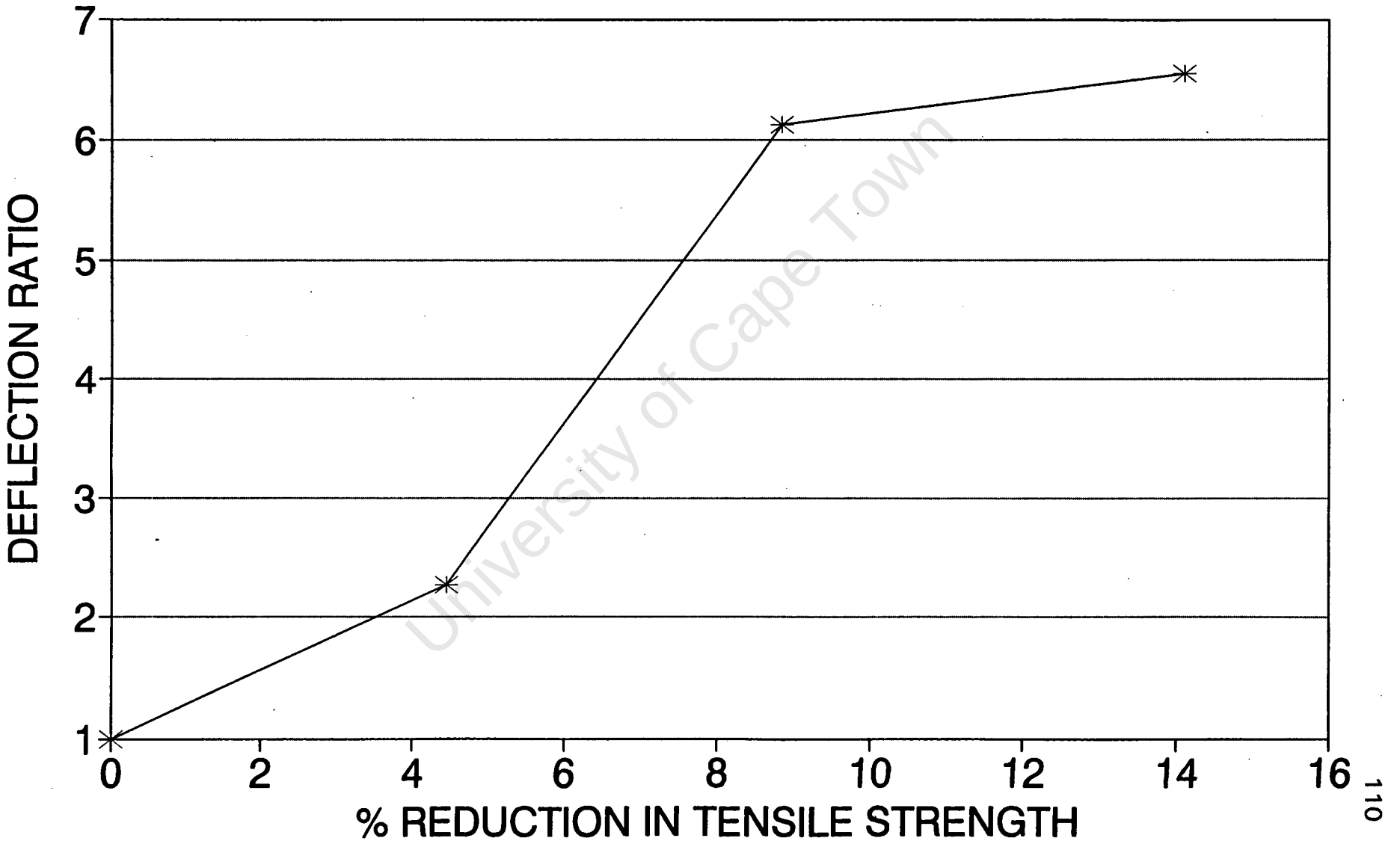

DEFLECTION RATIO (SERVICE LOAD)

FIGURE 4.1.5

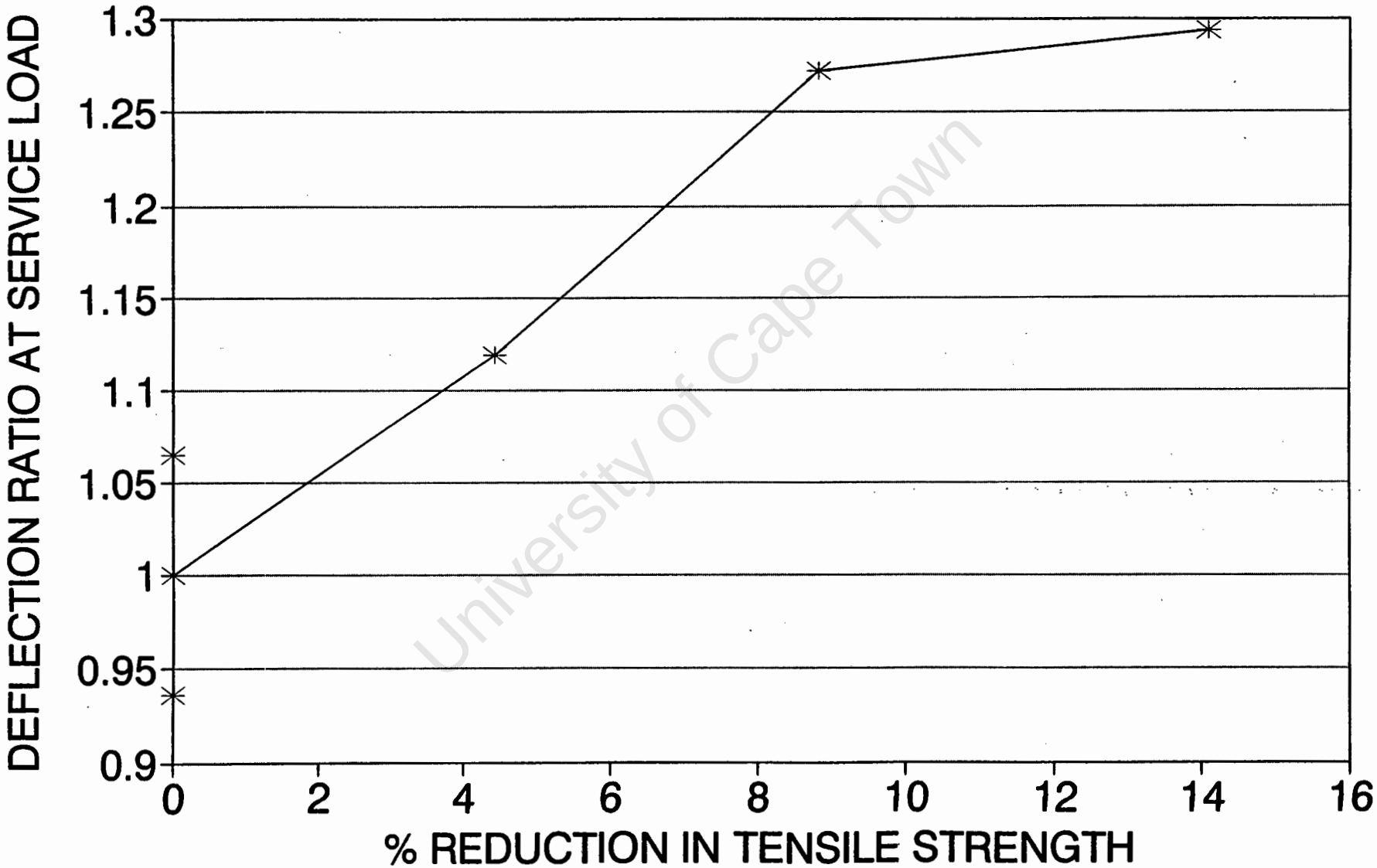

RATIO OF WORK DONE TO MAX LOAD

FIGURE 4.1.6

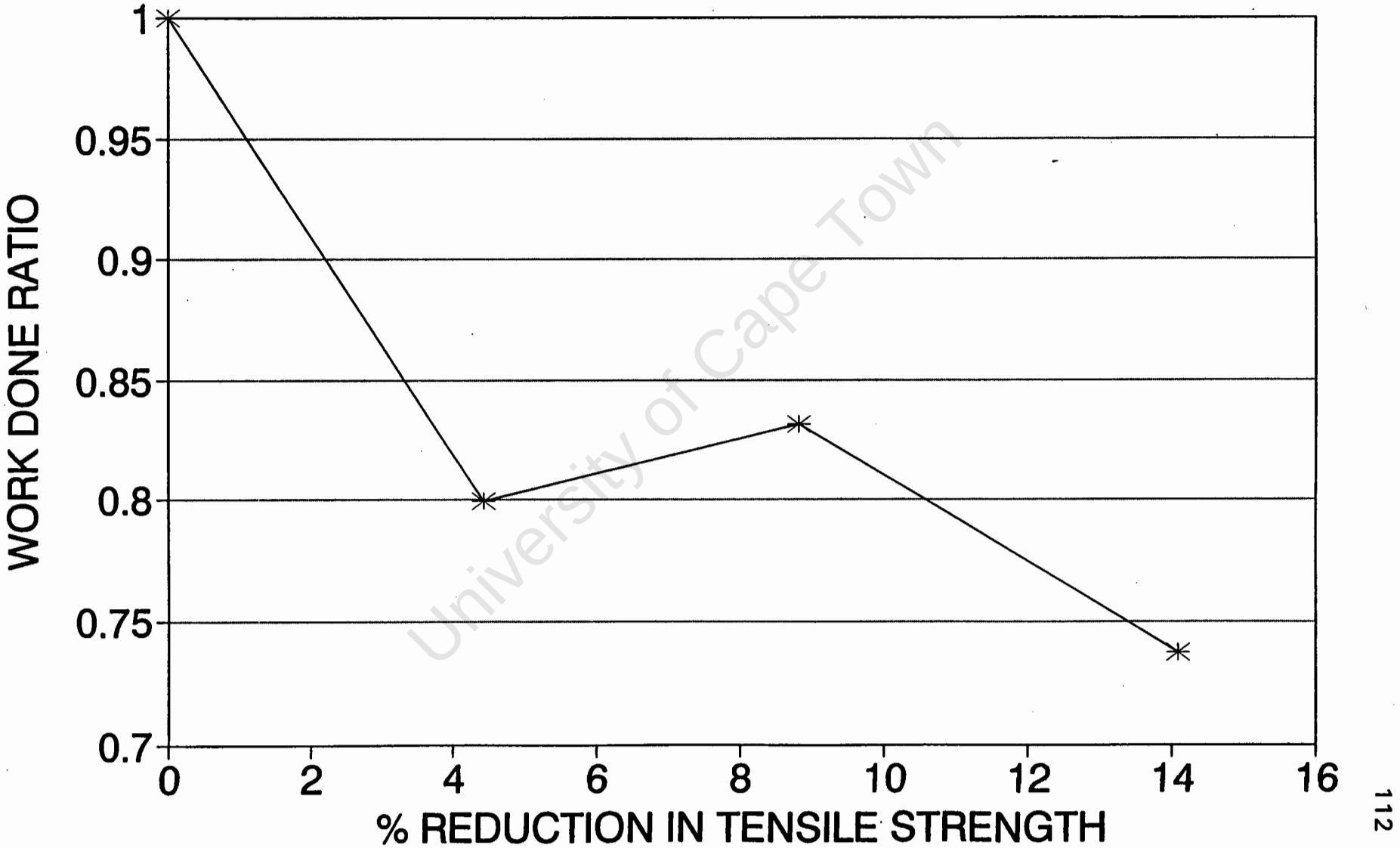

DUCTILITY RATIO

FIGURE 4.1.7

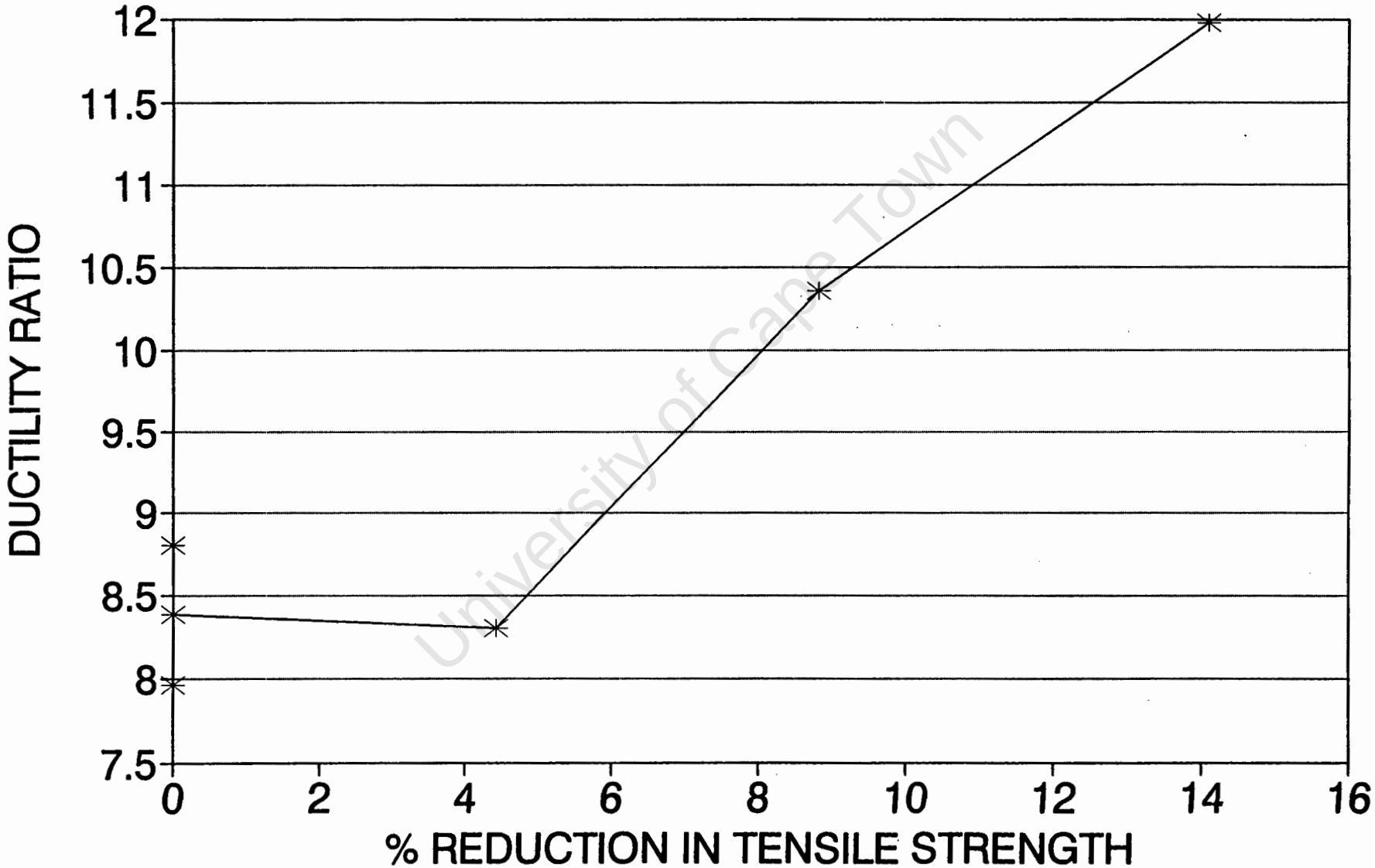

DUCTILITY RATIO (GRAPHIC METHOD)

FIGURE 4.1.8

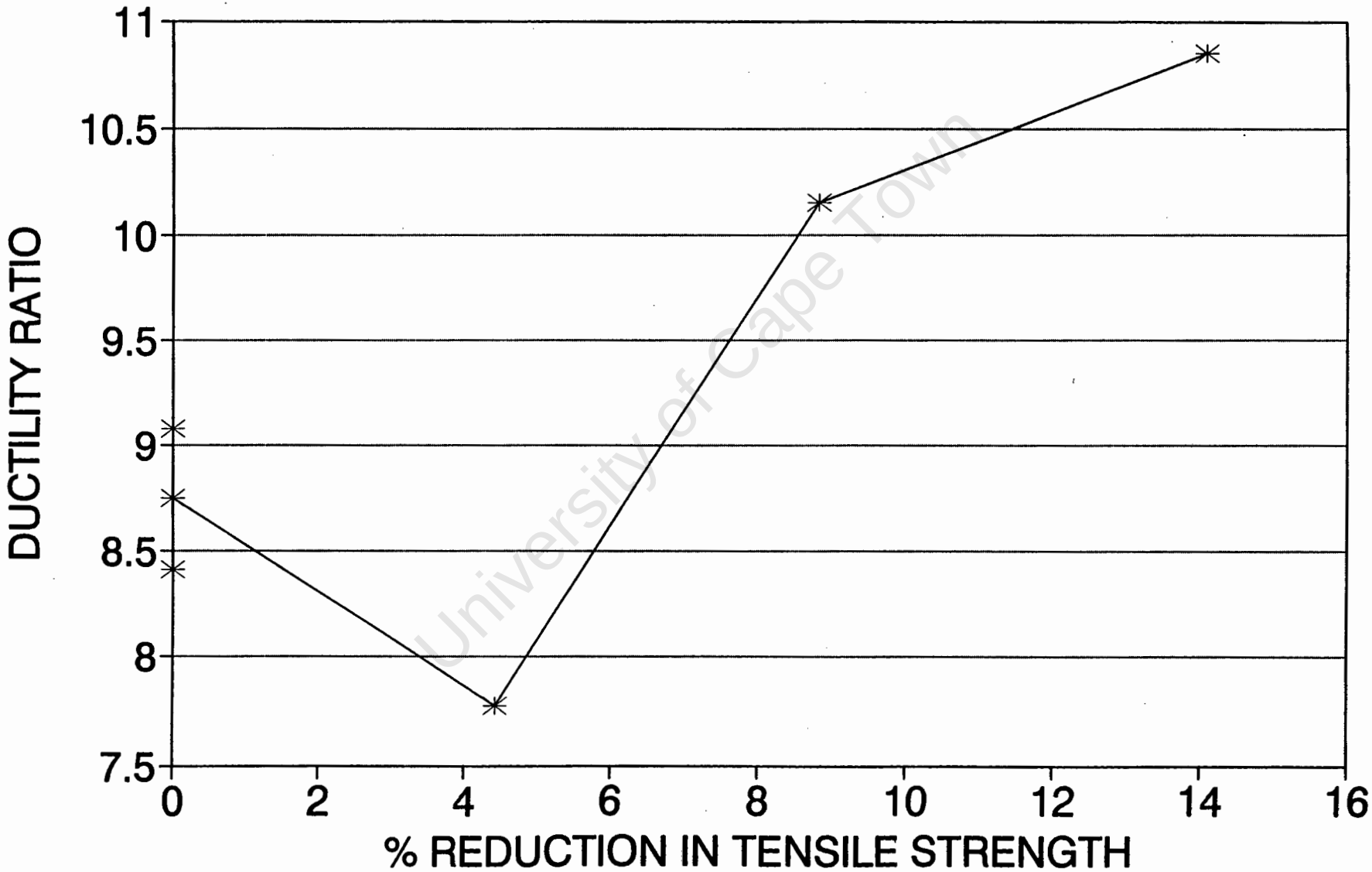

TOUGHNESS INDEX (MAXIMUM LOAD)

FIGURE 4.1.9

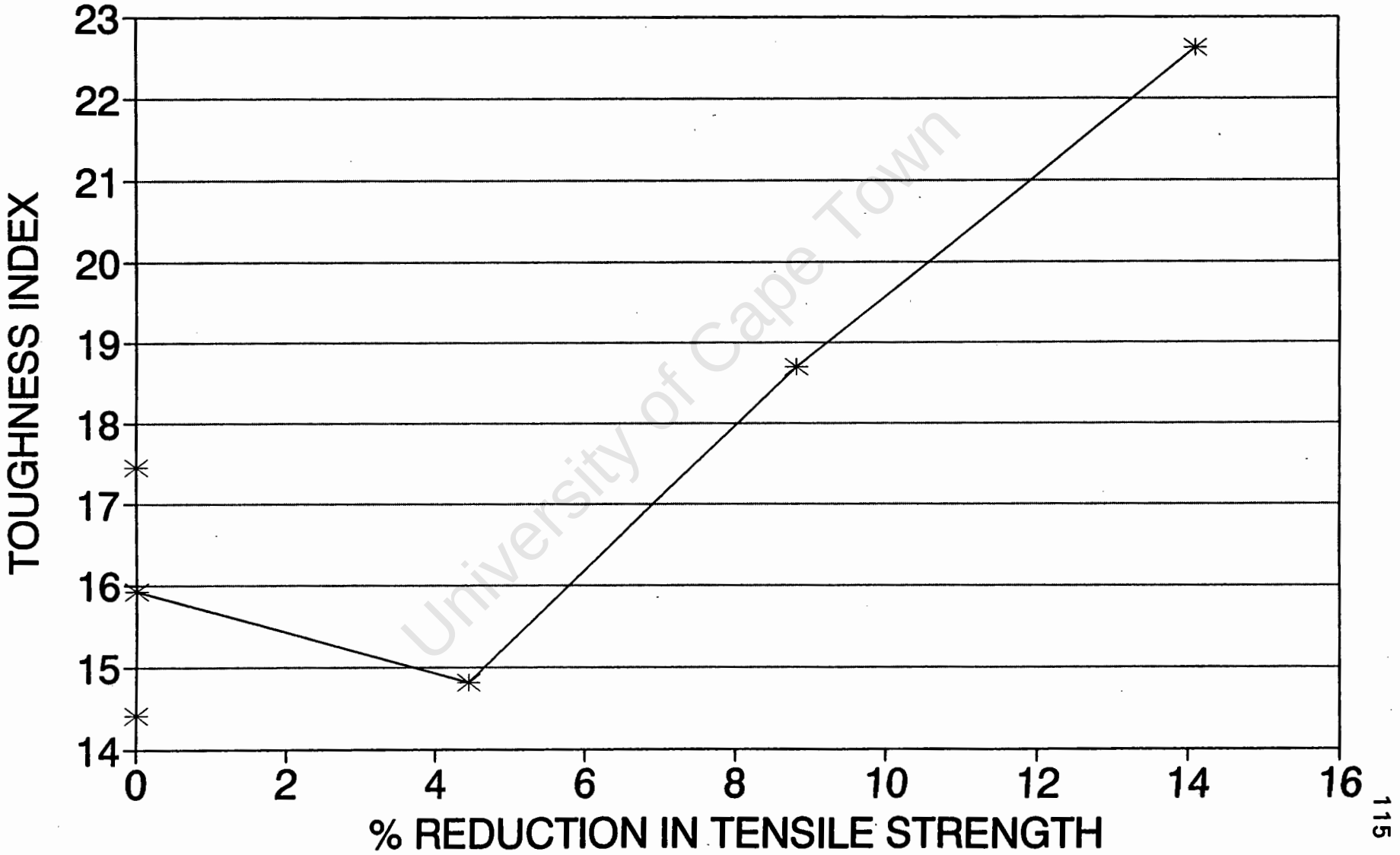

TOUGHNESS INDEX (FAILURE LOAD)

FIGURE 4.1.10

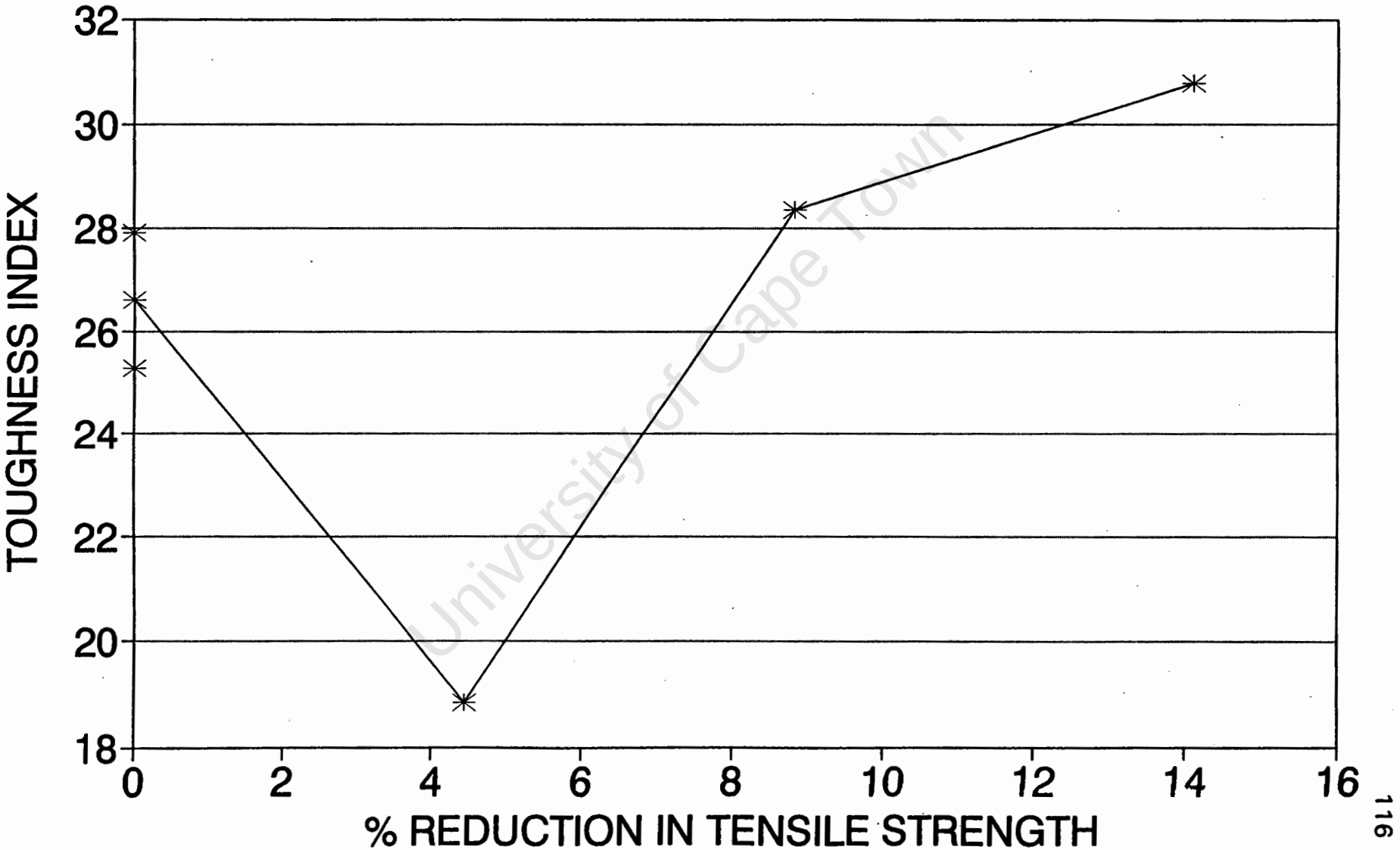

4.3 References

4.1) Beeby, A.W., Cracking, Cover, and corrosion of reinforcement, *Concrete International*, February, 1983, pp. 35-40.

4.4) Schiessl, P.(ed), *Corrosion of Steel in Concrete*, London :Chapman & Hall, 1988.

4.5) van Rensburg, J., *Van Wyk & Louw Consulting Engineers*, Personal communication, Pretoria, October, 1993.

4.6) Abdul-Hamid J. Al-Tayyib and Mohammad Shamim Khan, Corrosion rate measurements of reinforcing steel in concrete by electrochemical techniques, *ACI Materials Journal*, May-June, 1988, pp. 172-177.

4.7) Tachibana, Y., Kajikawa, Y. and Kawamura, M., The mechanical behaviour of RC beams damaged by corrosion of reinforcement, *Concrete Library of Japanese Society of Civil Engineers*, No 14, March, 1990, pp. 177-188.

4.8) Misra, S. and Uomoto, T., Effect of corrosion of reinforcement on the load carrying capacity of RC beams, *Procedings of the Japan Concrete Institute*, Vol. 9, No 2, pp. 675-680.

4.9) ASTM G1-81, Standard Practice for Preparing, Cleaning, and Evaluating Corrosion Test Specimens, July, 1981, pp. 89-94.

Chapter Five

Comparison of results with those from other investigators, and guidelines for the development of a possible analytical model to predict the effects of reinforcement corrosion on the load carrying capacity of reinforced concrete beams

5.0 Introduction

This chapter summarizes the effect of corrosion on the structural parameters studied in Chapters 3 and 4 and compares them with results obtained by other researchers. The significance of the effects of reinforcement corrosion is examined to highlight the need to be able to predict the effects of reinforcement corrosion. Guidelines are given for the development of an analytical model that could be used to predict the effects of reinforcement corrosion on the load carrying capacity of reinforced concrete beams.

5.1 Significance of the effects of reinforcement corrosion on the performance of reinforced concrete beams

The effects of reinforcement corrosion in a structure can have economic as well as structural implications. The economic consequences of reinforcement corrosion will depend on the type of element and its use. If the deterioration of the element aesthetically does not pose any problems then reinforcement corrosion does not have any economic consequences. If however the corrosion causes structural deterioration or aesthetic deterioration that cannot be tolerated, then the effects

of corrosion have to be taken into account at the design or repair stage, in which case corrosion will have economic consequences. The effects of reinforcement corrosion on structural or other performance criteria of reinforced concrete elements highlight the need to be able to make accurate service life predictions. Accurate service life predictions improve safety and reduce the costs associated with using reinforced concrete.

The four most important effects on the structural performance of reinforced concrete beams affected by corrosion are :

- Decrease in the maximum load carrying capacity.
- Increase in the deflection at the same load level.
- Decrease in the amount of work required to reach the maximum load.
- Smoothing of the load-deflection curve.

Decrease in the maximum load carrying capacity

A reduction in the maximum load carrying capacity is a disadvantage from a safety point of view as the design maximum load may after a certain amount of corrosion be more than the remaining maximum load carrying capacity of the element. When this occurs failure may be imminent even when the element is still under service loads and normally considered as safe. The severe rust staining and cracking of corroding reinforced concrete usually provide sufficient early warning that deterioration is occurring. There are however many examples where the structural integrity of an element has been severely impaired even though there are no external signs of deterioration. This type of deterioration poses major safety problems.

Increase in the deflection at the same load level

The increase in deflection obviously poses economic consequences if this effect is allowed for in the design stage. Additional deflections in the plastic range are however beneficial as they will provide more early warning signs that the element is being affected by corrosion in the event that rust staining and spalling is not occurring.

Decrease in the amount of work required to reach the maximum load

A decrease in the amount of work required to deform a structure has serious implications for the dynamic load resistance of a structure. Most gravity loads in practice become dynamic loads if the structure deflects rapidly. A decrease in the dynamic load resistance with increasing amounts of corrosion would obviously make the structure more susceptible to dynamic failures and more unsafe.

Smoothing of the load-deflection curve

The stepped behaviour observed in uncorroded beams, such as the control beams in this investigation, as local bond and anchorage failures occur was not observed in the corroded specimens. The greater the corrosion extent was the smoother the load-deflection curve was. Sudden large increases in the deflection, as is possible with gravity loads, can be sufficient to approximate dynamic loading. If the dynamic load is close to the maximum load capacity of the element then a sudden catastrophic failure may result. Corrosion of reinforcement therefore has beneficial effect on the structures response to loading, therefore making the element more resistant to dynamic loads and safer. This effect is however likely to be reversed at very high levels of corrosion were the corrosion products surrounding the steel may cause a sudden widening of cracks as the ribs on the bars move relative to the surrounding concrete. Corrosion therefore could increase the stepped behaviour thus making the structure more susceptible to dynamic failure.

5.2 Summary of the effects of reinforcement corrosion on structural performance of reinforced concrete beams

Table 5.2.1 is a summary of the parameters for both series 1 and 2. The parameters are defined in section 3.3. The table shows the general trend for each parameter with increasing amounts of corrosion. These trends can be taken as valid only for the particular specimens examined and only for the range of corrosion that was used in this investigation. Hinting that the trends will continue beyond the examined range is merely speculative, the actual trends may in fact change completely at much higher extents of corrosion.

Table 5.2.1 Summary of structural parameters.

Areas where reinforcement was corroded	Series one	Series two
Maximum load ratio		
Top	Constant	
Bot	Constant	
Top + Bot	Constant	Decreases
Yield load ratio		
Top	Constant	
Bot	Constant	
Top + Bot	Constant	Decreases
Deflection ratio at maximum load		
Top	Increases	
Bot	Increases	
Top + Bot	Increases	Increases
Deflection ratio at service load		
Top	Decreases	
Bot	Decreases	
Top + Bot	Decreases	Increases
Ratio of the work done to the maximum load		
Top	Decreases	
Bot	Decreases	
Top + Bot	Decreases	Decreases
Ductility ratio		
Top	Decreases	
Bot	Decreases	
Top + Bot	Decreases	Increases
Ductility ratio (graphic)		

Areas where reinforcement was corroded	Series one	Series two
Top	Decreases	
Bot	Decreases	
Top + Bot	Decreases	Increases
Toughness index using maximum load		
Top	Increases	
Bot	Increases	
Top + Bot	Increases	Increases
Toughness index using failure load		
Top	No clear trend	
Bot	No clear trend	
Top + Bot	No clear trend	Decreases then increases

The summary of the data shows that for some of the parameters in the series one tests, the results are in disagreement with the results from the series two specimens. Differences should be expected since the beams from series two were shorter, were reinforced more heavily and contained stirrups. The effect of including stirrups can play a significant role in the behaviour of the beams. Stirrups have the effect of confining the concrete and thus improving the ductility. The confining effect is especially important in concrete affected by reinforcement corrosion where cracking and spalling affect the compressive section. Stirrups also allow much greater loads to be carried by preventing shear failures (beam T1T was the only beam that displayed shear cracks) which could have resulted in a much lower load carrying capacity.

The critical level of corrosion damage above which corrosion has a significant negative effect on the structural performance may also be reached at different levels of corrosion for different types of specimens. If this is the case then differences between series one and two can be explained if series one represents

the changes in the early stages of corrosion and series two the changes in more advanced stages of corrosion.

5.2.1 Discussion of results

Maximum load carrying capacity

Other investigators[5.1,5.2] have performed similar tests on corroded beams of similar dimensions and with stirrups, and found that the maximum load carrying capacity of the beams decreased with increasing amounts of corrosion. This is in agreement with the results obtained in this investigation with series two beams (with stirrups). If the behaviour of the series one beams represents the behaviour in the early stages of corrosion (no corroding stirrups were present to cause additional disruption of the concrete), then the constant maximum load found in this investigation in series one beams could represent the behaviour before the beams are significantly affected by corrosion. Once this critical level has been reached then the maximum load carrying capacity starts to reduce. Al-Sulaimani et al[5.3] performed similar tests over a wide range of corrosion extents. They clearly established a critical level beyond which the maximum load carrying capacity was affected. This level was at 1,5% metal mass loss, about twice the level at which the first cracks appeared. For series one the critical level is above 1,85% metal loss (12,5% tensile loss) and below 0,65% metal loss (14,1% tensile loss) for series two beams. From a theoretical point of view, a decrease in the maximum load carrying capacity of the beams can be expected as corrosion is decreasing the amount of steel that is available to resist the applied loads.

Yield load

The yield load can similarly be expected to reduce with increasing amounts of corrosion as the steel cross-section is decreasing. The constant yield load experienced in series one tests could be results that are below the critical corrosion level, where the loss of load carrying capacity of the steel does not affect the load carrying capacity of the beam as a whole. Series one beams did not have stirrups which would cause an additional disruption to the concrete if they were corroded. It is therefore possible that the less damaged series one beams could be below the

critical damage level. Series two beams represent results above the critical corrosion level where greater extents of corrosion damage reduce the load carrying capacity of the steel and concrete sufficiently to reduce the load carrying capacity of the beam as a whole.

Deflection ratio

Misra and Uomoto[5.1] also found that the deflections at maximum load increased with increasing amounts of corrosion which is in accordance with the results from both series. It is possible that the deflection could initially decrease as the bond strength improves at low levels of corrosion, and thereafter increase as the corrosion products form a lubricating layer, weakening the bond and disrupting the concrete's structural integrity. The deflections at the service load are in conflict with each other with series one showing a decrease and series two an increase with increasing amounts of corrosion. This supports the idea that different types of specimens are affected by corrosion at different levels of corrosion. Theoretically deflections are essentially governed by the bond in the elastic and early plastic ranges and then mainly by the amount of steel in the section in the plastic range. As both these parameters are decreasing it can be expected that the deflections should be increasing with increasing amounts of corrosion.

Ratio of the work done up to the maximum load

The decreasing amount of work required to deflect the beams up to the maximum load is in agreement with the results of Misra and Uomoto.[5.1] A decreasing amount of energy required to deflect the beams means that the load reduction is occurring at a faster rate than the deflection is increasing.

Ductility ratio

Series one results showed a decreasing ductility ratio (a more brittle failure) which is in contrast with the results from series two that displayed more ductile behaviour with increasing amounts of corrosion. The ductility ratio does not provide much useful information as it is the ratio of two parameters on a particular specimen. This ratio can therefore show little or no variation even though the behaviour of the beam is changing if both parameters are being affected in a similar way.

Toughness index using P_{max}

Series one and series two are in agreement with the toughness index increasing with increasing amounts of corrosion. For the toughness index to be increasing with increasing amounts of corrosion the difference between the energy up to the maximum load and the energy up to the yield load is increasing. For this to occur, corrosion must be having a greater effect on the post yield behaviour than the elastic behaviour.

5.2.2 Comparison with other researchers' results

The limited number of results available from other researchers makes valid comparison with other results questionable. The difference between the specimens, the method of corrosion as well as different load conditions could have a significant, as yet undefined effect, which could invalidate comparisons. The available results for the maximum loads and the deflections at the maximum load have been made dimensionless and have been defined here as the 'Load number' and the 'Deflection number'. A 'Corrosion number', defined in terms of the corrosion current density and the time under corrosion, has been used as the basis for comparisons. The corrosion number is a prediction, similar to Faraday's mass loss prediction which was shown in section 3.3 not to be a good basis for comparison. The current density and time are the commonly quoted parameters when referring to galvanic corrosion and were therefore used as the basis for comparison. The dimensionless numbers have been defined here in such a way as to include structural properties such as cube strength, span, section breadth and depth because these properties are known to affect the load carrying capacity and deflection of beams. The dimensionless numbers and the corrosion number have been defined as follows :

$$\textit{Corrosion number} = \textit{Current density} \,.\, \textit{Time} \qquad (5.2.1)$$

Where : Current density is in (m.Amp/cm^2)
Time is the time under corrosion (Days)

$$Load\ number = \frac{P_{max}}{f_{cu}.b.h} \quad (5.2.2)$$

$$Deflection\ number = \frac{Span}{\Delta_{Pmax}} \quad (5.2.3)$$

f_{cu} is the concrete cube strength (MPa)
b is the breadth of the beam (mm)
h is the depth of the beam (mm)
Span is the beam's span (mm)

Figure 5.2.1 (pp. 128) shows the load number for : series 1 and 2, Misra and Uomoto's series A and B results[5.1] and Tachibana et al's results[5.2]. **Figure 5.2.2** (pp. 129) shows the deflection number for : series 1 and 2, Misra and Uomoto's series A results[5.1] and Tachibana et al's results[5.2]. **Tables 5.2.2 to 5.2.4** provide a summary of the investigators results used in Figures 5.2.1 and 5.2.2. The specimens in each of the three sets of results given were all corroded and tested in a similar way to the beams this investigation. Misra and Uomoto's series B specimens did however have two load points at the 1/3 and 2/3 span points and not a single midspan load point.

The general trend of a reduction in the load number with increasing corrosion number is evident in Figure 5.2.1. The large differences between the load numbers for each set of results is a reflection of how efficiently the section is being used. Misra's series A specimens have a 2% area of steel to concrete ratio, compared with the series two specimens that have a 0,46% area of steel to concrete ratio. From this it can be expected that Misra's series A specimens would have a greater load number as more efficient use is being made of the section's capacity, and the series 2 results would have a lower load number as less efficient use is being made of the section's capacity.

Figure 5.2.2 shows an increasing deflection number (i.e. a decreasing deflection) with increasing corrosion number. The results from series 2 are the only ones that show an increase in the deflection with increasing amounts of corrosion. The

different definition of the deflection ratio, using the maximum load level in the corroded beam to obtain the deflection in the uncorroded beam, accounts for the different trend between the deflection ratio and the deflection number. The differences in the deflection numbers between the sets of results is also a reflection of how efficiently the section is being used. The more heavily reinforced sections of Misra and Tachibana can be expected to have a bigger deflection number (i.e. small deflections for the given span) than the lighter reinforced sections of series 1 and 2 (which would have big deflections for the given span).

Table 5.2.2 Summary of Tachibana et al's results[5.2]

b mm	h mm	A_s	Stirrups ?	f_{cu} MPa	Span mm	m.Amp. Days /cm^2	P_{max} kN	Δ_{Pmax} mm
150	200	2Y16	None	35,6	1500	0	61,6	10,0
						1,5	61,4	10,0
						3,0	55,3	8,5
						5,0	52,5	6,5
						7,5	54,2	6,5

Table 5.2.3 Summary of Misra and Uomoto's results, Series A[5.1]

b mm	h mm	A_s	Stirrups ?	f_{cu} MPa	Span mm	m.Amp. Days /cm^2	P_{max} kN	Δ_{Pmax} mm
100	200	2Y16	R6 @ 170 mm	29,4	1700	0	94,2	12,0
						2,0	90,3	10,5
						4,0	86,3	8,8

LOAD NUMBER

FIGURE 5.2.1

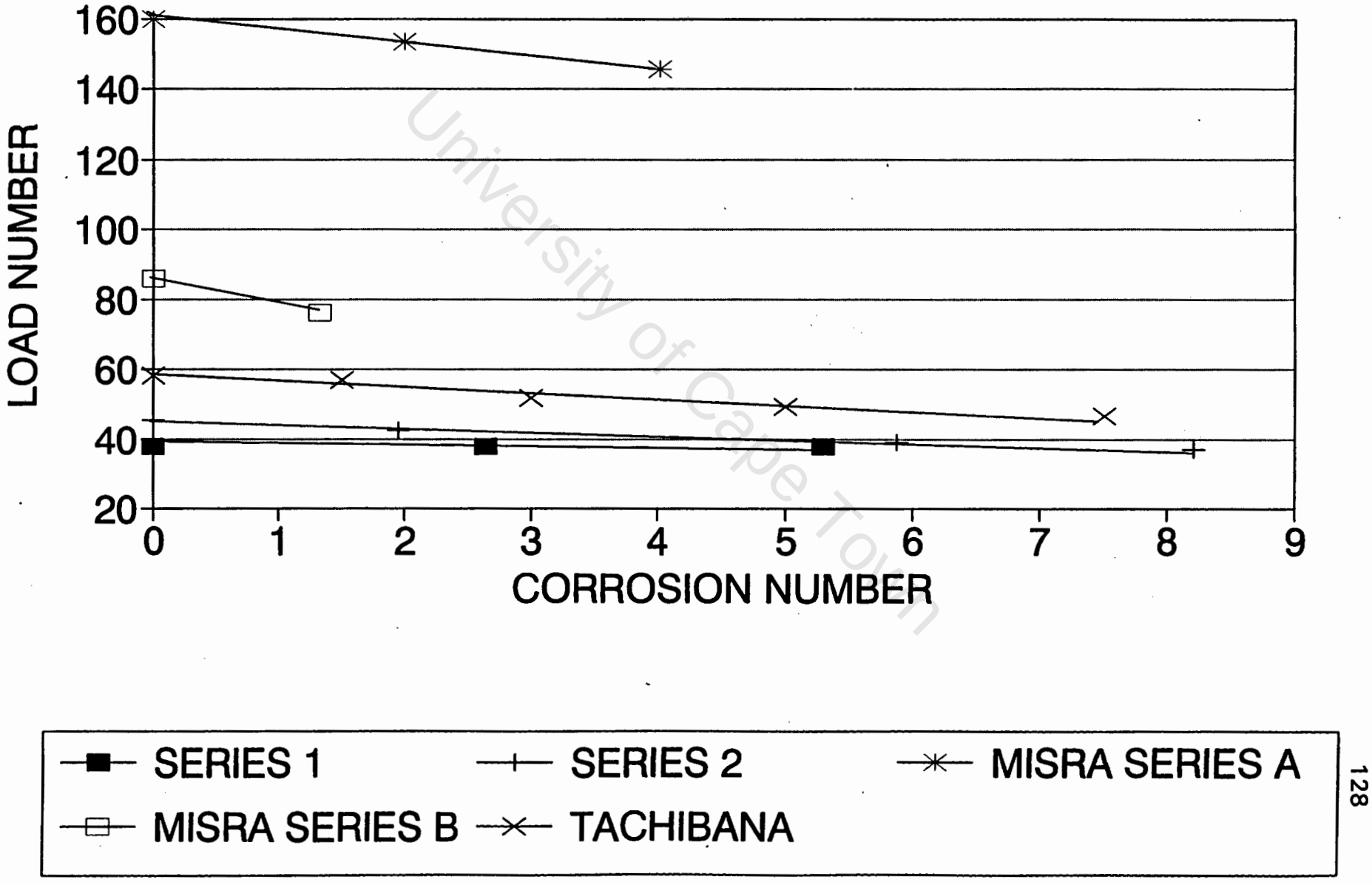

DEFLECTION NUMBER

FIGURE 5.2.2

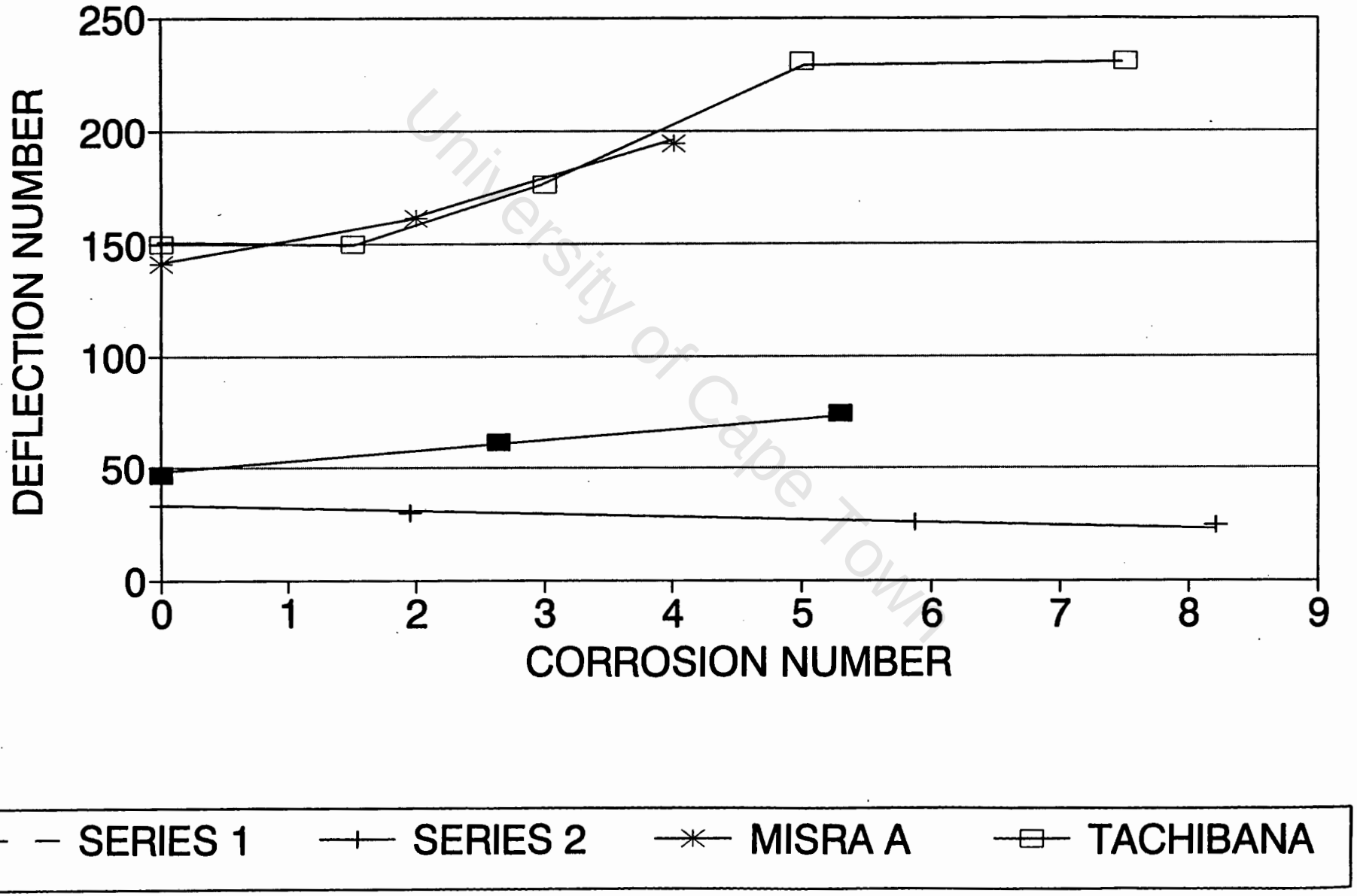

Table 5.2.4 Summary of Misra and Uomoto's results, Series B[5.1]

b mm	h mm	A_s	Stirrups ?	f_{cu} MPa	Span mm	m.Amp. Days /cm^2	P_{max} kN	Δ_{Pmax} mm
100	150	2Y10	None	37,3	1000	0	48,0	-
						1,3	40,2	-

5.3 Guidelines for the development of an analytical model to predict the effects of reinforcement corrosion on the ultimate load carrying capacity of reinforced concrete beams

The effect that corrosion has on the structural performance of reinforced concrete beams is a result of several factors that affect the performance. It can be assumed that these factors also interact in such a way that they further affect the performance of the concrete. The principle effects that corrosion has on reinforced concrete sections are as follows :

- Reduction in the area of (tension) steel
- Reduction in the available area of concrete in compression
- Reduction in bond strength

The development of an analytical model should isolate the effect that each of the above has on the structural performance and then try to incorporate all the effects into one model. The load carrying capacity of beams is one of the most important structural performance criteria and therefore will be considered in the development of this model.

5.3.1 Loss of the area of steel

Corrosion reduces the amount of steel available to resist applied loads. In the case of chloride induced corrosion, the loss of steel may be very localized causing deep pits. At certain intervals along the bar the cross-sectional area may be reduced significantly while at other parts there may be no reduction at all. The parts where the cross-section has been reduced the most are the critical areas and the reduction at these points should be assumed over the entire length of the bar when using the model.

Assuming a SABS 0100[5.4] concrete compression block (as shown in **Figure 5.3.1**), for axial equilibrium :

$$0{,}45f_{cu}(0{,}9x)b = 0{,}87f_y A_s \qquad (5.3.1)$$

where : f_{cu} is the concrete cube strength
x is the depth to the neutral axis
b is the breadth of the beam
f_y is the yield stress of the steel
A_s is the area of tension steel

For a simply supported beam of span L with a single transverse concentrated load of P at midspan, moment equilibrium about the centroid of the concrete compression block gives :

$$\frac{P}{2}.\frac{L}{2} = 0{,}87f_y A_s(d-0{,}45x) \qquad (5.3.2)$$

From Equation 5.3.1

$$x = \frac{0{,}87f_y}{0{,}405f_{cu}\,b}.A_s \qquad (5.3.3)$$

If A_s is reduced to α_s, then x is reduced to Equation 5.3.4
and P is reduced to P^*_s as given by Equation 5.3.5

$$x = \frac{0{,}87 f_y}{0{,}405 f_{cu}\, b}(\alpha_s A_s) \qquad (5.3.4)$$

$$P_s^* = \frac{3{,}48 f_y}{L}(\alpha_s A_s)(d - 0{,}45(\alpha_s x)) \qquad (5.3.5)$$

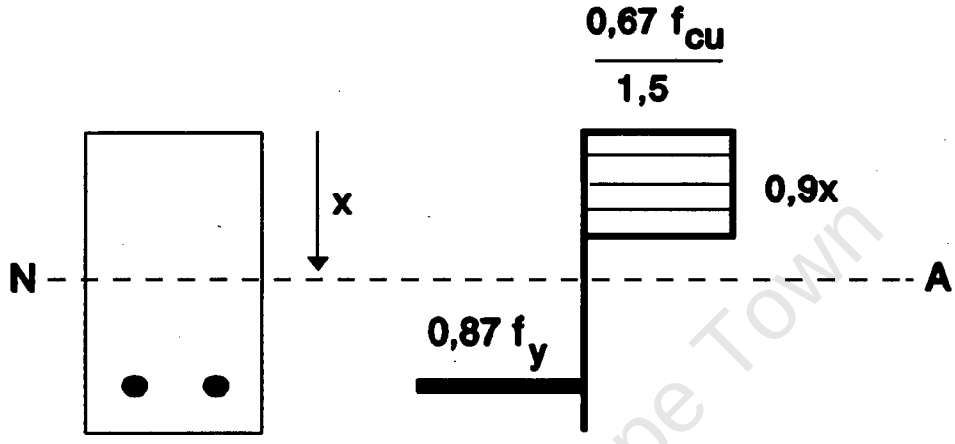

Figure 5.3.1 SABS 0100[5.4] compression block at ultimate conditions.

5.3.2 Loss of compression zone

If corrosion of steel in the compression zone occurs then there will be a reduction in the area of concrete available for compression resistance. If it is assumed that the concrete is disrupted to a depth of $\alpha_c x$ (from the top surface), then Equation 5.3.2 can be developed into :

$$P_c^* = \frac{3{,}48 f_y}{L}(A_s)[(d - \alpha_c x) - (1 - \alpha_c)0{,}45x] \qquad (5.3.6)$$

The depth can only be disrupted up to a depth equal to the cover plus the bar diameter.

5.3.3 Loss of bond

The load carrying capacity of a reinforced concrete beam is directly related to the bond strength between the steel and the concrete. If there was no bond or end

anchorage at all then a beam would be able to carry almost no load and the force in the tension reinforcing would be zero. If the bond strength is assumed to be at its maximum then the force in the tension reinforcing at ultimate would be equal to ($0{,}87f_yA_s$). Ignoring the effects of strain incompatibility and a changed load carrying mechanism, if the bond strength is reduced to α_b then Equation 5.3.2 can be developed into :

$$P_b^* = \alpha_b\left(\frac{3{,}48f_y\ A_s}{L}\right)\left(d-\frac{(\alpha_b\ x)}{2}\right) \qquad (5.3.7)$$

5.3.4 Loss of steel, loss of compression zone and loss of bond

From Equations 5.3.5, 5.3.6 and 5.3.7 the effect of a simultaneous loss of tension steel, compression zone and bond strength changes Equation 5.3.2 into :

$$P^* = \alpha_b\frac{3{,}48f_y}{L}(\alpha_s\ A_s)[(d-\alpha_c x)-\alpha_s(1-\alpha_c)\alpha_b\ 0{,}45x] \qquad (5.3.8)$$

The alpha factors vary with the percentage of corrosion as shown schematically in **Figure 5.3.2**. The variation of each of these with the percentage of corrosion can be substituted into Equation 5.3.8 to give the variation of the load carrying capacity with percentage of corrosion. It has been shown in section 2.6.4 that bond strength initially increases until the corrosion products act as a lubricating layer between the steel and the concrete causing a reduction in the bond strength, α_b therefore shows an initial increase. Thereafter the bond strength will continue to reduce to some level and then remain constant (or nearly constant) as no further loss of bond would occur once the bond strength has reduced to the frictional bond strength. The remaining area of steel, α_s, is a straight line relationship, with α_s equal to zero when there has been 100% steel mass loss. This would be a straight line for mass loss or tensile loss as both are linear relationships. The α_c factor increases with increasing amounts of corrosion until $\alpha_c x$ equals either the cover plus bar diameter or the depth to the neutral axis, x, α_c remaining constant

thereafter. Initially there will be no disruption to the concrete, at higher amounts of corrosion increasing amounts of disruption will occur, hence the initial curved shape.

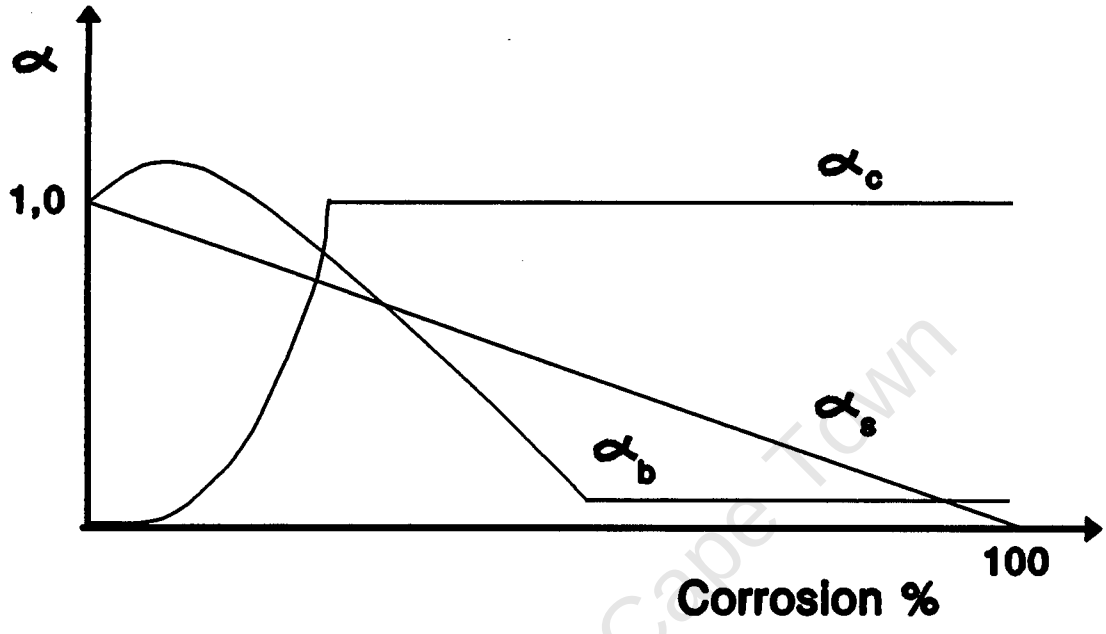

Figure 5.3.2 Variation of alpha factors with percentage corrosion (schematic)

5.3.5 Comparison of series two results with model

Cabrera and Ghoddoussi[5.5] obtained the variation of bond strength with the percentage of corrosion (mass loss). **Figure 5.3.3** is derived from their results by expressing the bond strength in terms of the uncorroded value to give the variation of α_b with the corrosion percentage mass lost. **Figure 5.3.4** (pp. 136) shows the maximum load ratio as predicted by the model (Equation 5.3.8) together with the results from series 2 beams. The corrosion percentage is the percentage tensile loss in the steel. The minor effect that α_c has on the load carrying capacity has been ignored in Figure 5.3.4. From 4 percent corrosion the α_b factor was kept constant with increasing amounts of corrosion to make the model fit the experimental points at 8,8% and 14,1% corrosion. The bond strengths given in Figure 5.3.3 were obtained from pull out tests of bars imbedded in cubes. The deviation of the model from the experimental points at corrosion percentages

greater than 8,8% could suggest that the pull-out test results are not totally valid for beams (assuming the model is correct). If the point were the bond strength no longer decreases for beams is at a lower corrosion percentage than for pull-out tests, then using a constant α_b factor from a certain level of corrosion can be justified.

The limited number of results in series 2, especially at low percentages of corrosion, make comparisons difficult. The initial increase in the load carrying capacity may have been displayed if there were specimens between 0 and 2 percent corrosion. The exact variation of the alpha-factors with corrosion percentage could make this model accurate enough to be used to predict the load carrying capacity of beams at different levels of corrosion. This model is highly sensitive to the large reductions in bond strength that result from small amounts of corrosion. The relatively slow decrease in the area of steel with percentage corrosion results in the loss of area of steel playing only a minor role in the load reduction in this model. A better definition of how these and other possible factors vary with corrosion is therefore essential if the model is to be able to predict the effect of corrosion on the load carrying capacity.

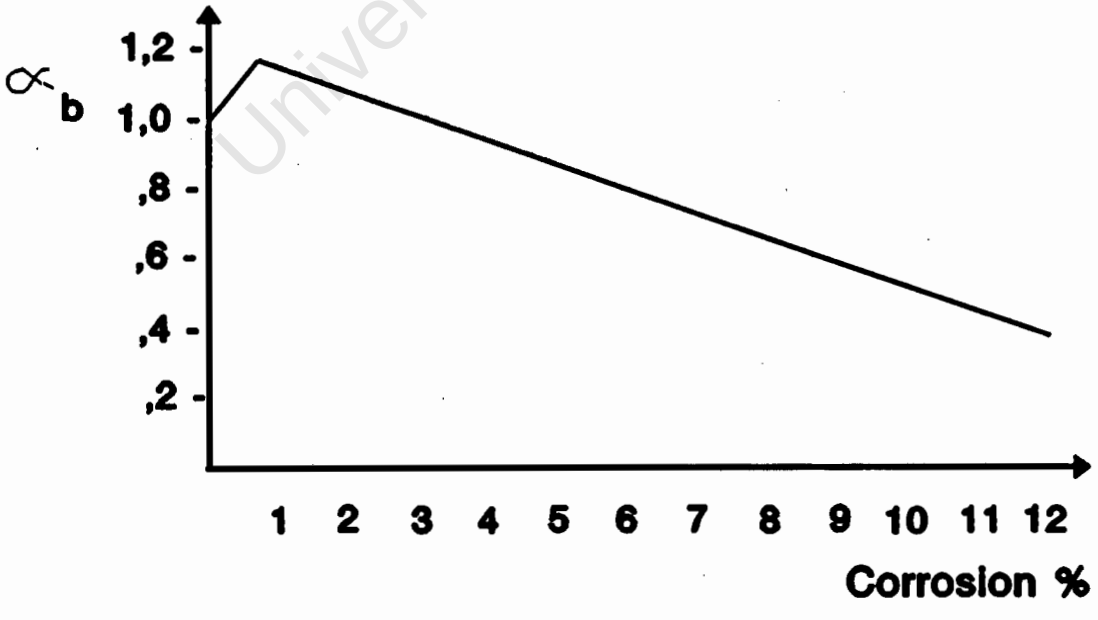

Figure 5.3.3 Variation of α_b with percentage corrosion

MAXIMUM LOAD RATIO

FIGURE 5.3.4

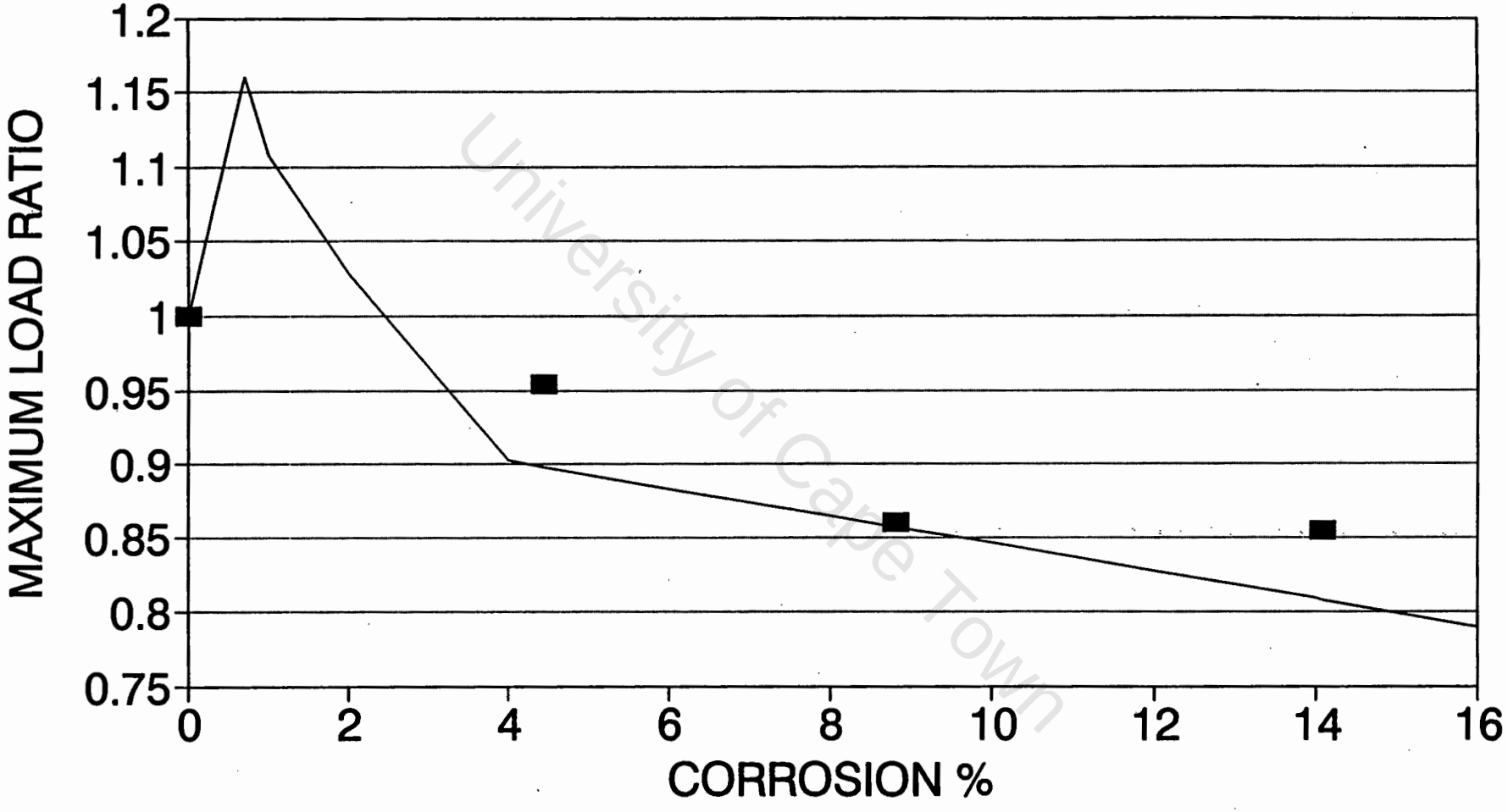

5.4 Guidelines for the development of an analytical model to predict the effects of reinforcement corrosion on the deflection at ultimate load in reinforced concrete beams

The factors which affect the deflection characteristics of reinforced concrete beams affected by reinforcement corrosion are :

- Reduction in the area of (tension) steel
- Reduction in the section depth
- Reduction in bond strength
- Reduction in the section stiffness

The development of a model to predict the deflection characteristics of beams affected by reinforcement corrosion is extremely complex. The deflection characteristics are dependant on the integral of the above effects along the length of the beam, whereas the load carrying capacity is only dependant on these effects at the most critical point. The development of a model similar to the one in section 5.3 would be too simplified and will therefore not be considered here.

5.5 Closure

This chapter has presented the significance of the effects of reinforcement corrosion on the performance of reinforced concrete beams in general terms, and how these effects could influence the design process. The summary of the results of this investigation were presented and discussed in relation to results of other researchers before making comparisons of the results. The guidelines presented for the development of the analytical model emphasized the need to have the variation of the alpha factors with corrosion more clearly defined.

5.6 References

5.1) Misra, S. and Uomoto, T., Effect of corrosion of reinforcement on the load carrying capacity of RC beams, *Proc. Japan Conc. Inst,* Vol 9, No 2, 1987, pp. 675-681.

5.2) Tachibana, Y., Kajikawa, Y., Kawamura, M., The mechanical behaviour of RC beams damaged by corrosion of reinforcement, *Concrete Library of Japanese Society of Civil Engineers*, No. 14, March 1990.

5.3) Al-Sulaimani, G.J., Kaleemullah, M., Basunbul, I.A. and Rasheeduzzafar, Influence of corrosion and cracking on bond behaviour and strength of reinforced concrete members, *ACI Structural Journal*, March-April, 1990, pp. 220-231.

5.4) SABS 0100-Part 1 : 1992, The Structural use of concrete : Design, *South African Bureau of Standards*, 1992.

5.5) Cabrera, J.G., and Ghoddoussi, P., The effect of reinforcement corrosion on the strength of the steel/concrete bond, *Proceedings of the Conference on Bond in Concrete*, Latvia, CEB, October 1992, pp. 11-24.

Chapter Six

Closure

6.1 Closure

Chapters one and two reviewed the relevant literature to provide a background to this investigation. The experimental results for series one and two were presented and discussed in Chapters three and four. Series one beams were 155x220x2200 mm long and were reinforced with 2Y10 high tensile ribbed steel in both the compression and tension zones with no shear steel. Series two beams were of the same cross-sectional dimensions except that they were 2000 mm long, and were reinforced with 2Y12 high tensile ribbed bars in the tension zone, R8 mild steel link carriers and R8 links spaced at 140 mm centres. Both series had a 28 day cube strength of 30 MPa. The beams were simply supported and were loaded at midspan. The structural parameters examined were affected as follows :

Maximum load carrying capacity

The maximum load carrying capacity of the beams in series 2 (with stirrups) reduced with increasing amounts of corrosion. The series 1 beams (no stirrups) showed little variation in the maximum load carrying capacity. A critical level of corrosion damage was suggested, which first needs to be reached before there is a reduction in the load carrying capacity. In terms of this assumption, series 1 beams were below this critical damage level and series 2 beams were above this damage level. The added damage to the concrete caused by the corroding stirrups in series 2 was sufficient to exceed the critical damage level and therefore reduce the load carrying capacity of the beams, which was not the case with the series 1 beams.

Deflection at maximum load

The deflection at maximum load was found to increase with increasing amounts of corrosion in both series of tests. The smaller amount of corrosion damage in series 1 beams (with no corroding stirrups), initially had no effect on the deflection of the beams, but once the critical corrosion damage level was reached the deflection was found to increase. The critical corrosion damage level in this work was found to be at a loss of approximately 5,5% of the tensile strength of the reinforcing bars.

Work done up to the maximum load

The amount of work required to reach the maximum load was found to decrease with increasing amounts of corrosion in series 2 tests. From this it was concluded that the load reduction was occurring at a faster rate than the rate at which the deflection was increasing.

Toughness index using the maximum load

The toughness index was defined as the ratio of the work done up to the maximum load to the work done up to the yield load. The toughness index was found to increase with increasing amounts of corrosion suggesting that corrosion has a greater effect on the post-yield behaviour than on the elastic behaviour of beams.

The non-dimensional comparison of the results of this investigation with the results of other researchers revealed similar trends of decreasing load carrying capacity and increasing deflections with increasing amounts of corrosion. The analytical model suggested modeled the maximum load carrying capacity of the beams in series 2 reasonably well when the appropriate alpha factors were used. The exact variation of the alpha factors with varying amounts of corrosion would be very useful in refining the model. A greater number of experimental results is also essential if the validity of the model is to be assessed, which was not possible using the limited results of this investigation.

6.2 Further research to be done

The classification of reinforcement corrosion by a method that is quick and easy and that can be used on existing structures is of great importance. The development of the method should aim at providing the link between the amount of corrosion and the degree to which the structure has deteriorated structurally.

The differences between accelerated corrosion and normal corrosion should be studied, especially the effect of corroding elements while under load. An attempt should also be made to try and relate the time of accelerated corrosion to the time of normal corrosion.

A more detailed study of the effects of reinforcement corrosion on the structural performance of reinforced concrete beams should be undertaken. A much wider range of the extent of corrosion and beam types should be looked at in order to be able to quantify the effects of corrosion more generally. The response to dynamic loading as well as to cyclic loading is also seen as an area of major importance.

A greater number and range of experimental results will assist in the development of an analytical model when assessing the validity of the model. The development of an analytical model should be the focus of research if this work or any work leading on from it is to have any use in the design stage.

Appendix 1

Load-Deflection graphs for series 1

1) Beam C1

2) Beam C2

3) Beam T1

4) Beam B1

5) Beam TB1

6) Beam T2

7) Beam B2

8) Beam TB2

BEAM C1

LOAD-DEFLECTION CURVE

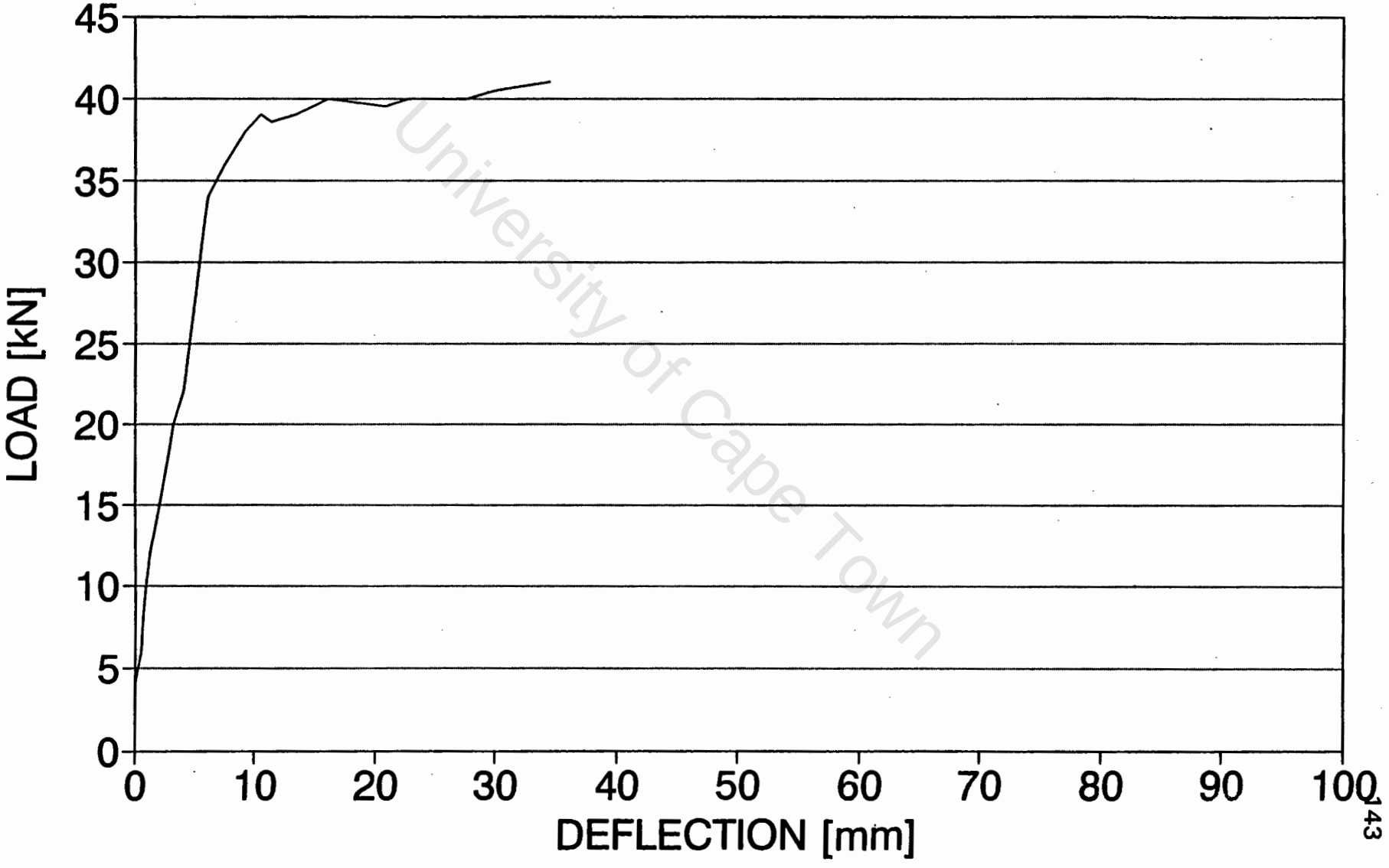

BEAM C2

LOAD-DEFLECTION CURVE

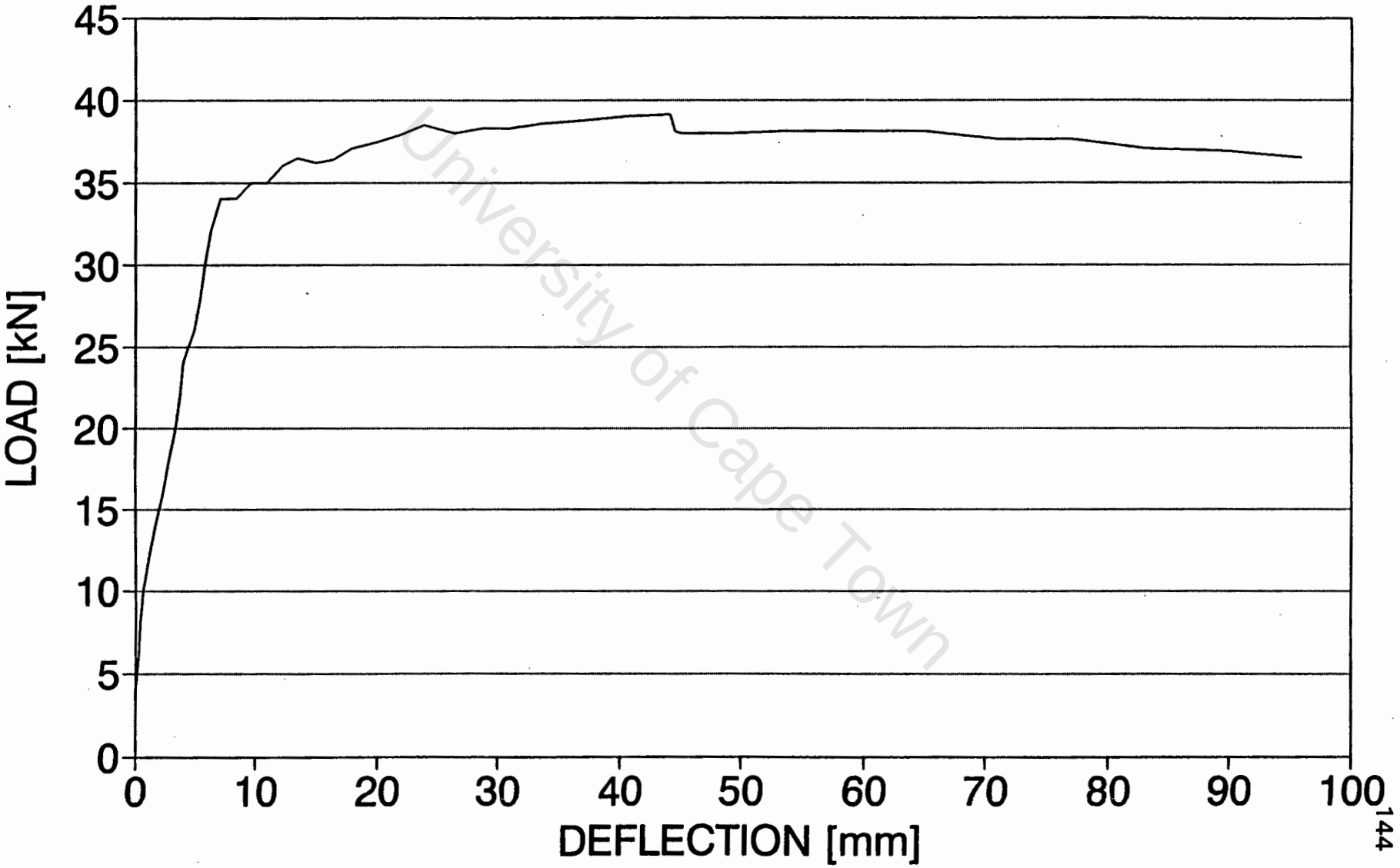

BEAM T1
LOAD-DEFLECTION CURVE

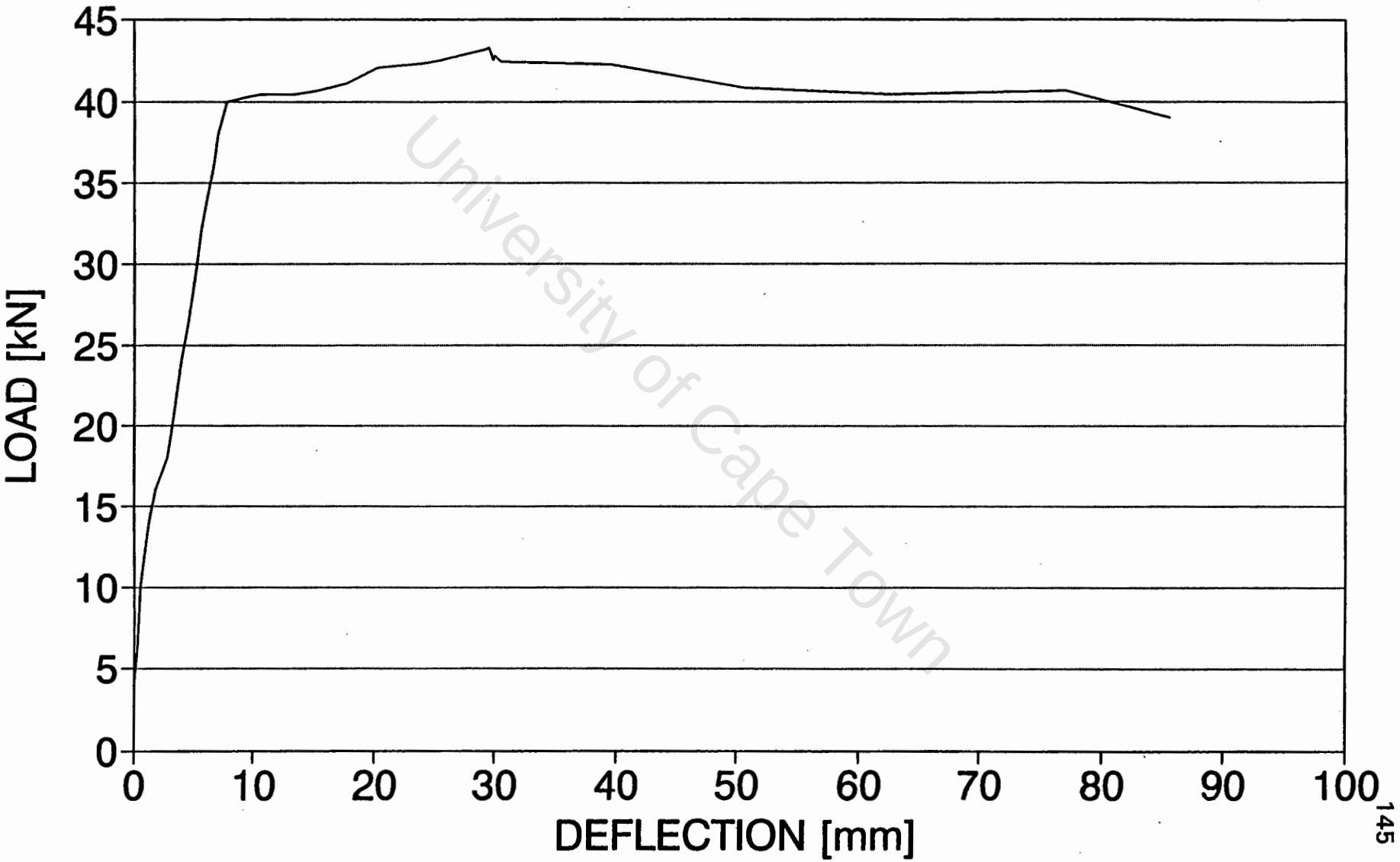

BEAM B1
LOAD-DEFLECTION CURVE

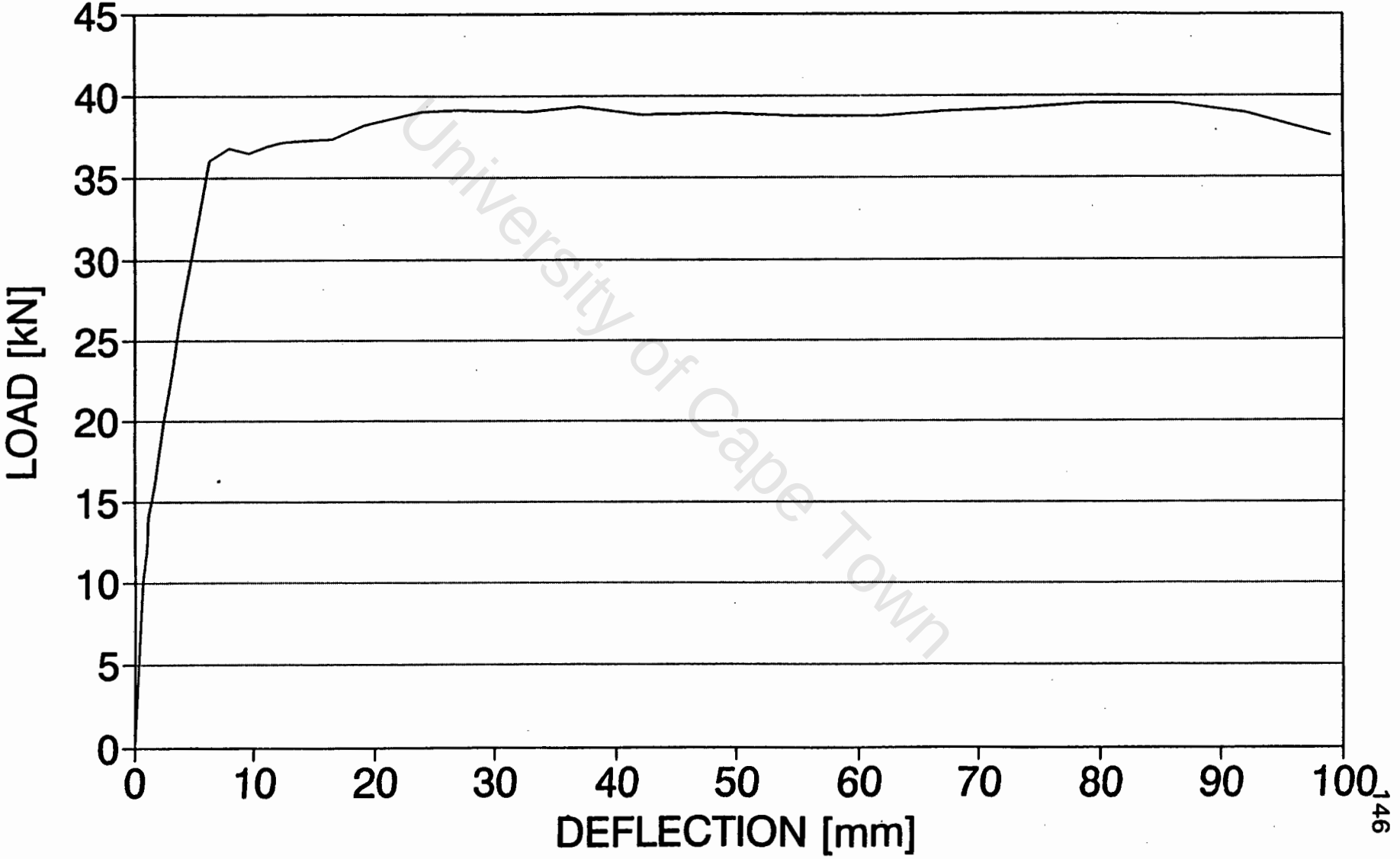

BEAM TB1
LOAD-DEFLECTION CURVE

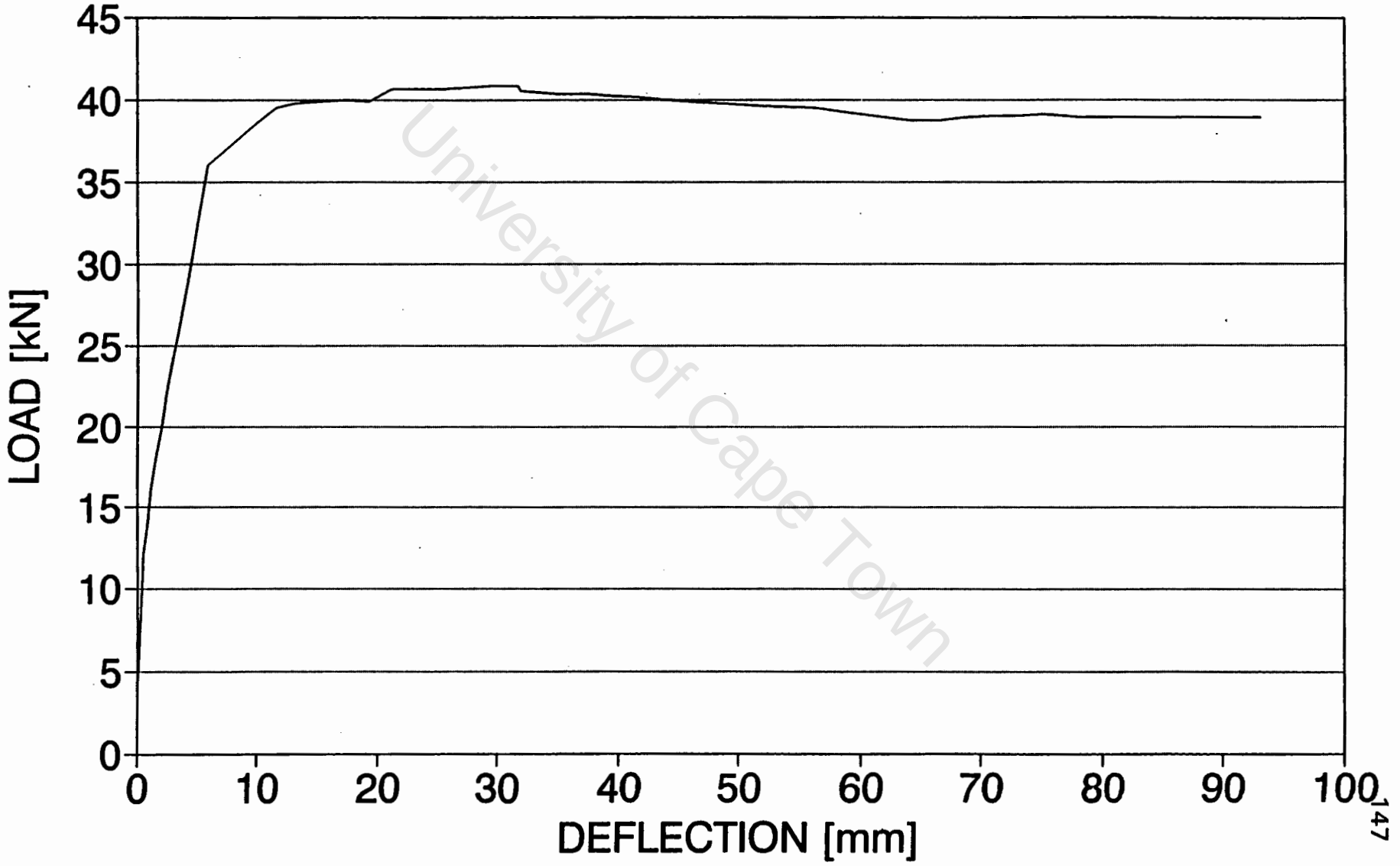

BEAM T2

LOAD-DEFLECTION CURVE

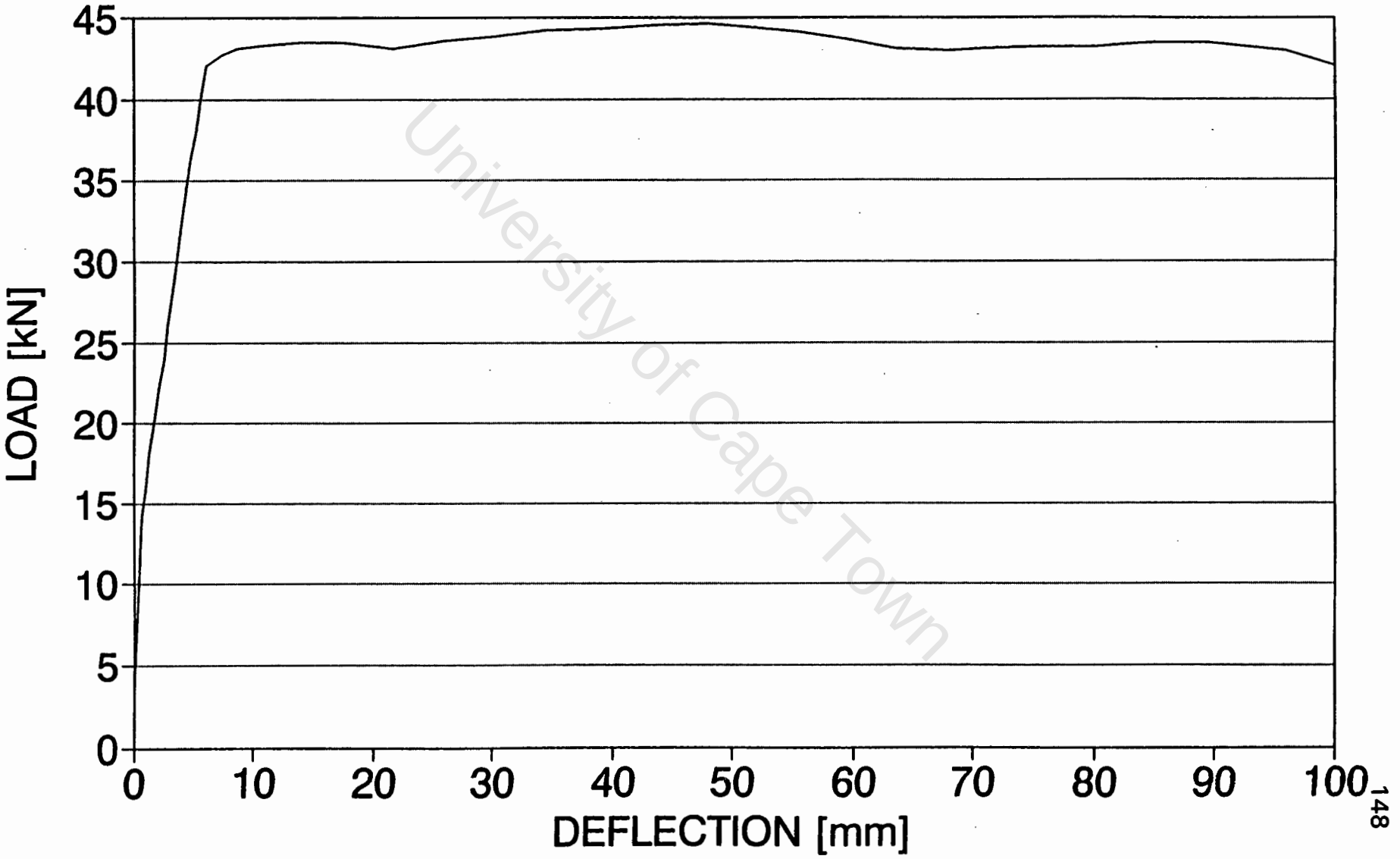

BEAM B2

LOAD-DEFLECTION CURVE

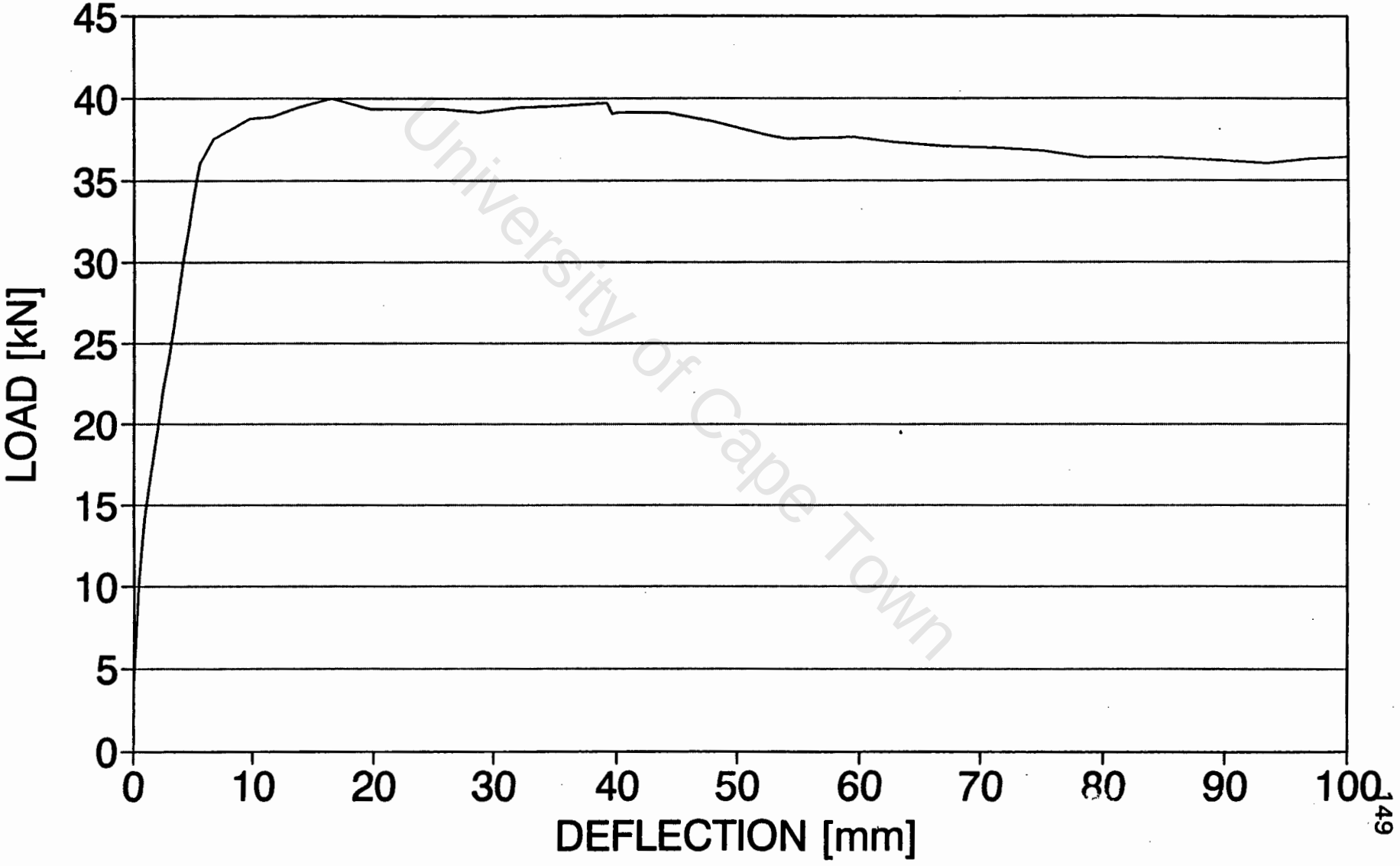

BEAM TB2

LOAD-DEFLECTION CURVE

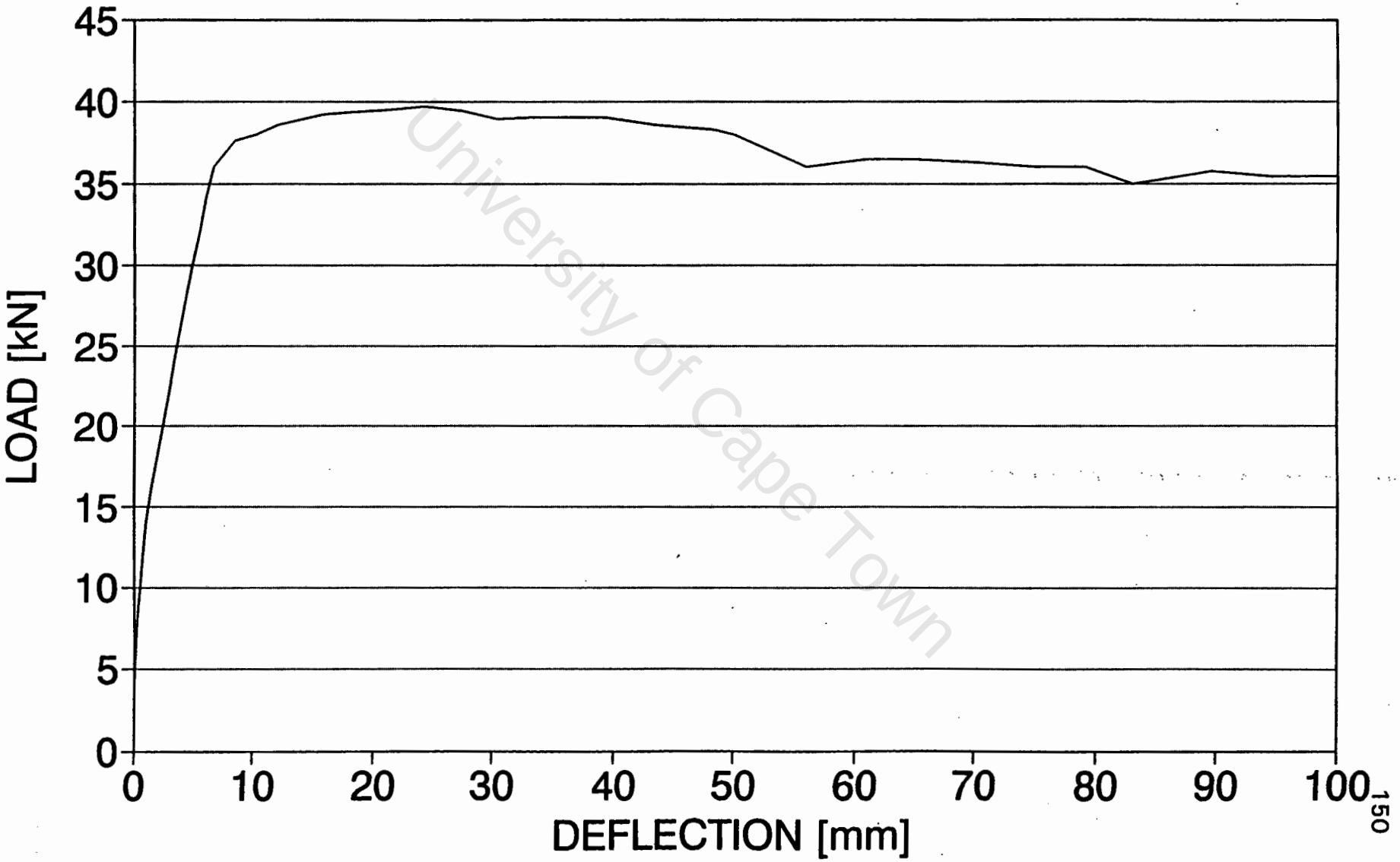

Appendix 2

Load-Deflection graphs for series 2

1) Beam C1T

2) Beam C2T

3) Beam T1T

4) Beam T2T

5) Beam T3T

6) Beam T4T

BEAM C1T
LOAD-DEFLECTION CURVE

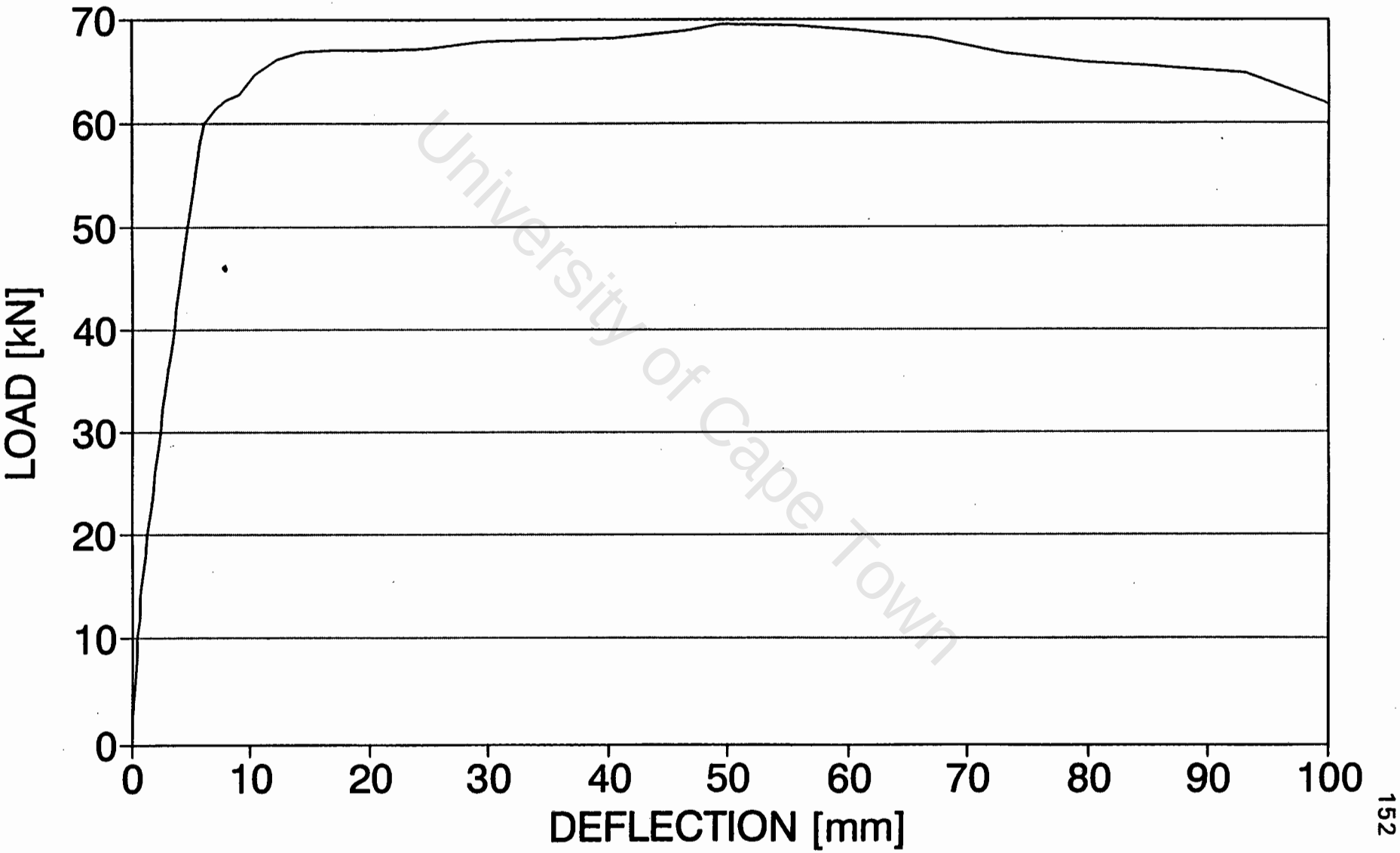

BEAM C2T
LOAD-DEFLECTION CURVE

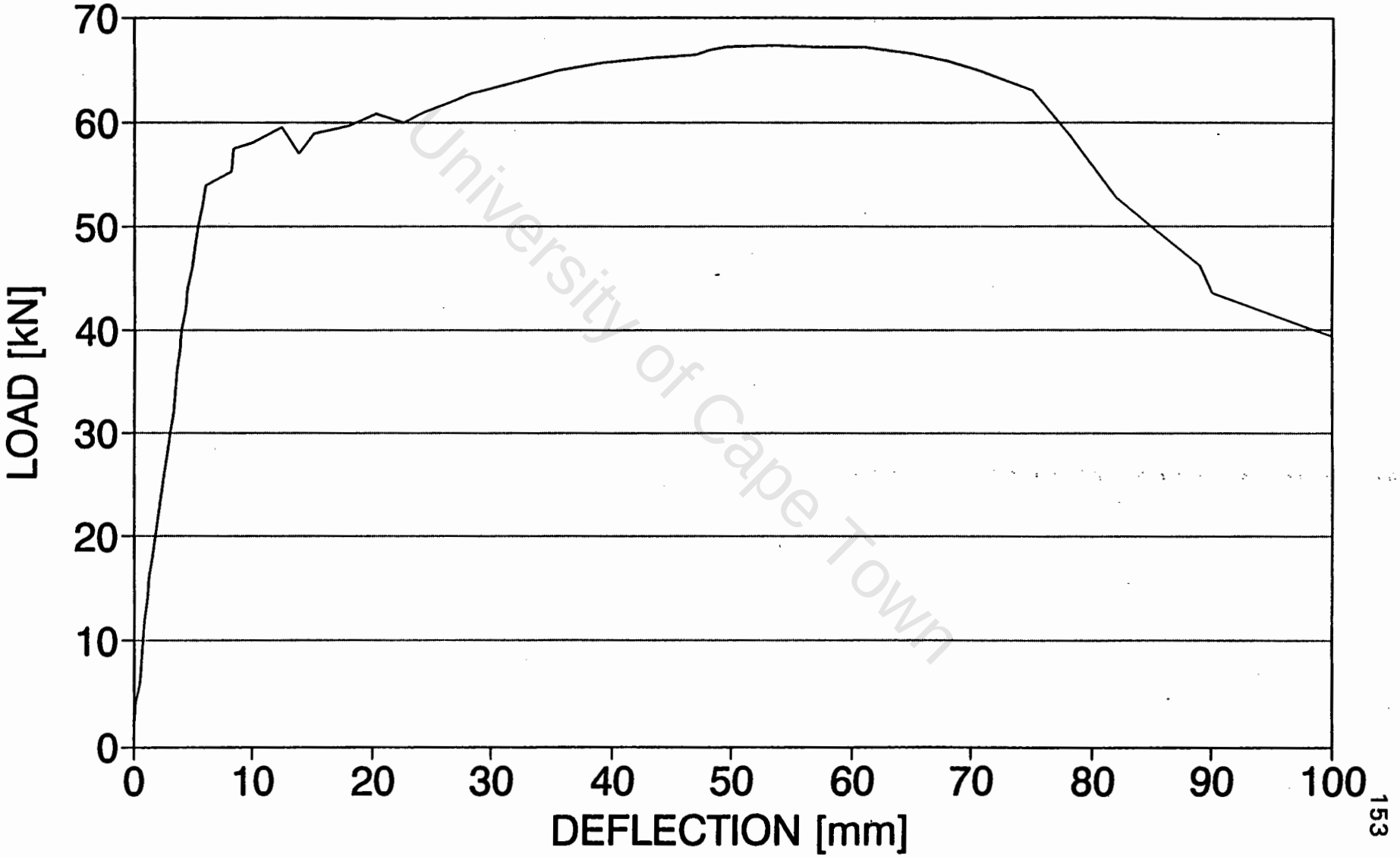

BEAM T1T

LOAD-DEFLECTION CURVE

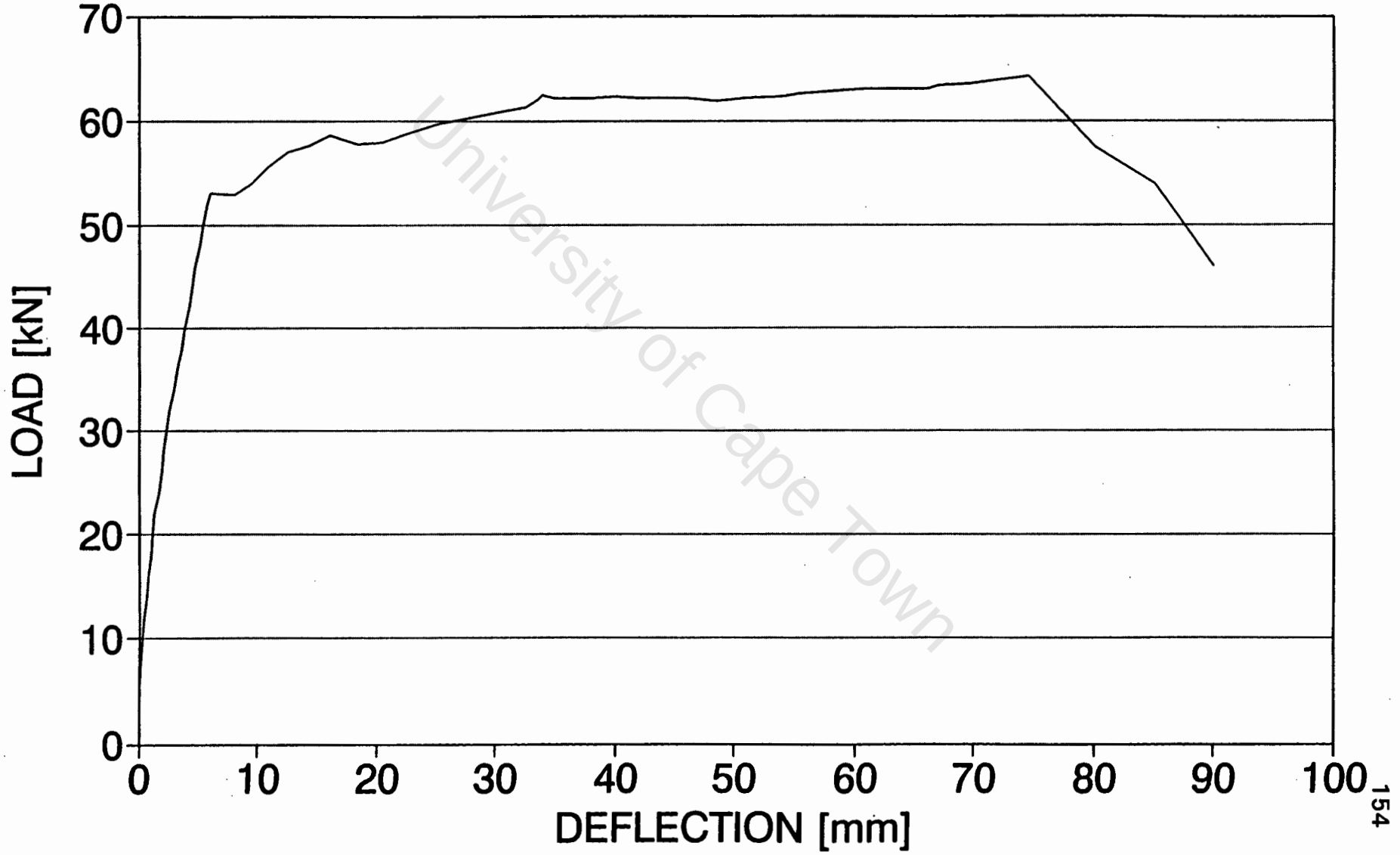

BEAM T2T

LOAD-DEFLECTION CURVE

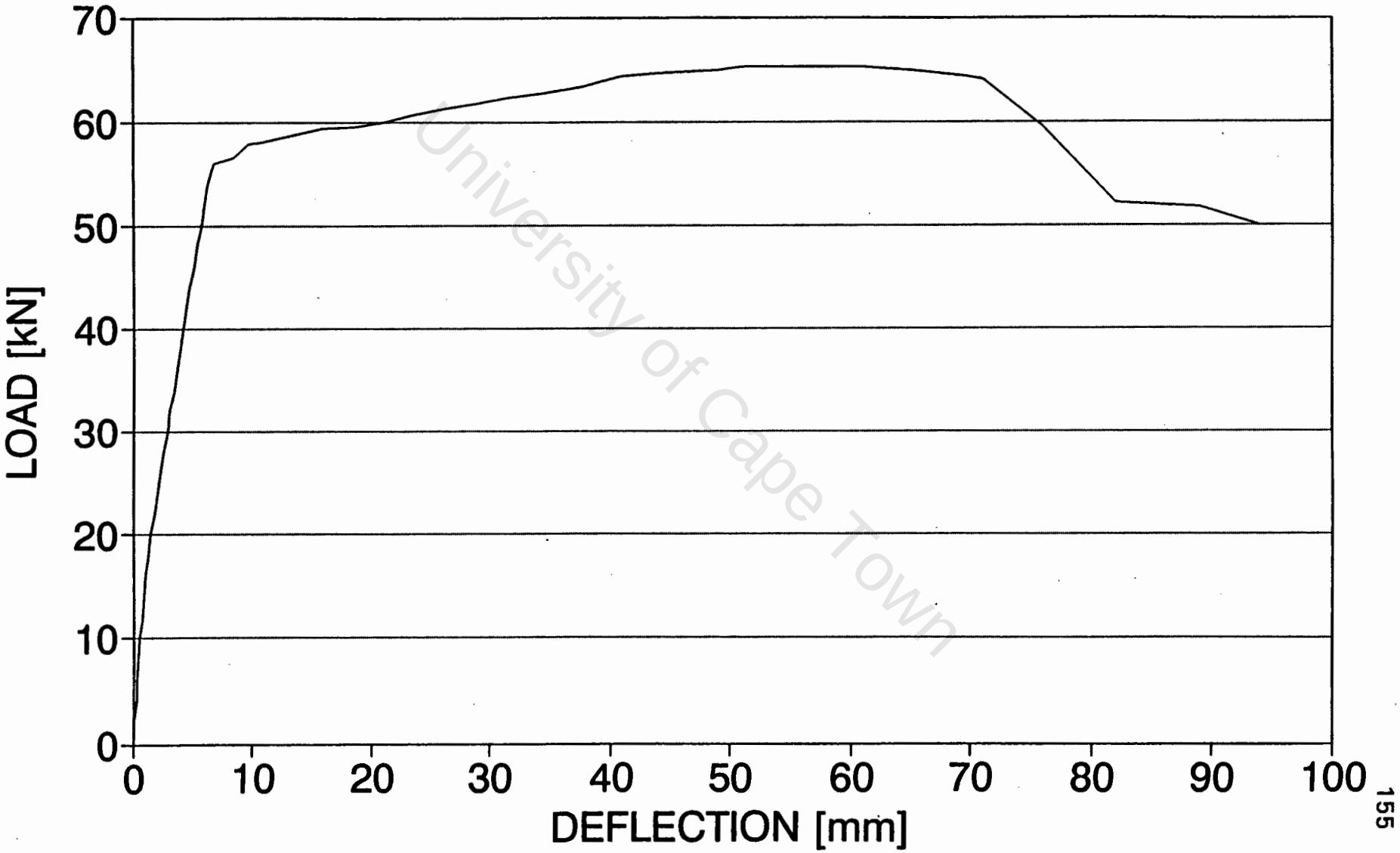

BEAM T3T
LOAD-DEFLECTION CURVE

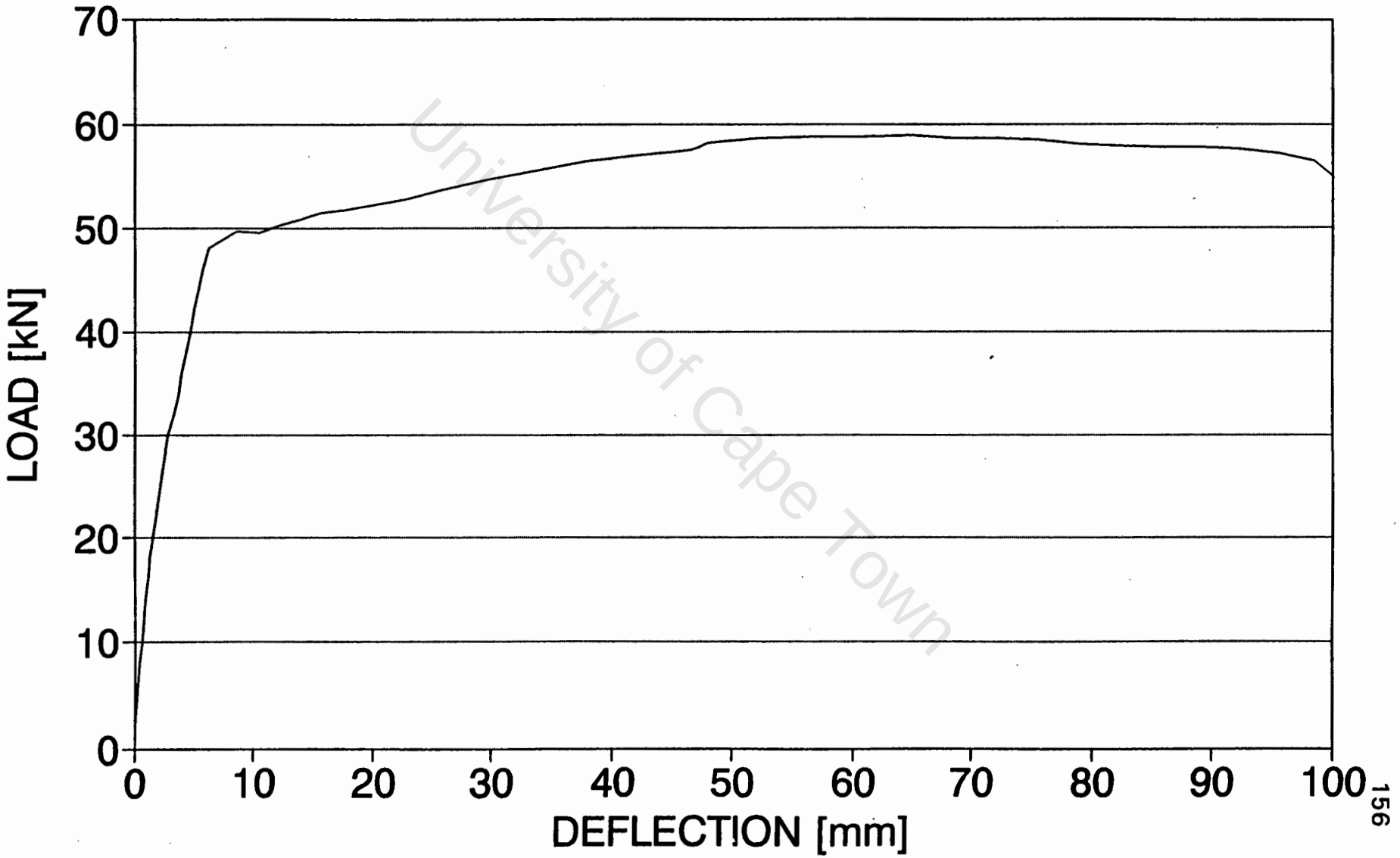

BEAM T4T
LOAD-DEFLECTION CURVE